



National Library  
of Canada

Bibliothèque nationale  
du Canada

Canadian Theses Service

Service des thèses canadiennes

Ottawa, Canada  
K1A 0N4

## NOTICE

The quality of this microform is heavily dependent upon the quality of the original thesis submitted for microfilming. Every effort has been made to ensure the highest quality of reproduction possible.

If pages are missing, contact the university which granted the degree.

Some pages may have indistinct print especially if the original pages were typed with a poor typewriter ribbon or if the university sent us an inferior photocopy.

Reproduction in full or in part of this microform is governed by the Canadian Copyright Act, R.S.C. 1970, c. C-30, and subsequent amendments.

## AVIS

La qualité de cette microforme dépend grandement de la qualité de la thèse soumise au microfilmage. Nous avons tout fait pour assurer une qualité supérieure de reproduction.

S'il manque des pages, veuillez communiquer avec l'université qui a conféré le grade.

La qualité d'impression de certaines pages peut laisser à désirer, surtout si les pages originales ont été dactylographiées à l'aide d'un ruban usé ou si l'université nous a fait parvenir une photocopie de qualité inférieure.

La reproduction, même partielle, de cette microforme est soumise à la Loi canadienne sur le droit d'auteur, SRC 1970, c. C-30, et ses amendements subséquents.

THE UNIVERSITY OF ALBERTA

MULTIRATE ADAPTIVE INFERENTIAL CONTROL  
OF DISTILLATION COLUMNS

by



YAN SUNG YIU

A THESIS

SUBMITTED TO THE FACULTY OF GRADUATE STUDIES AND RESEARCH  
IN PARTIAL FULFILLMENT OF THE REQUIREMENTS FOR THE DEGREE  
OF MASTER OF SCIENCE

IN

PROCESS CONTROL

THE DEPARTMENT OF CHEMICAL ENGINEERING

EDMONTON, ALBERTA

SPRING, 1990



National Library  
of Canada

Bibliothèque nationale  
du Canada

Canadian Theses Service

Service des thèses canadiennes

Ottawa, Canada  
K1A 0N4

## NOTICE

The quality of this microform is heavily dependent upon the quality of the original thesis submitted for microfilming. Every effort has been made to ensure the highest quality of reproduction possible.

If pages are missing, contact the university which granted the degree.

Some pages may have indistinct print especially if the original pages were typed with a poor typewriter ribbon or if the university sent us an inferior photocopy.

Reproduction in full or in part of this microform is governed by the Canadian Copyright Act, R.S.C. 1970, c. C-30, and subsequent amendments.

## AVIS

La qualité de cette microforme dépend grandement de la qualité de la thèse soumise au microfilmage. Nous avons tout fait pour assurer une qualité supérieure de reproduction.

S'il manque des pages, veuillez communiquer avec l'université qui a conféré le grade.

La qualité d'impression de certaines pages peut laisser à désirer, surtout si les pages originales ont été dactylographiées à l'aide d'un ruban usé ou si l'université nous a fait parvenir une photocopie de qualité inférieure.

La reproduction, même partielle, de cette microforme est soumise à la Loi canadienne sur le droit d'auteur, SRC 1970, c. C-30, et ses amendements subséquents.

ISBN 0-315-60264-3

THE UNIVERSITY OF ALBERTA

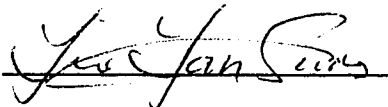
RELEASE FORM

Name of author Yan Sung Yiu  
Title of thesis Multirate Adaptive Inferential Control of  
Distillation Columns  
Degree Master of Science  
Year this degree granted Spring, 1990

Permission is hereby granted to the University of Alberta library to reproduce single copies of this thesis and to lend or sell such copies for private, scholarly or scientific research purposes only.

The author reserves other publication rights, and neither the thesis nor extensive extracts from it may be reprinted or otherwise reproduce without the author's written permission.

(SIGNED)



PERMANENT ADDRESS :

69, G/F, Man Chun House,

Tze Man Estate,

Kowloon, Hong Kong

DATED Sep 28 1989

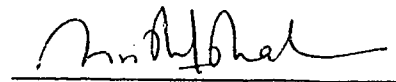
THE UNIVERSITY OF ALBERTA  
FACULTY OF GRADUATE STUDIES AND RESEARCH

The undersigned certify that they have read, and recommend to the Faculty of Graduate Studies and Research for acceptance, a thesis entitled **Multirate Adaptive Inferential Control of Distillation Columns** submitted by **Yan Sung Yiu** in partial fulfillment of the requirements for the degree of **Master of Science in Process Control**.



Dr. R.K. Wood

Supervisor



Dr. S.L. Shah



Dr. K.A. Stromsmoe

DATE DEC 22 / 89

**To my parents,  
brothers and sisters**

## Abstract

This thesis evaluates the performance of three multirate inferential estimation schemes which infer intersample values of the controlled output from a more rapidly sampled secondary plant output. Three estimator equations based on using first and second order plant models are employed. Each of these estimators is combined with a fixed parameter PI controller to form an adaptive inferential control (AIC) scheme. The control performance of each AIC scheme was compared with the control behavior of a conventional PI feedback control strategy.

The AIC schemes have been evaluated, by simulation, for bottoms composition control of a binary distillation column and of a five component depropanizer. The binary column control behavior was simulated using a transfer function model while simulation of the control behavior of the depropanizer was performed using a general purpose distillation column simulator, DYCONDIST. For both columns, the AIC schemes used a tray temperature as the secondary output. Simulation results showed that the standard AIC scheme, which required the identification of twelve parameters when a first order plant model was assumed, provided the best control performance for control of the bottoms composition of the binary column modelled by transfer functions when there are changes in feed, set point or process parameters. However, for control of the bottoms composition of the depropanizer, this scheme was not able to cope with the nonlinear behavior of the process while the simplified algorithm, which has only three model parameters when a first order plant model is employed, resulted in the best control response. Use of a dead-band on AIC strategies was found to stabilize the control behavior during the initial adaptation period so its

use is strongly recommended for practical applications.

The performance of the AIC algorithms were also examined experimentally for control of the bottoms composition of a pilot scale binary distillation column. The experimental results further demonstrated the robust control performance of the SM-1 algorithm because only three parameters needed to be estimated. Although the controller settings of the fixed PI controller used in the AIC schemes were never tuned, the SM-1 algorithm outperformed the SM-2 simplified and the conventional PI schemes for the cases with -20% step disturbance in feed rate or one mass percent set point changes.

In general, the simulation and experimental results show the potential for successful application of the SM-1 control algorithm to industrial processes.



## Acknowledgement

The author would like to thank Dr. R.K. Wood for his guidance and supervision during the course of this research. Special thanks are also due to Mr. David Shook without whom the experimental work would not have been possible.

My gratitude is extended to Ms. Andree Koenig, Mr. Don Sutherland, Mr. Keith Faulder and the staff of both the electronics and machine shops for their prompt assistance in keeping the distillation column functional.

The work on this thesis was made more enjoyable by other graduate students. In particular, I owe much to discussions with Dr. Weiping Lu, Eric Lau, Kun-yu Kwok, Mike Foley and David Shook. Appreciation is also extended to Dr. Coorus Mohtadi of Oxford University for his valuable suggestions during his visit in the Department of Chemical Engineering. The fun time with the graduate students in the 5th floor "bull-pen" and the "Control Group Food Mart" will never be forgotten.

The financial support from the Department of Chemical Engineering is gratefully acknowledged.

Finally, I take the opportunity to thank my parents, brothers and sisters in Hong Kong for their constant support and encouragement over so many years.

## Table of Contents

Chapter	Page
1. Introduction and Literature Survey . . . . .	1
1.1 Introduction . . . . .	1
1.2 Literature Review . . . . .	3
1.1.1 Non-adaptive Schemes for Inferring Process Outputs . . . . .	3
1.1.2 Adaptive Schemes for Inferring Process Outputs . . . . .	8
1.3 Thesis Organization . . . . .	13
2. Development of the Multirate Adaptive Inferential Estimation Algorithm . . . . .	15
2.2 Introduction . . . . .	15
2.2 Derivation of the Multirate Adaptive Inferential Estimation Algorithm . . . . .	15
2.2.1 Plant Model . . . . .	17
2.2.2 The Standard Algorithm . . . . .	20
2.2.3 The Simplified Algorithm . . . . .	21
2.2.4 The Truncated Standard Algorithm . . . . .	23
2.3 Recursive Least Squares Identification Algorithms . . . . .	23
2.3.1 Recursive Least Squares with Exponential Data Weighting . . . . .	24
2.3.2 Recursive Least Squares with Constant Trace Covariance Matrix through Variable Forgetting Factor . . . . .	25
2.3.3 Recursive Least Squares with Exponential Data Weighting and Covariance Resetting . . . . .	26
2.4 Adaptive Inferential Control Using a Dead-band . . . . .	26
3. Multirate Adaptive Inferential Control of a Linear System . . . . .	28
3.1 Introduction . . . . .	28

3.2	Linear Model of the Pilot Scale Binary Column	28
3.3	Implementation of the Adaptive Inferential Control Algorithm	31
3.3.1	Estimation Equations and the Control Law	31
3.3.2	Selection of the Secondary Output, Identification and Initial Parameters	34
3.4	Simulation Results	35
3.4.1	Control of a Time-Invariant Process	35
3.4.2	Control of a Time-Variant Process	52
3.5	Summary	58
4.	Multirate Adaptive Inferential Control of a Nonlinear System.	60
4.1	Introduction	60
4.2	The DYCONDIST Simulator	60
4.3	Description of the Depropanizer Column	63
4.4	Implementation of the Adaptive Inferential Control Algorithm	65
4.4.1	Selection of the Secondary Output	65
4.4.2	Estimation Equations, Identification and Initialization	67
4.5	Simulation Results	70
4.5.1	Single Tray Temperature Feedback Control	70
4.5.2	Control Performance of the Adaptive Inferential Control Scheme Using a Sensitive Secondary Output	73
4.5.3	Sensitivity of the Control Performance of the Adaptive Inferential Control Scheme to Selection of Secondary Output	102
4.5.4	Control Performance of the Truncated Standard Algorithm	110
4.6	Summary	111

5.	Experimental Results	116
5.1	Introduction	116
5.2	Description of the Equipment	116
5.2.1	Software	119
5.2.2	Communications	119
5.2.3	Top Composition Control	120
5.2.4	Feed Flow Control	120
5.2.5	Bottoms Composition Control	121
5.2.6	Temperature Measurements	122
5.3	Estimation Equations, Identification and Initialization	122
5.4	Results	125
5.4.1	Step Increase in Feed Rate of 25%	125
5.4.2	Step Decrease in Feed Rate of 20%	132
5.4.3	Servo Control Performance	136
5.5	Summary	142
6.	Conclusions and Recommendations for Future Work	143
6.1	Conclusions	143
6.2	Recommendations for Future Work	146
	References	149
Appendix A		
	The Concept of Observability	158
Appendix B		
	Tray Liquid Holdup Data and Thermodynamic Parameters for Depropanizer Column	164

## List of Tables

Table	Page
3.1 Parameters for the Transfer Model of the Binary Distillation Column . . . . .	30
3.2 Tuned Controller Constants for the AIC Schemes . . . . .	35
3.3 Summary of Control Performance for a -25% Step Change in Feed Rate . . . . .	36
3.4 Summary of Control Performance for a -25% Step Change in Feed Rate with Liquid Temperature on Tray 6 Used as the Secondary Output for the AIC Schemes . . . . .	47
3.5 Summary of Control Performance for a -25% Step Change in Feed Rate with Changes in Process Gains and Time Delays . . . . .	53
4.1 Depropanizer Operating Conditions . . . . .	64
4.2 Tuned Controller Settings for the AIC Schemes Using Stage 23 Liquid Temperature as the Secondary Output . . . . .	68
4.3 Description of the Tests Used in Simulation of Control of the Depropanizer . . . . .	71
4.4 Summary of Control Performance for a -20% Step Change in Feed Rate . . . . .	77
4.5 Effect of Employing a 15% Dead-band on Control Performance of the AIC Schemes for a 20% Step Change in Feed Rate . . . . .	88
4.6 Summary of Control Performance for Step Change in the Concentrations of the Components in the Feed Stream . . . . .	94
4.7 Summary of Control Performance for a -20% Step Change in Set Point . . . . .	102

4.8	Effect of Using Stage 27 Liquid Temperature as the Secondary Output on Control Performance of the AIC Schemes . . . . .	103
4.9	Comparison of Control Performance of the TST-2 and ST-1 AIC Schemes . . . . .	111
5.1	Typical Steady State Operating Conditions of the Binary Distillation Column . . . . .	118
5.2	Summary of Control Performance for a +25% Step Change in Feed Rate . . . . .	129
5.3	Summary of Control Performance for a -20% Step Change in Feed Rate . . . . .	135
5.4	Summary of Control Performance for Step Changes of One Mass Percent Methanol Concentration in Bottoms Composition Set Point . . . . .	140
B.1	Tray Liquid Holdup Profile . . . . .	164
B.2	Equilibrium Data . . . . .	165
B.3	Liquid Enthalpy Data . . . . .	165
B.4	Vapor Enthalpy Data . . . . .	166

## List of Figures

Figure	Page
1.1 The Inferential Control Scheme (Using Secondary Outputs)	6
1.2 The Adaptive Inferential Control Scheme of Shen and Lee (1989)	11
2.1 Multirate Adaptive Inferential Feedback Control Scheme with a Fixed Parameter Controller	16
3.1 Multirate Adaptive Inferential Control of the Bottoms Composition of a Distillation Column	32
3.2 Comparison of Conventional PI and ST-1 AIC Control Performance for a -25% Step Change in Feed Rate and AIC Parameter Trajectories	37
3.3 Comparison of Conventional PI and SM-1 AIC Control Performance for a -25% Step Change in Feed Rate and AIC Parameter Trajectories	38
3.4 Comparison of Conventional PI and SM-2 AIC Control Performance for a -25% Step Change in Feed Rate and AIC Parameter Trajectories	39
3.5 Comparison of Predicted Bottoms Composition versus Actual Bottoms Composition for a -25% Step Change in Feed Rate	41
3.6 Control Performance of the ST-1 AIC Scheme Using Tray 6 Liquid Temperature as the Secondary Output for a -25% Step Change in Feed Rate and AIC Parameter Trajectories	44
3.7 Control Performance of the SM-1 AIC Scheme Using Tray 6 Liquid Temperature as the Secondary Output for a -25% Step Change in Feed Rate and AIC Parameter Trajectories	45
3.8 Control Performance of the SM-2 AIC Scheme Using Tray 6 Liquid Temperature as the Secondary Output for a -25% Step Change in Feed Rate and AIC Parameter Trajectories	46

3.9	Comparison of Conventional PI and ST-1 AIC Control Performance for a Step Increase of One Mass Percent Methanol Concentration in the Bottoms Composition Set Point and AIC Parameter Trajectories . . . . .	49
3.10	Comparison of Conventional PI and SM-1 AIC Control Performance for a Step Increase of One Mass Percent Methanol Concentration in the Bottoms Composition Set Point and AIC Parameter Trajectories . . . . .	50
3.11	Comparison of Conventional PI and SM-2 AIC Control Performance for a Step Increase of One Mass Percent Methanol Concentration in the Bottoms Composition Set Point and AIC Parameter Trajectories . . . . .	51
3.12	Comparison of Conventional PI and ST-1 AIC Control Performance for Changes in the Transfer Function Gains and Time Delays and AIC Parameter Trajectories . . . . .	54
3.13	Comparison of Conventional PI and SM-1 AIC Control Performance for Changes in the Transfer Function Gains and Time Delays and AIC Parameter Trajectories . . . . .	55
3.14	Comparison of Conventional PI and SM-2 AIC Control Performance for Changes in the Transfer Function Gains and Time Delays and AIC Parameter Trajectories . . . . .	56
4.1	Open Loop Responses of Four Tray Liquid Temperatures to Step Changes in Feed Rate (-10% F at t=0 ; +10% F at t=50) . . . . .	66
4.2	Single Tray Temperature Feedback Control of Bottoms Composition for +20% and -20% Step Changes in Feed Rate . . . . .	72
4.3	Comparison of Conventional PI and ST-1 AIC Control Performance for a -20% Step Change in Feed Rate and AIC Parameter Trajectories (No Dead-band with AIC) . . . . .	74
4.4	Comparison of Conventional PI and SM-1 AIC Control Performance for a -20% Step Change in Feed Rate and AIC Parameter Trajectories (No Dead-band with AIC) . . . . .	75



4.5	Comparison of Conventional PI and SM-2 AIC Control Performance for a -20% Step Change in Feed Rate and AIC Parameter Trajectories (No Dead-band with AIC)	76
4.6	Comparison of Predicted Bottoms Composition versus Actual Bottoms Composition for a -20% Step Change in Feed Rate (No Dead-band with AIC).	78
4.7	Comparison of Conventional PI and ST-1 AIC Control Performance for a +20% Step Change in Feed Rate and AIC Parameter Trajectories (No Dead-band with AIC)	80
4.8	Comparison of Conventional PI and SM-1 AIC Control Performance for a +20% Step Change in Feed Rate and AIC Parameter Trajectories (No Dead-band with AIC)	81
4.9	Comparison of Conventional PI and SM-2 AIC Control Performance for a +20% Step Change in Feed Rate and AIC Parameter Trajectories (No Dead-band with AIC)	82
4.10	Comparison of Conventional PI and ST-1 AIC Control Performance for a +20% Step Change in Feed Rate and AIC Parameter Trajectories (15% Dead-band with AIC)	85
4.11	Comparison of Conventional PI and SM-1 AIC Control Performance for a +20% Step Change in Feed Rate and AIC Parameter Trajectories (15% Dead-band with AIC)	86
4.12	Comparison of Conventional PI and SM-2 AIC Control Performance for a +20% Step Change in Feed Rate and AIC Parameter Trajectories (15% Dead-band with AIC)	87
4.13	Effect of Using a Dead-band with ST-1 AIC on Control Performance for a +20% Step Change in Feed Rate	89
4.14	Comparison of Conventional PI and ST-1 AIC Control Performance for Step Changes in the Concentrations of the Components in the Feed Stream and AIC Parameter Trajectories (15% Dead-band with AIC)	91
4.15	Comparison of Conventional PI and SM-1 AIC Control Performance for Step Changes in the Concentrations of the Components in the Feed Stream and AIC Parameter Trajectories (15% Dead-band with AIC)	92

4.16	Comparison of Conventional PI and SM-2 AIC Control Performance for Step Changes in the Concentrations of the Components in the Feed Stream and AIC Parameter Trajectories (15% Dead-band with AIC)	93
4.17	Comparison of Conventional PI and SM-1 AIC Control Performance for Simultaneous Increases in Feed Rate and Analyzer Cycle Time and AIC Parameter Trajectories (15% Dead-band with AIC)	96
4.18	Comparison of Conventional PI and SM-2 AIC Control Performance for Simultaneous Increases in Feed Rate and Analyzer Cycle Time and AIC Parameter Trajectories (15% Dead-band with AIC)	97
4.19	Comparison of Conventional PI and ST-1 AIC Control Performance for a -20% Step Change in Bottoms Composition Set Point and AIC Parameter Trajectories (15% Dead-band with AIC)	99
4.20	Comparison of Conventional PI and SM-1 AIC Control Performance for a -20% Step Change in Bottoms Composition Set Point and AIC Parameter Trajectories (15% Dead-band with AIC)	100
4.21	Comparison of Conventional PI and SM-2 AIC Control Performance for a -20% Step Change in Bottoms Composition Set Point and AIC Parameter Trajectories (15% Dead-band with AIC)	101
4.22	Control Performance of ST-1 AIC Scheme Using Stage 27 Liquid Temperature as Secondary Output and AIC Parameter Trajectories for a +20% Step Change in Feed Rate (15% Dead-band with AIC)	104
4.23	Control Performance of SM-1 AIC Scheme Using Stage 27 Liquid Temperature as Secondary Output and AIC Parameter Trajectories for a +20% Step Change in Feed Rate (15% Dead-band with AIC)	105
4.24	Control Performance of SM-2 AIC Scheme Using Stage 27 Liquid Temperature as Secondary Output and AIC Parameter Trajectories for a +20% Step Change in Feed Rate (15% Dead-band with AIC)	106
4.25	Control Performance of SM-1 AIC Scheme Using Stage 27 Liquid Temperature as Secondary Output and AIC Parameter Trajectories for Simultaneous Increases in Feed Rate and Analyzer Cycle Time (15% Dead-band with AIC)	107

4.26	Control Performance of SM-2 AIC Scheme Using Stage 27 Liquid Temperature as Secondary Output and AIC Parameter Trajectories for Simultaneous Increases in Feed Rate and Analyzer Cycle Time (15% Dead-band with AIC)	108
4.27	Comparison of Conventional PI and TST-2 AIC Control Performance for a +20% Step Change in Feed Rate and AIC Parameter Trajectories (15% Dead-band with AIC)	112
4.28	Comparison of Conventional PI and TST-2 AIC Control Performance for Simultaneous Increases in Feed Rate and Analyzer Cycle Time and AIC Parameter Trajectories (15% Dead-band with AIC)	113
5.1	Schematic Diagram of the Binary Distillation Column	117
5.2	Comparison of Conventional PI and ST-1 AIC Control Performance for a +25% Step Change in Feed Rate and AIC Parameter Trajectories	126
5.3	Comparison of Conventional PI and SM-1 AIC Control Performance for a +25% Step Change in Feed Rate and AIC Parameter Trajectories	127
5.4	Comparison of Conventional PI and SM-2 AIC Control Performance for a +25% Step Change in Feed Rate and AIC Parameter Trajectories	128
5.5	Comparison of Predicted Bottoms Composition versus Actual Bottoms Composition for a +25% Step Change in Feed Rate	131
5.6	Comparison of Conventional PI and SM-1 AIC Control Performance for a -20% Step Change in Feed Rate and AIC Parameter Trajectories	133
5.7	Comparison of Conventional PI and SM-2 AIC Control Performance for a -20% Step Change in Feed Rate and AIC Parameter Trajectories	134
5.8	Comparison of Predicted Bottoms Composition versus Actual Bottoms Composition for -20% Step Change in Feed Rate	137

5.9	Comparison of Conventional PI and SM-1 AIC Control Performance for Step Changes of One Mass Percent Methanol Concentration in the Bottoms Composition Set Point . . . . .	138
5.10	Comparison of Conventional PI and SM-2 AIC Control Performance for Step Changes of One Mass Percent Methanol Concentration in the Bottoms Composition Set Point . . . . .	139
5.11	Comparison of Predicted Bottoms Composition versus Actual Bottoms Composition for Step Changes of One Mass Percent Methanol Concentration in Bottoms Composition Set Point . . . . .	141

## Nomenclature and Notation

### Alphabetical

$A(q^{-1})$	Polynomial corresponding to process output (c.f. Eq. 2.5)
$A(q^{-J})$	Polynomial corresponding to process output in the transformed process model (c.f. Eq. 2.21); equivalent to $A_J(q^{-J})$ .
$\underline{\underline{A}}$	System model matrix in Eq. A.4; $\underline{\underline{A}}_{ij}$ is a sub-matrix of $\underline{\underline{A}}$ .
$\overline{\underline{\underline{A}}}$	A similar system model matrix of $\underline{\underline{A}}$ (see Eq. A.11).
$a_i$	Coefficients of $A(q^{-1})$ or $A(q^{-J})$ ; $a_0 = 1$ .
$a_{Ji}$	Coefficients of $A_J(q^{-J})$ ; $a_{J0} = 1$ .
$\overline{a}_i$	Entries in the system model matrix in Eq. 2.1.
$B(q^{-1})$	Polynomial corresponding to process input (c.f. Eqs. 2.6 and 2.23).
$B_J(q^{-1})$	Polynomial corresponding to process input in the transformed process model (c.f. Eq. 2.18); equivalent to $B(q^{-1})$ in Eq. 2.23.
$\underline{\underline{B}}$	System input vector in Eq. A.4; $\underline{\underline{B}}_i$ is a sub-vector of $\underline{\underline{B}}$ .
$\overline{\underline{\underline{B}}}$	A similar system input matrix of $\underline{\underline{B}}$ (see Eq. A.11).
$b_i$	Entries in the system model vector describing the effect of process input on the state (c.f. Eq. 2.1).
$C$	The total number of components in a distillation column (c.f. Section 4.2).
$C(q^{-1})$	Polynomial corresponding to secondary output in the transformed process model (c.f. Eq. 2.24).

$C_j(q^{-1})$	Polynomial corresponding to secondary output in the transformed process model (c.f. Eq. 2.16).
$\bar{C}(q^{-1})$	Polynomial corresponding to secondary output (c.f. Eq. 2.7).
$\underline{C}$	System output vector in Eq. A.5; $\underline{C}_i$ is a sub-vector of $\underline{C}$ .
$\bar{\underline{C}}$	A similar system output matrix of $\underline{C}$ (see Eq. A.11).
$c_i$	Coefficients of $C(q^{-1})$ .
$c_{ji}$	Coefficients of $C_j(q^{-1})$ .
$D$	Diagonal Matrix.
$D(q^{-1})$	Polynomial corresponding to the white noise in process output (c.f. Eq. 2.11).
$\bar{D}(q^{-1})$	Polynomial as defined by Eq. 2.12.
$d$	Time delay between input and primary output.
$d_i$	Coefficients of $D(q^{-1})$ .
$E(q^{-1})$	Polynomial corresponding to the white noise term in Eq. 2.14.
$E_j(q^{-1})$	Polynomial corresponding to the white noise term in the transformed process model (c.f. Eq. 2.16).
$e_i$	Coefficients of $E(q^{-1})$ .
$e_{ji}$	Coefficients of $E_j(q^{-1})$ .
$e(t)$	The prediction error in the cost function $J_K$ .
$h$	Coefficient relating secondary output to process output.
$I$	Identity matrix.
$J$	Sampling interval of process output.
$J_K$	Cost function in the recursive least squares algorithm.
$K$	The upper time limit of the cost function $J_K$ .
$K(t)$	Kalman gain.
$M$	Order of polynomials $B(q^{-1})$ , $C(q^{-1})$ and $E(q^{-1})$ in Eq. 2.21.

$N$	Order of polynomials $B_j(q^{-1})$ , $C_j(q^{-1})$ and $E_j(q^{-1})$ in Eq. 2.16; the total number of stages in a distillation column (c.f Section 4.2).
$n$	Order of the process model.
$nv$	Observability index of secondary output.
$ny$	Order of polynomial $A(q^{-1})$ .
$P(t)$	Covariance matrix.
$q^{-1}$	Backward shift operator.
$R(q^{-1})$	Polynomial corresponding to disturbance sequence in Eq. 2.4.
$r(t)$	A factor defined by Eq. 2.39.
$r_i(t)$	Entries in the vector corresponding to disturbance sequence in process model (c.f. Eq. 2.1).
$T$	Basic sampling time.
$\text{Tr}(P)$	Trace of matrix $P$ .
$U$	Upper-triangular matrix.
$u(t)$	Manipulated variable.
$v(t)$	Secondary output.
$w(t)$	Random and unmeasured load disturbance of zero mean and finite variance.
$\underline{x}(t)$	State vector.
$\bar{\underline{x}}(t)$	A state vector that is similar to $\underline{x}(t)$ (see Eq. A.12).
$x_i$	The $i$ th state of the system.
$\underline{Y}$	System output vector in Eq. A.5.
$y(t)$	Primary (controlled) output.
$z(t)$	White noise sequence.

### Greek

$\alpha$	Parameter used to reset the covariance matrix.
$\phi(t)$	Regressor vector.
$\Psi$	Observability matrix.
$\lambda$	Forgetting factor.
$\theta(t)$	Process model parameter vector.
$\Omega$	A nonsingular matrix which transforms one realization of a linear system to another "similar" realization.
$\xi_v$	Uncorrelated random sequence of zero mean and finite variance corresponding to secondary output (c.f. Eq. 2.2).
$\xi_y$	Uncorrelated random sequence of zero mean and finite variance corresponding to primary output (c.f. Eq. 2.2).
$\zeta$	Uncorrelated random sequence of zero mean and finite variance (c.f. Eq. 2.12).

### Subscripts

$y_e(t)$	Estimated value of $y(t)$ .
$\phi_e(t)$	Regressor vector using $y_e(t)$ instead of $y(t)$ .
$y_{nom}$	Nominal value of $y$ .
$y_{sca}$	Scaling factor of $y$ .



### Superscripts

$\hat{a}$	Estimated value of $a$ .
$\tilde{y}$	Scaled deviation value of $y$ .
$E'$	Matrix or vector $E$ obtained from using the secondary output $v'(t)$ (see Eq. A.13).
$E''$	Matrix or vector $E$ obtained from using the secondary output $v''(t)$ (see Eq. A.14).
$P^T$	Transpose of the matrix $P$ .

### Abbreviations

AIC	Adaptive inferential control.
AIE	Adaptive inferential estimation.
RLS	Recursive least squares.
SM-1	Simplified AIC algorithm using a first order plant model.
SM-2	Simplified AIC algorithm using a second order plant model.
ST-1	Standard AIC algorithm using a first order plant model.
TST-2	Truncated ST-1 standard AIC algorithm using two parameters for secondary output and for manipulated variable.

## **Chapter 1 : Introduction and Literature Survey**

### **1.1 Introduction**

In chemical process control, the control problems are often related to the control of product quality. A typical example is the control of product quality of distillation columns. Although the sensitivity, reliability and speed of response of on-line process analyzers, such as gas chromatographs, have been vastly improved in recent years, the use of an on-line analyzer for product quality control frequently introduces long time delay to the control systems, resulting in poor control performance. To circumvent this problem, considerable ingenuity has been expended on developing different ways to infer product compositions.

In addition to the problem of limited measurements of process outputs, the time-varying nature of most chemical processes often presents serious problems for conventional control strategies. In order to improve the control performance for processes which have nonlinear and/or time-varying characteristics and limited availability of process outputs, an adaptive scheme which can predict the process outputs at a rate faster than they are measured is required.

The objective of this thesis is to obtain a solution for the above problems. The work includes a systematic evaluation of the multirate adaptive inferential estimation (AIE) scheme proposed by Lu (1989). This scheme infers intersample values of the controlled output, which is sampled at a slower rate because of the long cycle time of an on-line analyzer, from a more rapidly measured secondary plant output. The work by Lu has provided a solid theoretical basis for multirate adaptive inferential estimation and control. However, it is still at its early stage of theoretical development

and the algorithm is only derived for linear systems. For industrial applications, the assumption of linear systems is usually violated. Since the assessment of the AIE scheme based on a rigorous mathematical approach is difficult so the validity of the AIE scheme for application in industrial processes has to be examined experimentally. Furthermore, Lu's scheme is proposed in a fundamental form which is essential to a theoretical study but not practical to the control of a real chemical process. Therefore, many additional issues must be addressed. For example, the robustness of the estimation scheme and some implementation details have to be considered. Only combined with a extensive study of these important issues can the multirate adaptive inferential estimation and control be an integral contribution to the ~~area~~ of process control.

To achieve the stated goal, the thesis includes a thorough study of the performance of the multirate adaptive inferential estimation and control strategy for control of distillation columns bottoms compositions. Linear and nonlinear process models were used in the simulation phase. The multirate scheme were further evaluated experimentally using a pilot scale binary distillation column. This systematic evaluation fills the gap between the theory and application aspects of the multirate adaptive inferential estimation technique and highlights the potential of immediate application of the AIE scheme to the control of an industrial chemical process.

In Chapter 1.2, a literature survey of previous studies related to inferential estimation using sampled plant outputs, with the emphasis on the topic of distillation column control, is presented. Distillation control has been the subject of academic and industrial research because of its key role in

many chemical processing industry. Excellent reviews of the distillation control field, covering the literature published in this area from 1970 to 1984, have been done by Tolliver and Waggoner (1980) and McAvoy and Wang (1985). The organization of this thesis will be outlined in Section 1.3.

## 1.2 Literature Survey

### 1.1.1 Non-adaptive Schemes for Inferring Process Outputs

For distillation column product quality control, probably the most commonly used technique is regulation of the temperature of a selected tray at an appropriate set point. The selection of the location of the control tray has been the subject of numerous papers. Rademaker *et al.* (1975) presented a well-organized summary of the various criteria proposed over the years. Most criteria proposed before 1970 are based on steady state information (e.g. Wood, 1968). In these approaches, the steady state temperature profile is plotted and a tray liquid temperature is in the region where the temperature is changing fairly rapidly from tray to tray is selected (Desphande, 1985; Buckley *et al.*, 1985). Other authors (e.g. Rademaker *et al.*, 1975; Shinsky, 1984) disagree with this approach and suggest that dynamic considerations are also important. In addition to the problem of control tray selection, single tray temperature feedback control will generally result in offset because maintaining a constant tray temperature does not necessarily result in constant product composition when there is a feed disturbance, as shown experimentally by Pakte *et al.* (1982). As pointed out by Luyben (1969), controlling an intermediate tray temperature is usually unsatisfactory for columns separating close-boiling products since control over a very narrow temperature range is required.

Furthermore, pressure variations, which are quite common in practice, can reverse the effects of composition changes on temperatures changes.

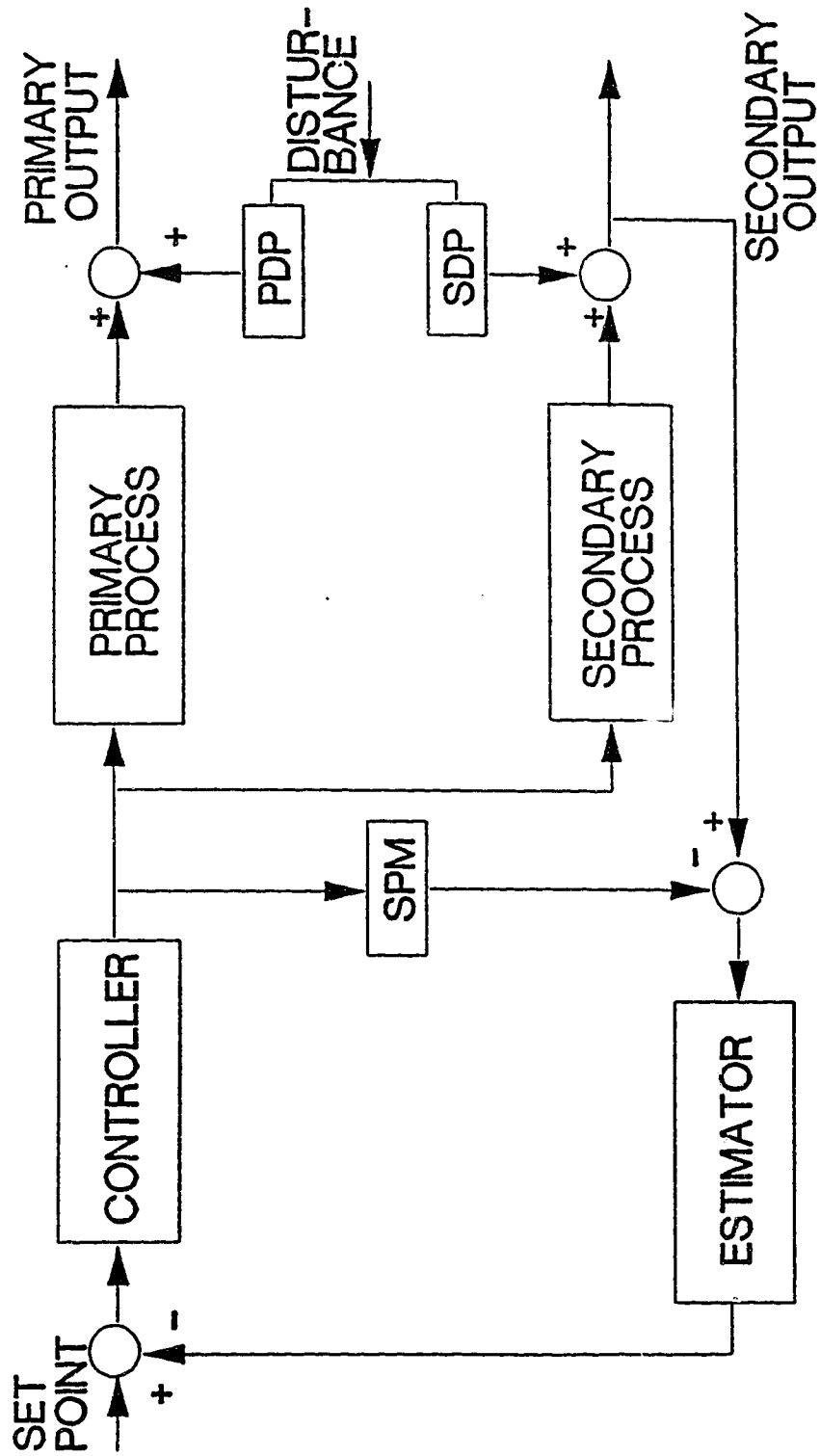
Besides single tray temperature feedback control, various heuristic schemes have also been proposed to regulate product compositions of distillation columns. To avoid pressure effects, a popular technique is to control a differential temperature ( $\Delta T$ ). In this scheme, the difference between two temperatures on two trays in the same section of the column is controlled. As pointed out by Webber (1959), some potential problems can arise as a result of using the  $\Delta T$  control strategy. Firstly, the relationship between  $\Delta T$  and product composition is not monotonic. Thus, the controller action had to be reversed for desired values of composition that were on different sides of the extremum point on the  $\Delta T$  versus composition plot. Secondly, feed composition disturbances in the heavy components caused poor control performance.

Luyben (1969) proposed a double differential temperature control scheme for distillation column control. The basic idea is to measure and control the difference between two temperature differentials. However, the procedure for selecting two appropriate temperature differentials is quite complex. The simulation results presented by Luyben (1969) showed very little improvement in control performance compared with that achieved by the  $\Delta T$  and single temperature feedback control schemes.

Yu and Luyben (1984) suggested the use of multiple temperature for the control of multicomponent distillation columns. The two schemes presented were the temperature/differential temperature (TDT) and the temperature/dual differential temperature ( $TD^2T$ ) schemes. The TDT control structure used a temperature differential to reset the set point of the temperature

controller of an "optimal" single temperature control tray. However, this technique did not work satisfactorily for feed composition changes in key components (light key and heavy key). In the TD<sup>2</sup>T control scheme, two temperature differentials were used to adjust the set point of the temperature controller of a properly selected tray. Simulation results showed that TD<sup>2</sup>T control performed well for different feed composition changes. Nevertheless, this scheme required a significant amount of design effort and the applicability seemed very case-dependent. Moreover, the TD<sup>2</sup>T control scheme could not handle disturbances in feed flow rate (Yu and Luyben, 1984) so the potential of this scheme for practical applications is very limited.

Brosilow and co-workers (Joseph and Brosilow, 1978a, 1978b; Brosilow and Tong, 1978) proposed a more complicated control algorithm called *inferential control*. This algorithm uses available secondary measurements to minimize the steady state error of a least squares based estimator, and the selected measurements are used to infer and counteract the effect of the unmeasured disturbances on the primary (controlled) process output, as shown in Fig. 1.1. Methods for optimal selection of secondary measurements for state estimation have been suggested by Joseph and Brosilow (1978a, 1978b) and were further refined by Morari and Stephanopoulos (1980a, 1980b). As may be expected, the performance of this inferential control strategy depends heavily on the accuracy of the secondary process model. As well, in order to improve the transient response of the estimator, heuristically derived lead-lag elements should be incorporated into the inferential control framework. As may be expected, since most chemical processes are nonlinear and often time-varying in nature, the changing dynamic



**PDP : PRIMARY DISTURBANCE PROCESS**  
**SDP : SECONDARY DISTURBANCE PROCESS**  
**SPM : SECONDARY PROCESS MODEL**

Figure 1.1 The Inferential Control Scheme (Using Secondary Outputs)

characteristics of the process can easily degrade the performance of an inferential control system that has been designed on the basis of a particular process model. A comparative study of the performance of the inferential control system with the conventional feedback control system has been performed experimentally (Pakte *et al.*, 1982). Although all results showed that the inferential control strategy was superior to a conventional feedback control scheme in rejecting unmeasured load disturbance, steady state offset was found to be a potential problem with the inferential control system (Pakte *et al.*, 1982) because of the nonlinear and time-varying behavior of the process. Another shortcoming of this inferential control scheme is the requirement that all the gains and approximate time constants that relate the primary and secondary outputs to all plant disturbances and manipulated variables be known for a particular operating condition.

The concept on which this inferential control system is based has been extended by Garcia and Morari (1982), Morari (1983) and by Parrish and Brosilow (1985) to develop an inferential control system which only uses the measurement of the primary output to infer the effect of disturbances on process output. This type of control was designated as "internal model control" by Garcia and Morari (1982). In this scheme, the effect of the manipulated variable on the primary process model (i.e. the primary process model output) is subtracted from the measured primary output. If the primary process model is perfect, the feedback signal to the controller will be due to the disturbance only. Thus, the controller can be designed and tuned to eliminate the effect of the disturbance on the primary output. The main disadvantage of using this internal model controller is that its



performance depends heavily on the accuracy of the process model as well as the on-line tuning. Parrish and Brosilow (1985) proposed some heuristic rules for on-line tuning of the controller parameters. Their simulation results showed that superior performance could be obtained using the inferential control strategy compared with that achieved by using conventional PID control. Parrish and Brosilow (1988) extended their inferential control scheme for application to control of a nonlinear process. Results from two illustrative examples, a laboratory heat exchanger and a simulated neutralization process, are presented. Their results indicated that a substantial improvement in control was possible using the nonlinear inferential controller.

None of the inferential control strategies reviewed in the preceding material employed measurement of the primary output at long sample intervals in conjunction with simultaneous frequent measurement of a secondary output. It is this type of strategy that is considered in this work. This approach, as explained in the material presented in Chapter 2, is different from a scheme proposed by Luyben (1973). Luyben's strategy involved the use of a parallel cascade control scheme which used measurement of a primary output in a controller to vary the set point of a secondary output controller. Although this approach eliminates steady state offset, the transient response is often poor (Pakte *et al.*, 1982) because the set point of the secondary output controller can only be changed when an infrequent measurement of the primary output is available.

### 1.2.2 Adaptive Schemes for Inferring Process Outputs

Conventional control strategies do not always provide satisfactory

control performance because no adaptive features are incorporated to handle nonlinear and/or time-varying behaviors of most processes. In recent years, there has been extensive research activity in adaptive control systems. In this work, adaptive control systems are defined as those systems which adjust the parameters of their plant models and/or controllers to compensate for changes in the process or the environment. There has been extensive interest in the adaptive control systems in the last decade because of the breakthroughs in microelectronics that have made it possible and economical to implement adaptive controllers for practical applications. An excellent survey of adaptive control strategies for process control has been included in Seborg *et al.* (1986). Although this survey article emphasizes fundamental concepts and alternative controller design strategies, potential operating problems associated with some adaptive control schemes as well as a critical review of recursive parameter estimation techniques are also presented.

Some adaptive controllers or estimators have been formulated to control the infrequently sampled plant outputs at a faster rate. Söderström (1980) developed, for first-order plant models, several minimum variance controllers which enable the manipulated input to be adjusted during the intersample interval of the plant output. Scattolini (1988) proposed a multi-input multi-output self-tuning control algorithm for processes with infrequent and delayed output sampling. Although the simulation results demonstrate the satisfactory performance of this control algorithm, no comparative results are presented. Recently, Lu and Fisher (1989) derived a multirate adaptive estimation scheme which can be employed to predict the infrequently sampled output at a faster rate, the rate at which corrective

changes of the manipulated variable can be introduced. Convergence and stability properties are also proved for open loop operation. This idea has been extended to obtain a servo control law with input constraints (Lu *et al.*, 1989) with simulation examples demonstrating the excellent performance of the multirate estimation schemes.

The adaptive algorithms reviewed above do not make use of the dynamic information available from other (secondary) plant outputs. It may be advantageous to use the primary and secondary plant outputs simultaneously to improve control performance. Shen and Lee (1989) modified the inferential control scheme of Brosilow and co-workers (Joseph and Brosilow, 1978a, 1978b; Brosilow and Tong, 1978) to obtain an adaptive inferential control algorithm for controlling processes with intermittent measurements of the controlled output. In this adaptive scheme, shown in Fig. 1.2, frequent measurements of the secondary process output are used to update the secondary process model on-line and estimate the effect of any load disturbance. The parameters of the inferential controller are adapted using infrequent measurements of the process output. The controller design is based on a discrete inverse convolution model (Shen and Lee, 1985 and 1988) which is a stable approximation of the inverse of the primary process model. Simulation results indicated that this adaptive inferential control system provided improvement over conventional PID and inferential control in the presence of unmeasured load disturbances and variations in process characteristics. However, it is doubtful if this scheme can provide satisfactory control performance in practice because two process models have to be identified recursively on-line and the number of parameters that need to be estimated will be large for a process with long analyzer cycle time.

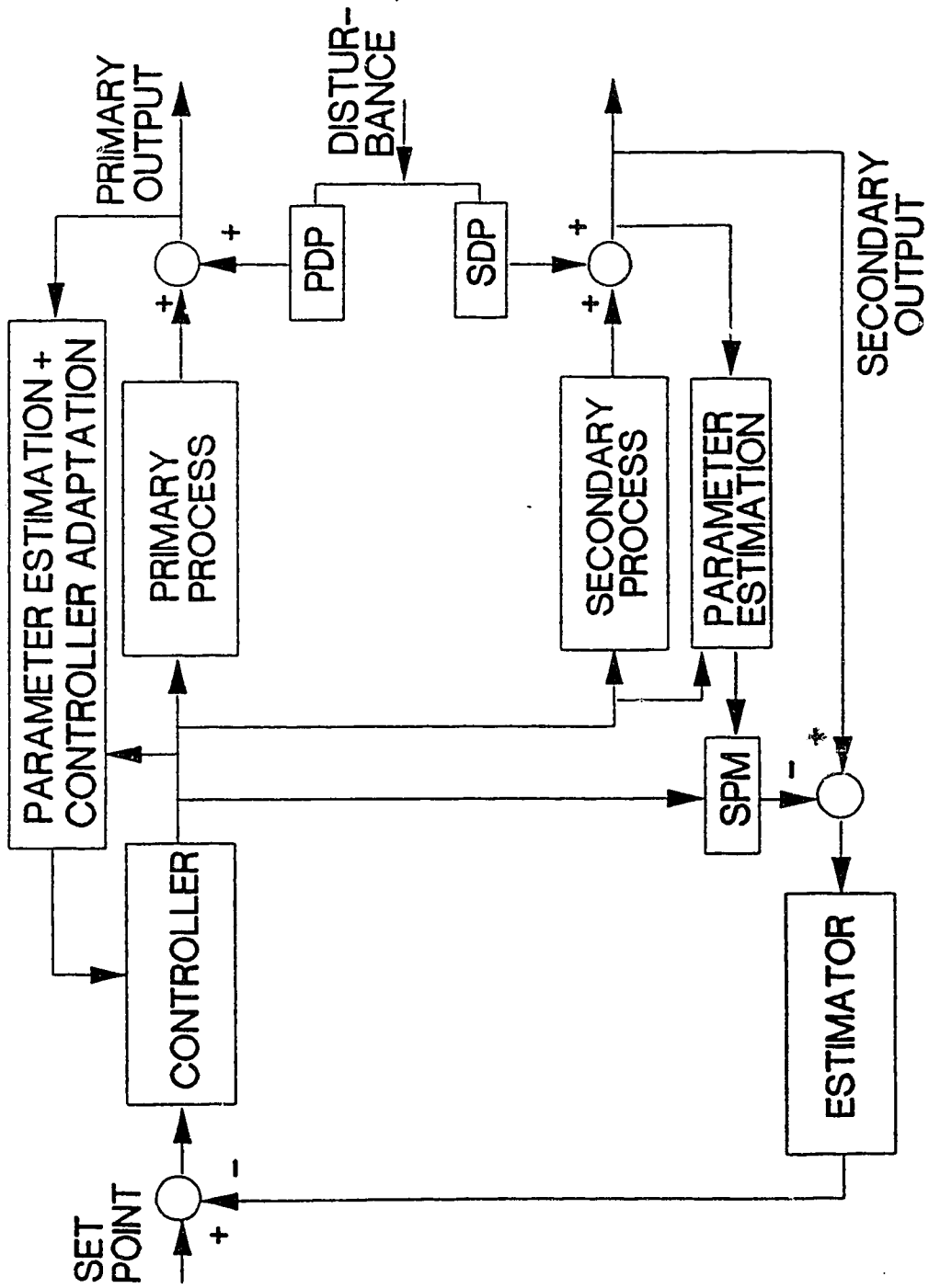


Figure 1.2 The Adaptive Inferential Control Scheme of Shen and Lee (1989)

Guilandoust *et al.* (1987, 1988a, 1988b) recently proposed two multirate adaptive inferential estimators for inferring infrequently measured process output from other more rapidly sampled secondary output. One estimator is derived from a state-space model of the process while the other is based upon an input-output representation of the plant. These adaptive estimation techniques require minimal design effort compared with the non-adaptive inferential control scheme. Estimates of the controlled output are generated at the fast rate at which the secondary output is measured and these estimates can then be used with either a fixed parameter controller or an adaptive controller to regulate the controlled output. Since the parameters of the estimator models can be updated on-line, the proposed algorithms are able to cope with slow time-varying process dynamics. Their results obtained from simulation and industrial evaluation indicate the potential of their schemes for practical applications. However, as pointed out by Lu (1989), several very restrictive assumptions were employed when Guilandoust *et al.* (1987, 1988a, 1988b) derived the control algorithms. In their state-space formulation, complete observability of the process from a secondary output is required, a condition which is not common in practice. When they derived the working equation from an input-output relation, two process models were assumed, one for the controlled output,  $y(t)$ , and one for the secondary output,  $v(t)$ . However, in order to obtain a working equation which related  $y(t)$  to  $v(t)$  and the manipulated variable  $u(t)$ , the same stationary random load disturbance vector must be present in both models. In other words, the link of  $y(t)$  to  $v(t)$  and  $u(t)$  is only via the external white noise disturbance and so the working equation is theoretically not applicable when there are no disturbances.

Lu (1989) has formulated two similar multirate adaptive inferential schemes in a more formal manner. His work has a sound theoretical foundation and the restrictive assumptions used by Guilandoust *et al.* (1987, 1988a, 1988b) are not required. It is the objective of this research to evaluate, by simulation and experimental testing, the multirate adaptive inferential algorithms of Lu (1989). The basis of comparison is the control performance that is achieved by a conventional feedback PI control scheme.

### 1.3 Thesis Organization

The multirate adaptive inferential estimation schemes proposed by Lu (1989) are derived in Chapter 2. This chapter also describes the recursive least squares identification algorithms used in this work. Some issues concerning the practical applications of the adaptive schemes are also discussed in this chapter.

In Chapter 3, the control performance of the adaptive inferential control (AIC) schemes is studied by simulation using a transfer function model of a binary distillation column. The control behavior is assessed by computing the integral of absolute error (IAE) values for changes in feed rate, reflux rate, and set point. The robustness of the AIC schemes is tested by changing the parameters in the transfer function model.

Chapter 4 is devoted to a evaluation of the control performance of the AIC schemes when they are employed to control the bottoms composition of a simulated multicomponent distillation column. The simulations are performed using a general purpose multicomponent distillation column simulator, DYCONDIST (Carling and Wood, 1986). The column model used in this simulator and the depropanizer tower specifications are also described.

Chapter 5 presents experimental results obtained when the AIC schemes are applied to control the bottoms composition of a pilot scale binary distillation column. The control performance of the AIC schemes are compared to that achieved using a conventional proportional plus integral feedback controller.

Chapter 6 summarizes conclusions from this study and presents recommendations for future work.

## **Chapter 2 : Development of the Multirate Adaptive Inferential Estimation Algorithms**

### **2.1 Introduction**

The multirate adaptive inferential estimation (AIE) algorithm that is the focus of this work is derived in Section 2.2. The derivation concentrates on the development of the equations that form the basis for the multirate AIE strategy. The output convergence properties have been considered in detail by Lu (1989) and will not be repeated here. In addition to the standard and simplified algorithms presented by Lu (1989), another simplified version of the standard scheme, designated as the truncated standard algorithm, is also described in the next section.

In Section 2.3, the underlying theoretical basis for the basic recursive least squares (RLS) identification algorithm is presented. Three variants of this basic RLS method used in this work are also outlined.

For practical application of the multirate AIE strategy, in common with other advanced computer control techniques, some precaution is required. In this work, it is suggested that a dead-band be employed. The definition of this dead-band can be found in Section 2.4.

### **2.2 Derivation of the Multirate Adaptive Inferential Estimation Scheme**

The multirate adaptive inferential estimation and control scheme evaluated in this study is shown in block diagram form in Fig. 2.1. This scheme, first proposed by Guilandoust *et al.* (1985, 1987, 1988) used an algorithm based on either a state space or on an input-output approach. Their governing equations, although original and practical, were based on some very restrictive assumptions. For example, the process must be



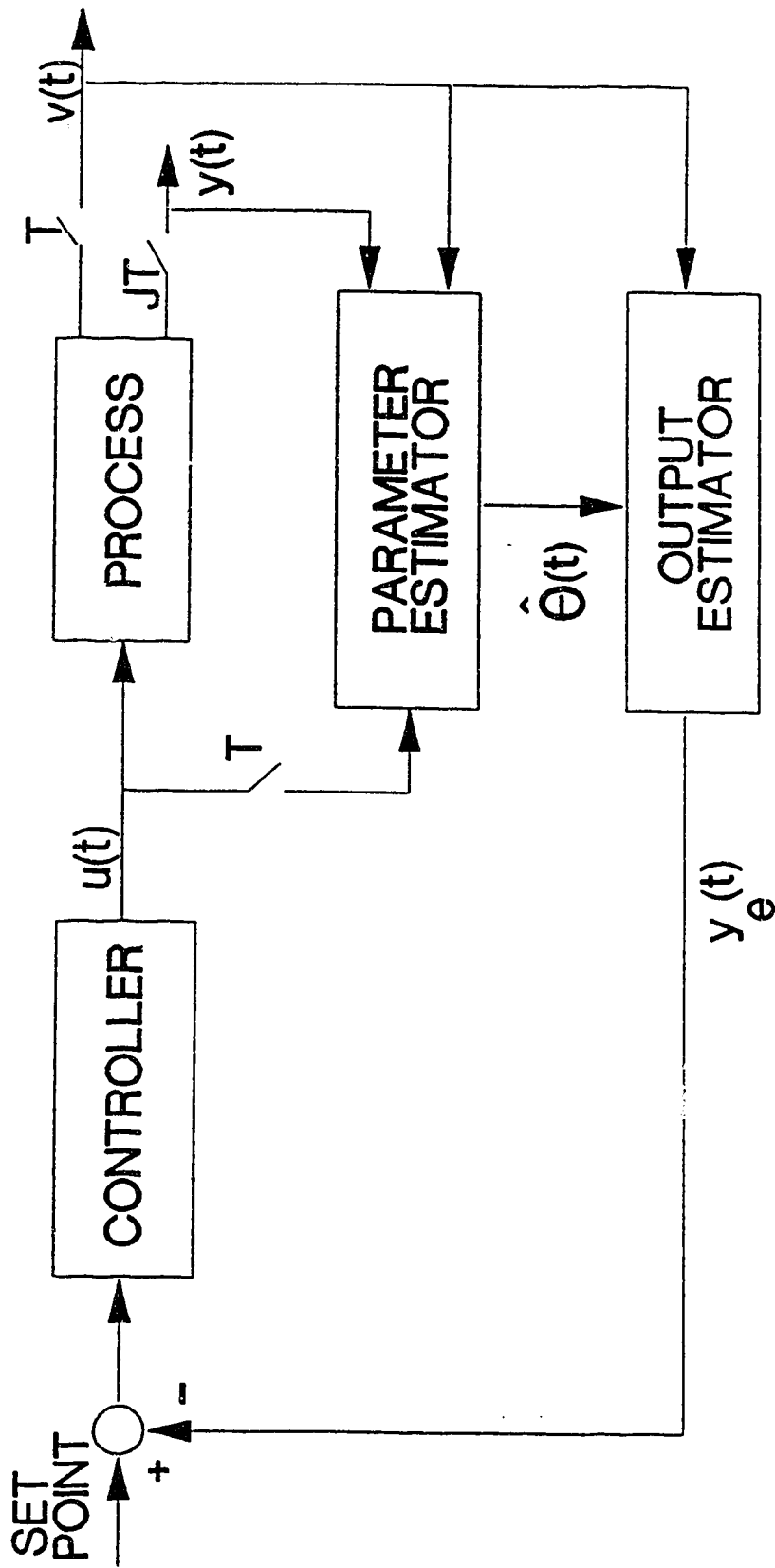


Figure 2.1 Multirate Adaptive Inferential Feedback Control Scheme with a Fixed Parameter Controller

completely observable from the secondary output when the state space model is used. A detailed discussion of these restrictive assumptions can be found in Lu (1989).

### 2.2.1 Plant Model

The adaptive inferential strategy is based on the assumption that the primary controlled output,  $y(t)$ , is sampled every  $JT$  time units while the measured value of the secondary output,  $v(t)$ , is available every  $T$  time units. The manipulated variable,  $u(t)$ , is changed at the basic sampling time  $T$ . Assuming that the process is completely observable from  $v(t)$  and  $y(t)$  and for  $T$  taken as the unit time, it follows from the theory of linear systems (Wolovich, 1974) that the system can be represented by

$$\underline{x}(t+1) = \begin{bmatrix} 0 & \dots & 0 & -a_1 & 0 & \dots & 0 & -\bar{a}_1 \\ & & I_{nv-1} & \vdots & \vdots & & \vdots & \vdots \\ & & & -a_{nv} & 0 & \dots & 0 & -\bar{a}_{nv} \\ 0 & \dots & 0 & -a_{nv+1} & 0 & \dots & 0 & -\bar{a}_{nv+1} \\ \vdots & & \vdots & \vdots & & & \vdots & \\ 0 & \dots & 0 & -a_n & & & I_{ny-1} & -\bar{a}_n \end{bmatrix} \underline{x}(t) + \begin{bmatrix} b_1 \\ \vdots \\ b_{nv} \\ b_{nv+1} \\ \vdots \\ b_n \end{bmatrix} u(t) + [r_1 \quad \dots \quad r_{nv} \quad r_{nv+1} \quad \dots \quad r_n]^T w(t) \quad (2.1)$$

$$v(t) = x_{nv}(t) + \xi_v(t) \quad (2.2)$$

$$y(t) = hx_{nv}(t) + x_n(t) + \xi_y(t) \quad (2.3)$$

where

$w(t)$ ,  $\xi_v(t)$  and  $\xi_y(t)$  = independent random Gaussian sequences with zero mean and finite variance

$nv$  = the observability index of  $v(t)$

$n$  = the order of the process

$\underline{x}(t)$  = the state vector

$ny = n - nv$ .

(NOTE : The implication of the observability index is discussed in Appendix A.)

The time delay between  $u$  and  $y$  will be considered later. By successive substitution, it can be shown that the input-output relation from  $u(t)$ ,  $v(t)$  and  $w(t)$  to  $y(t)$  is

$$\begin{aligned} A(q^{-1})[y(t) - hv(t) + h\xi_v(t) - \xi_y(t)] = \\ B(q^{-1})u(t) + \bar{C}(q^{-1})v(t) + R(q^{-1})w(t) \end{aligned} \quad (2.4)$$

where

$$A(q^{-1}) = 1 + \bar{a}_1 q^{-1} + \bar{a}_2 q^{-2} + \dots + \bar{a}_{nv+1} q^{-ny} \quad (2.5)$$

$$B(q^{-1}) = b_n q^{-1} + b_{n-1} q^{-2} + \dots + b_{nv+1} q^{-ny} \quad (2.6)$$

$$\bar{C}(q^{-1}) = -a_n q^{-1} - a_{n-1} q^{-2} - \dots - a_{nv+1} q^{-ny} \quad (2.7)$$

$$R(q^{-1}) = r_n q^{-1} + r_{n-1} q^{-2} + \dots + r_{nv+1} q^{-ny} \quad (2.8)$$

Eq. 2.4 can be rewritten as

$$\begin{aligned} A(q^{-1})y(t) = B(q^{-1})u(t) + C(q^{-1})v(t) + D(q^{-1})\xi_y(t) \\ + \bar{D}(q^{-1})\zeta(t) \end{aligned} \quad (2.9)$$

where

$$\begin{aligned}
C(q^{-1}) &= \bar{C}(q^{-1}) + hA(q^{-1}) & (2.10) \\
&= c_0 + c_1 q^{-1} + c_2 q^{-2} + \dots + c_{ny} q^{-ny}
\end{aligned}$$

$$D(q^{-1}) = hA(q^{-1}) = d_0 + d_1 q^{-1} + d_2 q^{-2} + \dots + d_{ny} q^{-ny} \quad (2.11)$$

$$\bar{D}(q^{-1})\zeta(t) = R(q^{-1})w(t) - hA(q^{-1})\xi_V(t) \quad (2.12)$$

Applying the spectral factorization principle (Åström, 1970), the last two terms of Eq. 2.9 can be replaced by  $E(q^{-1})z(t)$  where  $E(q^{-1})$  is defined by

$$E(q^{-1}) = e_0 + e_1 q^{-1} + e_2 q^{-2} + \dots + e_{ny} q^{-ny} \quad (2.13)$$

and  $z(t)$  is white noise with finite variance so Eq. 2.9 becomes

$$A(q^{-1})y(t) = B(q^{-1})u(t) + C(q^{-1})v(t) + E(q^{-1})z(t) \quad (2.14)$$

For the roots of  $A(q^{-1})$  designated as  $\alpha_i$  ( $i = 1, \dots, ny$ ), multiplication of both sides of Eq. 2.14 by the polynomial

$$\prod_{i=1}^{ny} \left[ 1 + (\alpha_i q)^{-1} + (\alpha_i q)^{-2} + \dots + (\alpha_i q)^{2-J} + (\alpha_i q)^{1-J} \right] \quad (2.15)$$

yields, as can be shown by mathematical induction (Lu, 1989),

$$A_J(q^{-J})y(t) = B_J(q^{-1})u(t) + C_J(q^{-1})v(t) + E_J(q^{-1})z(t) \quad (2.16)$$

where

$$A_J(q^{-J}) = 1 + a_{J1} q^{-J} + a_{J2} q^{-2J} + \dots + a_{Jny} q^{-Jny} \quad (2.17)$$

$$B_J(q^{-1}) = b_{J1} q^{-1} + b_{J2} q^{-2} + \dots + b_{JN} q^{-N} \quad (2.18)$$

$$C_J(q^{-1}) = c_{J0} + c_{J1} q^{-1} + \dots + c_{JN} q^{-N} \quad (2.19)$$

$$E_J(q^{-1}) = e_{J0} + e_{J1} q^{-1} + \dots + e_{JN} q^{-N} \quad (2.20)$$

for  $N = J \times ny$

Eqs. 2.16 to 2.20 form the basis for the multirate adaptive inferential

estimation and prediction algorithms evaluated in this work. It should be noted that in Eq. 2.16, the value of  $y(t)$  is required only every "J" sampling intervals instead of every sampling interval. For simplicity of notation, the "J" subscript is dropped,  $ny$  is replaced by  $n$  and  $JN$  is denoted by  $M$ . If there is a time delay of  $d$  between  $u$  and  $y$ , Eqs. 2.16 to 2.20 can be rewritten as

$$A(q^{-J})y(t) = B(q^{-1})u(t-d) + C(q^{-1})v(t-d) + E(q^{-1})z(t) \quad (2.21)$$

where

$$A(q^{-J}) = 1 + a_1q^{-J} + a_2q^{-2J} + \dots + a_nq^{-Jn} \quad (2.22)$$

$$B(q^{-1}) = b_1q^{-1} + b_2q^{-2} + \dots + b_Mq^{-M} \quad (2.23)$$

$$C(q^{-1}) = c_0 + c_1q^{-1} + c_2q^{-2} + \dots + c_Mq^{-M} \quad (2.24)$$

$$E(q^{-1}) = e_0 + e_1q^{-1} + e_2q^{-2} + \dots + e_Mq^{-M} \quad (2.25)$$

### 2.2.2 The Standard Algorithm

The standard algorithm formulated by Lu (1989) involves identification of the system parameters, whenever the measurement  $y(t)$  is available, using

$$y(t) = \phi_e(t-1)\hat{\theta}(t) \quad (2.26)$$

where

$$\phi_e(t-1) = [-y_e(t-J) \quad -y_e(t-2J) \quad \dots \quad -y_e(t-nJ) \quad (2.27)$$

$$u(t-1-d) \quad u(t-2-d) \quad \dots \quad u(t-d-M)$$

$$v(t-d) \quad v(t-1-d) \quad \dots \quad v(t-d-M)]$$

$$\hat{\theta}(t) = [\hat{a}_1(t) \quad \hat{a}_2(t) \quad \dots \quad \hat{a}_n(t) \quad (2.28)$$

$$\hat{b}_1(t) \quad \hat{b}_2(t) \quad \dots \quad \hat{b}_M(t)$$

$$\hat{c}_0(t) \quad \hat{c}_1(t) \quad \dots \quad \hat{c}_M(t)]^T$$

where  $y_e(t)$  is the predicted value of  $y(t)$  and " $\hat{\phantom{x}}$ " represents estimated value.

If a measurement of  $y(t)$  is available at time  $t$ , after updating the regressor vector (Eq. 2.27) using stored values of  $y_e$ ,  $u$  and  $v$ , the parameters in Eq. 2.28 can be estimated using an identification algorithm (e.g. a recursive least squares algorithm as used in this study). Use of the values of  $y_e$  instead of  $y$  in the regressor equation, Eq. 2.27, is the result of employing the output error method for parameter estimation (Lu, 1989; Goodwin and Sin, 1984). Although  $y(t-J)$ ,  $y(t-2J)$ , ... etc can be used in Eq. 2.27, these actual measurements are not used in the regressor because for the period  $t$  to  $t+J$ , the estimated values must be used to perform intersample predictions of  $y$  since  $y$  is available only every  $J$  sample intervals. Thus, for consistency,  $y_e(t-J)$ ,  $y_e(t-2J)$ , ... and  $y_e(t-nJ)$  are used in Eq. 2.27.

During the period from  $t$  to  $t+J$ , the estimated parameters can be used for the  $k$ -step ahead prediction of  $y$ , that is  $y_e(t+k)$ , using

$$y_e(t+k) = \phi_e(t-1+k)\hat{\theta}(t) \quad (2.29)$$

For the  $J$ -step ahead prediction, the number of unknown parameters is  $n(2J+1)+1$  and so for a first order plant model ( $n=1$ ) and  $J=5$ , 12 parameters ( $\hat{a}_1, \hat{b}_1, \dots, \hat{b}_5, \hat{c}_0, \dots, \hat{c}_5$ ) must be identified.

### 2.2.3 The Simplified Algorithm

A possible difficulty that may arise when the standard algorithm is applied to nonlinear and/or time-varying processes is the speed of parameter convergence due to the large number of parameters that must be identified.

When the standard algorithm is used with a first order plant model, an increase in  $J$  from 5 to 10 will require that 22 parameters be estimated instead of 12. A simplification of the estimation equations, Eqs. 2.26 to 2.28, to overcome this situation by reducing the number of  $\hat{b}_i$  and  $\hat{c}_i$  parameters to be identified has been suggested by Lu (1989). The extreme case presented by Lu (1989) is to set  $\hat{b}_{i+1}(t) = \hat{c}_i(t) = 0$  for  $i \neq 0, J, 2J, \dots, (n-1)J$  and so the number of parameters to be estimated is only  $3n$  and independent of  $J$ . In general, decreasing the number of parameters of the standard algorithm will increase the plant model mismatch. However, as pointed out by Lu (1989), the simplified algorithm can achieve exact model match (if  $\hat{c}_{nJ}$  is not set to zero and is included in the parameter estimate vector) at output sampling interval when there are no disturbances ( $E(q^{-1})z(t) = 0$  in Eq. 2.21) and the manipulated variable,  $u$ , is kept constant within the slower sampling interval (i.e. from time  $t$  to  $t+J$ ). For a nonlinear and/or time-varying system, where an exact plant model match is impossible even if the standard algorithm is employed, reducing the number of parameters to be identified will improve the numerical conditioning of the estimation algorithm, thus resulting in better overall control performance. It may be readily realized that during normal steady states operation and  $y$  is under conventional PI control,  $u$  and  $v$  are constant (except for process noises) within the slower sampling interval. Then, if no excitation signal is added into  $u$  during off-line identification, using the simplified algorithm may be better since the measurements of  $u$  and  $v$  within the slower sampling interval are not included in the regressor vector. Consequently, better initial parameter estimates can be obtained for the simplified algorithm.

Use of a first order plant model for this simplified scheme requires the estimation of only three parameters ( $\hat{a}_1$ ,  $\hat{b}_1$  and  $\hat{c}_0$ ) while the use of a second order model will involve identification of six parameters ( $\hat{a}_1$ ,  $\hat{a}_2$ ,  $\hat{b}_1$ ,  $\hat{b}_2$ ,  $\hat{c}_0$  and  $\hat{c}_5$ ). The performance that can be achieved for control of a linear and a nonlinear system using these algorithms with first and second order plant models has been investigated by simulation in this work. Experimental evaluation, involving the control of bottoms composition of a pilot scale binary distillation column, will be also presented.

#### 2.2.4 The Truncated Standard Algorithm

The simplified algorithm suggested by Lu (1989), to reduce the number of  $\hat{b}$  and  $\hat{c}$  parameters that must be estimated, represents an extreme simplification. Different techniques for reducing the number of unknown model parameters of the standard algorithm may be required depending on the application. Another approach to reduce the number of parameters to be estimated is to truncate the standard algorithm. This form of algorithm, designated as truncated standard algorithm, is presented here as one possible approach. Use of a first order model with the standard algorithm would involve identification of  $\hat{b}_1, \dots, \hat{b}_5$  and  $\hat{c}_0, \dots, \hat{c}_5$ . The effectiveness of the suggested truncated scheme, which involves setting  $\hat{b}_3, \hat{b}_4, \hat{b}_5$  and  $\hat{c}_2, \dots, \hat{c}_5$  to 0, is examined by simulation for control of a nonlinear system (c.f. Chapter 4).

### 2.3 Recursive Least Squares Identification Algorithms

The on-line estimation of unknown process and/or controller parameters is a crucial part of adaptive control scheme. Many books dealing with



identification methods have been published over the years (Graupe, 1976; Hsia, 1977; Ljung and Söderström, 1982; Goodwin and Sin, 1984; Ljung, 1987). Probably the most popular parametric identification method used in adaptive control is the recursive least squares (RLS) algorithm. Three variants of the basic RLS estimator used in this work will be briefly described.

### 2.3.1 Recursive Least Squares with Exponential Data Weighting

Assuming that the system to be identified is described by the following linear discrete model

$$y(t) = \phi^T(t)\theta(t) \quad (2.30)$$

where

$$\phi(t) = [y(t-1), y(t-2), \dots, u(t-1), u(t-2), \dots]^T \quad (2.31)$$

$$\theta^T(t) = [a_1, a_2, \dots, b_0, b_1, \dots] \quad (2.32)$$

The basic RLS method is the result of minimization of a quadratic cost function of the prediction error,  $e(t)$ , of the form (Ljung and Söderström, 1983)

$$J_K(\theta) = \frac{1}{K} \sum_{t=1}^K \lambda^{K-t} e(t)^2 = \frac{1}{K} \sum_{t=1}^K \lambda^{K-t} (y(t) - \phi^T(t)\hat{\theta}(t))^2 \quad (2.33)$$

The RLS parameter estimation law is given by the following equations :

Parameter vector update :

$$\hat{\theta}(t) = \hat{\theta}(t-1) + K(t) [y(t) - \hat{\theta}^T(t-1)\phi(t)] \quad (2.34)$$

Kalman gain vector update :

$$K(t) = \frac{P(t-1)\phi(t)}{\lambda + \phi^T(t)P(t-1)\phi(t)} \quad (2.35)$$

Covariance matrix update :

$$P(t) = \left[ P(t-1) - \frac{P(t-1)\phi(t)\phi^T(t-1)P(t-1)}{\lambda + \phi^T(t)P(t-1)\phi(t)} \right] \frac{1}{\lambda} \quad (2.36)$$

For the basic RLS algorithm,  $\lambda$ , the exponential forgetting factor, equals 1. A difficulty that may arise when the basic RLS algorithm is employed is that the algorithm does not retain its adaptivity (Goodwin and Sin, 1984). To retain the alertness of a RLS algorithm, a "forgetting" or discounting factor,  $\lambda$  ( $0 < \lambda < 1$ ), is employed in Eqs. 2.34 to 2.36. To improve numerical conditioning, the factorization algorithm of Bierman (1976) is employed.

This method is based on factorization of  $P$  into

$$P = U D U^T \quad (2.37)$$

where  $D$  and  $U$  are respectively diagonal and an upper-triangular matrices. A PASCAL subroutine for RLS estimation using the U-D factorization algorithm can be found in Åström and Wittenmark (1984). A FORTRAN version of this code, developed by Vermeer (1987), has been utilized in simulation of the control behavior of a linear system (c.f. Chapter 3).

### 2.3.2 Recursive Least Squares with Constant Trace Covariance Matrix through a Variable Forgetting Factor

Using a fixed forgetting factor in conjunction with the basic RLS algorithm works well only if the process has sufficient excitation; otherwise, exponential data forgetting will lead to covariance "blow-up" (Goodwin and Sin, 1984). In a recent paper, Sripada and Fisher (1987) have proposed four modifications to the basic least squares algorithm. One of the proposed modifications is to use a variable forgetting factor which will keep the trace of the covariance matrix,  $P(t)$ , constant. This technique has been used in the identification algorithm for the simulation of the control of a nonlinear multicomponent distillation column (c.f. Chapter 4). The

update equations for the parameter vector, Kalman gain vector and covariance matrix are as expressed by Eqs. 2.34 to 2.36 with the value of the variable forgetting factor,  $\lambda(t)$ , to keep the trace of P constant calculated by the expression

$$\lambda(t) = 1 - \left[ r(t) - \{r(t)^2 - \frac{4 \|\mathbf{P}(t-1)\phi(t)\|^2}{\text{tr } \mathbf{P}(t-1)}\}^{1/2} \right] \frac{1}{2} \quad (2.38)$$

where

$$\begin{aligned} \text{tr } \mathbf{P}(t-1) &= \text{the trace of } \mathbf{P}(t-1) \\ r(t) &= 1 + \phi(t)\mathbf{P}(t-1)\phi(t) \end{aligned} \quad (2.39)$$

### 2.3.3 Recursive Least Squares with Exponential Data Weighting and Covariance Resetting

The RLS algorithm with a fixed forgetting factor discussed in Section 2.3.1 is easy to implement and use because of its simplicity. However, several authors have suggested that it is advantageous to incorporate covariance resetting (Goodwin and Sin, 1984) into a RLS algorithm to improve numerical conditioning (Goodwin and Sin, 1984; Vermeer *et al.*, 1988) for practical applications. Therefore, a fixed forgetting factor and covariance resetting options have been incorporated into the RLS algorithm utilized in the experimental evaluation (c.f. Chapter 5) The covariance matrix, P, is reset to  $\alpha^*I$ , where I is the identity matrix and  $\alpha$  is a user specified constant, whenever the trace of P drops below a user specified value, i.e.

$$\mathbf{P}(t) = \alpha^*I \quad \text{if } \text{tr } \mathbf{P}(t-1) < P_{\min} \quad (2.40)$$

### 2.4 Adaptive Inferential Control Using a Dead-band

As can be readily appreciated, the prediction of the controlled output,

$y_e(t)$ , will not be reliable during the initial stage of adaptation following a disturbance. Since the parameters can only be updated at the cycle time of the analyzer and the adaptive inferential control (AIC) scheme utilizes the value of  $y_e(t)$  for the control calculation, it is appropriate to incorporate a dead-band into the AIC algorithm so that the controller output will not be calculated using an unreliable value of  $y_e(t)$ . The dead-band (DB) employed in this work is defined by

$$DB = \frac{|y(t) - y_e(t)|}{y(t)} \times 100 \% \quad (2.41)$$

When a measurement of  $y(t)$  is available, the accuracy of  $y_e(t)$  is checked by calculating a value of DB using Eq. 2.40. If the calculated DB is larger than a specified value, the AIC algorithm is "switched off" and the process will be controlled using a conventional fixed parameter PI control algorithm. The AIC algorithm will be "switched on" when DB is less than the specified value. This "safety check" method is better than the approach of restricting the change in  $u(t)$ , the manipulated variable, because there is no measure of the accuracy of the predicted value of  $y(t)$  by limiting the change in  $u(t)$ . The effect of introducing a dead-band will be addressed in Chapter 4.

## **Chapter 3 : Multirate Adaptive Inferential Control of a Linear System**

### **3.1 Introduction**

Three different adaptive inferential control (AIC) schemes, derived from the standard and simplified estimation algorithms, were evaluated using a linear model of the pilot scale binary distillation column located in the Department of Chemical Engineering at the University of Alberta. The control objective was regulation of the bottoms composition to its set point. The tests used to investigate the effectiveness of the AIC schemes were changes in feed rate, set point and process parameters (process gains and time delays). In Section 3.2, the parameters of the transfer function model are presented. The implementation of the control algorithms and other details are described in Section 3.3, followed by the simulation results and discussion in Section 3.4. The control performance of each AIC scheme is compared with that of a conventional proportional plus integral (PI) feedback control scheme which uses the composition measurement from the analyzer as the feedback signal. The effect of secondary output (tray temperature) selection on the performance of the AIC schemes was also investigated.

### **3.2 Linear Model of the Pilot Scale Binary Column**

For preliminary evaluation of the performance of control algorithms, linear models are often used because of their simplicity. The linear model used in the present study is a transfer function model of the pilot scale binary distillation column. This column has been used for several previous studies directed at evaluating different control algorithms (e.g. Chanh,

1971; Wood and Berry, 1973; Sastry *et al.*, 1977; Morris *et al.*, 1981; Martin-Sanchez and Shah, 1984) and it has also been used for experimental evaluation in this work. More details about this equipment are provided in Chapter 5.

The column separates a 50-50 percent mixture of methanol-water into top and bottom products of 95 and 5 mass percent methanol respectively. The control objective is regulation of the composition of methanol in the bottoms at its set point value despite changes in feed flow rate, set point or the process parameters. A tray temperature was used as the secondary output for the AIC schemes. The transfer function models for bottom composition,  $X_B$ , and liquid temperature on the  $i$ th stage,  $T_i$ , are of the form

$$X_B(s) = \frac{K_1 e^{-\tau_{d1}s}}{\tau_1 s + 1} S(s) + \frac{K_2 e^{-\tau_{d2}s}}{\tau_2 s + 1} F(s) + \frac{K_3 e^{-\tau_{d3}s}}{\tau_3 s + 1} R(s) \quad (3.1)$$

$$T_i(s) = \frac{K_4}{\tau_4 s + 1} S(s) + \frac{K_5 e^{-\tau_{d5}s}}{\tau_5 s + 1} F(s) + \frac{K_6 e^{-\tau_{d6}s}}{\tau_6 s + 1} R(s) \quad (3.2)$$

Parameters for Eq. 3.1 are given by Wood and Berry (1973). The transfer functions for  $T_i$ , originally established by Chanh (1971) as second order plus time delay transfer functions, have been approximated in this work by first order plus time delay models since Chanh (1971) found one of the time constants in each transfer function to be significantly larger than the other time constant. The values of the parameters of Eqs. 3.1 and 3.2 are summarized in Table 3.1. It should be noted that the cycle time of the analyzer is not included in Eq. 3.1. For all simulations, the cycle time is

Table 3.1

Parameters for the Transfer Function Model of the Binary Distillation Column

(a) Parameters for the Bottoms Composition Transfer Functions, Eq. 3.1

$K_1$	$\tau_1$	$\tau_{d1}$	$K_2$	$\tau_2$	$\tau_{d2}$	$K_3$	$\tau_3$	$\tau_{d3}$
-2.56	14.4	3.0	0.648	13.2	4.0	0.872	10.9	7.0

(b) Parameters for the Tray Temperature Transfer Functions, Eq. 3.2

Tray	$K_4$	$\tau_4$	$K_5$	$\tau_5$	$\tau_{d5}$	$K_6$	$\tau_6$	$\tau_{d6}$
1	22.28	15.6	-5.95	11.9	1.0	-7.8	12.5	2.0
2	35.49	15.9	-9.99	13.4	1.0	-17.0	18.2	2.0
3	40.00	16.2	-9.47	14.3	0.0	-16.6	19.0	2.0
4	19.48	16.4	-5.68	14.7	0.0	-10.0	17.6	1.0
5	20.20	16.6	-5.38	14.2	1.0	-10.8	19.6	1.0
6	13.99	16.1	-3.59	14.2	2.0	-8.4	20.7	1.0

NOTE :(1) The units for the transfer function parameters are :

$K_1, K_2, K_3 = \text{mass \% methanol}/(\text{g/s})$

$K_4, K_5, K_6 = \text{°C}/(\text{g/s})$

$\tau_1, \tau_2, \dots, \tau_6, \tau_{d1}, \dots, \tau_{d6} = \text{minutes}$

(2) Feed is introduced at tray 4.

(3) Trays are numbered from bottom to top.

assumed to be 5 minutes so the composition measurement for  $X_B$  is available every 5 minutes. The continuous temperature measurement is sampled at a 1 minute interval.

### 3.3 Implementation of the Adaptive and Partial Control Algorithms

#### 3.3.1 Estimation Equations and the Control Law

As discussed in Chapter 2, the number of parameters for the standard estimation algorithm depends on the assumed order of the plant,  $n$ , as well as the ratio ( $J$ ) of the larger sampling time to the smaller sampling time. Since the AIC schemes are to be applied in practice to systems which have a large value of  $J$ , the number of parameters involved for the standard algorithm will be large and so only a first order plant model will be assumed for the standard algorithm in this work. For the simplified algorithm, the number of parameters is equal to  $3n$ , which is independent of  $J$ . Using a second order model for the simplified algorithm will result in identification of only 6 parameters. Therefore, both first and second order plant models will be employed for the simplified algorithm in the simulations. The block diagram representation of the AIC schemes used to simulate the control of bottoms composition,  $X_B$ , of the binary column is shown in Fig. 3.1.

The equation for identification can be expressed as

$$y(t) = \phi_e(t-1)\hat{\theta}(t) \quad (3.3)$$

Since  $J=5$ , the 5-step ahead prediction equation is

$$y_e(t+5) = \phi_e(t-1+5)\hat{\theta}(t) \quad (3.4)$$

For the standard algorithm based on a first order plant model (scheme ST-1),



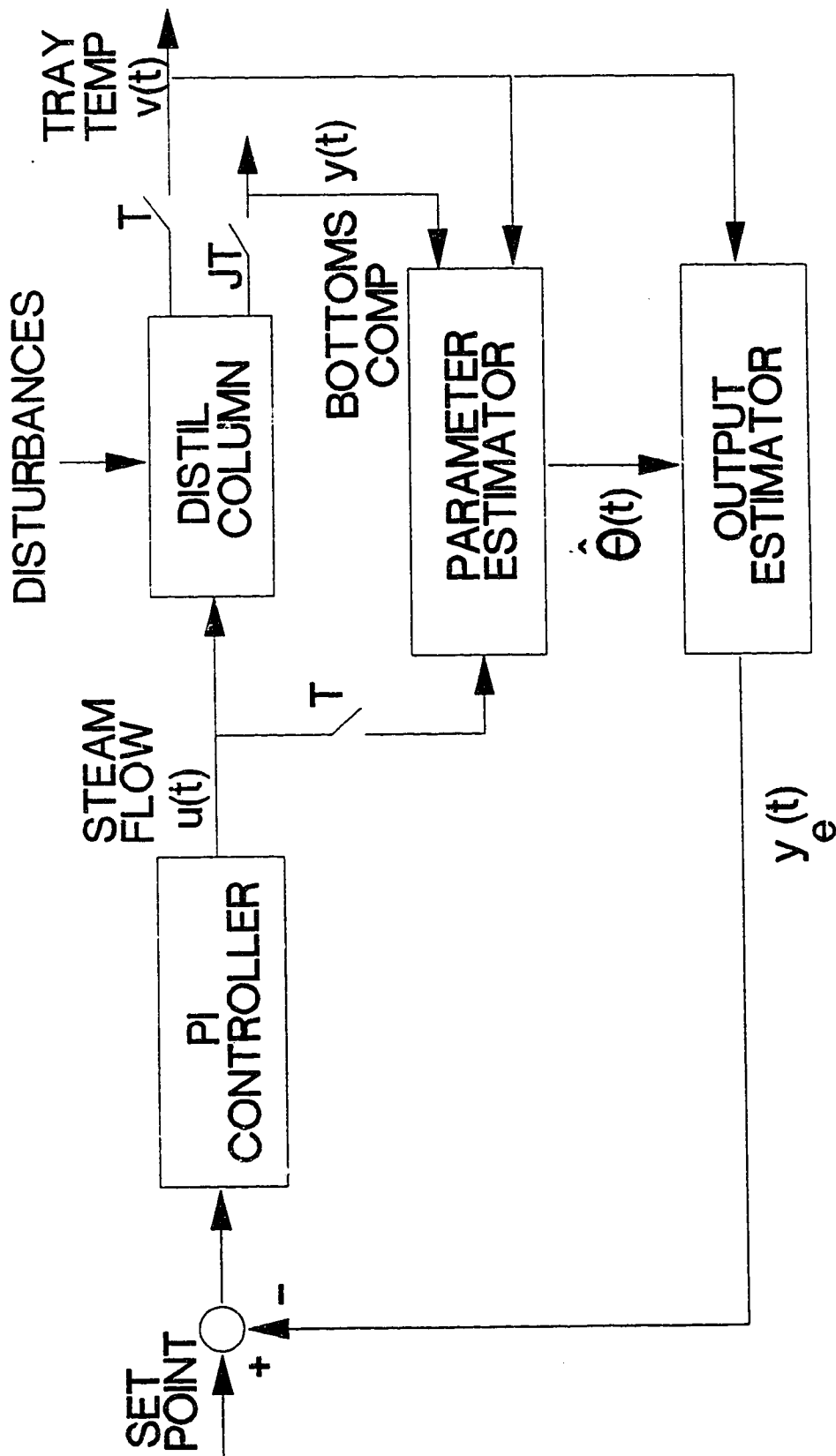


Figure 3.1 Multirate Adaptive Inferential Control of the Bottoms Composition of a Distillation Column

the governing equations (c.f. Eqs. 2.27 and 2.28) are

$$\phi_e(t-1) = \begin{bmatrix} y_e(t-5) & u(t-6) & u(t-7) & \dots & u(t-10) \\ v(t-5) & v(t-6) & \dots & v(t-10) \end{bmatrix} \quad (3.5a)$$

$$\hat{\theta}(t) = [\hat{a}_1 \quad \hat{b}_1 \quad \hat{b}_2 \quad \dots \quad \hat{b}_5 \quad \hat{c}_0 \quad \hat{c}_1 \quad \dots \quad \hat{c}_5]^T \quad (3.5b)$$

$$\phi_e(t-1+5) = \begin{bmatrix} y_e(t) & u(t-1) & u(t-2) & \dots & u(t-5) \\ v(t) & v(t-1) & v(t-2) & \dots & v(t-5) \end{bmatrix} \quad (3.5c)$$

In the case of the simplified algorithm, if a first order plant is assumed, the equations for this control system (scheme SM-1) become

$$\phi_e(t-1) = [y_e(t-5) \quad u(t-6) \quad v(t-5)] \quad (3.6a)$$

$$\hat{\theta}(t) = [\hat{a}_1 \quad \hat{b}_1 \quad \hat{c}_0]^T \quad (3.6b)$$

$$\phi_e(t-1+5) = [y_e(t) \quad u(t-1) \quad v(t)] \quad (3.6c)$$

while if a second order plant is selected the control algorithm for this scheme, designated as SM-2, is based on the following equations

$$\phi_e(t-1) = \begin{bmatrix} y_e(t-5) & y_e(t-10) & u(t-6) & u(t-11) \\ v(t-5) & v(t-10) \end{bmatrix} \quad (3.7a)$$

$$\hat{\theta}(t) = [\hat{a}_1 \quad \hat{a}_5 \quad \hat{b}_1 \quad \hat{b}_5 \quad \hat{c}_0 \quad \hat{c}_5]^T \quad (3.7b)$$

$$\phi_e(t-1+5) = \begin{bmatrix} y_e(t) & y_e(t-5) & u(t-1) & u(t-6) \\ v(t) & v(t-5) \end{bmatrix} \quad (3.7c)$$

Thus, the numbers of parameters to be identified for schemes ST-1, SM-1 and SM-2 are 12, 3 and 6 respectively.

As shown in Fig. 3.1, the predicted output,  $y_e(t)$ , is used as a feedback signal for the control calculation. In the conventional feedback control scheme, the measurement of  $y(t)$  from the analyzer is used as the feedback signal. The proportional plus integral (PI) control law used for

studying the performance of the AIC schemes and the conventional feedback control scheme is expressed as

$$OP = K_p ER + K_i \int_0^t ER dt + BIAS \quad (3.8)$$

### 3.3.2 Selection of Secondary Output, Identification and Initial Parameters

A tray temperature was chosen as the secondary output for the AIC schemes. From Table 3.1, it can be seen that the liquid temperature on the second tray ( $T_2$ ) is the most sensitive tray liquid temperature to changes in feed rate (F) and steam flow rate (S) while the liquid temperature on tray 6 ( $T_6$ ) is the most insensitive. Trays are numbered from bottom to top, with the feed being introduced at tray 4. To investigate the effect of secondary output selection on the performance of the AIC schemes, simulations were performed using  $T_2$  and also  $T_6$  as secondary output in the adaptive algorithms.

A recursive least squares (RLS) identification algorithm with U-D factorization (Åström and Wittenmark, 1984) and a constant forgetting factor of 0.97 was employed for estimating the parameters of the model equation. The covariance matrix was initialized to the identity matrix and covariance resetting was not employed. Initial parameter values for the parameter vector were obtained by exciting the process with a series of +5%/-5% changes in feed flow rate.

The initial proportional plus integral controller settings, obtained using the process reaction curve method and the Cohen-Coon formulae (Stephanopoulos, 1984), were calculated to be  $K_p = -0.14 \frac{\text{g/s}}{\text{mass \%}}$  and  $K_i = -0.103 \frac{\text{g/s}}{\text{mass \%} \cdot \text{min}}$ . For each control scheme, the controller was tuned for the case of -25 % step change in feed rate to obtain a minimum integral of absolute

error (IAE). For the conventional PI control scheme, the tuned controller settings were established to be  $K_p = -0.65 \frac{\text{g/s}}{\text{mass \%}}$  and  $K_I = -0.111 \frac{\text{g/s}}{\text{mass \%} \cdot \text{min}}$ . The tuned controller settings for the AIC schemes are summarized in Table 3.2.

Table 3.2  
Tuned Controller Constants for the AIC Schemes

Scheme	$K_p$ ((g/s)/mass %)	$K_I$ ((g/s)/mass %-min)
ST-1 <sup>(1)</sup>	-0.30	-0.033
SM-1 <sup>(1)</sup>	-0.30	-0.033
SM-2 <sup>(1)</sup>	-0.30	-0.033
ST-1 <sup>(2)</sup>	-0.20	-0.024
SM-1 <sup>(2)</sup>	-0.17	-0.019
SM-2 <sup>(2)</sup>	-0.17	-0.019

Note : (1) Liquid temperature at tray 2 is used as the secondary output  
(2) Liquid temperature at tray 6 is used as the secondary output

### 3.4 Simulation Results

#### 3.4.1 Control of a Time-Invariant Process

Regulatory and servo control performance for each the AIC scheme was compared with that of the conventional feedback PI control scheme. For the regulatory control case, a 25% step decrease in feed rate was introduced into the process at time  $t=0$  minute. For the servo control case, the set point was increased by 20% to a value of 6.0 mass percent methanol at time  $t=0$  minute.

(i) Step Disturbance in Feed Rate

Table 3.3 provides a summary of the IAE performance values for each AIC scheme and the conventional feedback PI control scheme when a 25% step decrease in feed rate was introduced into the process. The closed loop responses obtained using the ST-1, SM-1 and SM-2 control schemes are compared in Figs 3.2 to 3.4 with the controlled response obtained by employing the PI scheme. Also shown in these figures are the parameter trajectories of the AIC schemes. For the sake of clarity, only seven of the twelve parameters of the ST-1 scheme are shown in the parameter trajectories presented in Fig. 3.2 and in all subsequent parameter trajectories for the ST-1 scheme.

Table 3.3  
Summary of Control Performance for a -25% Step Change in Feed Rate

<u>Control Scheme</u>	<u>IAE (mass %-minute)</u>	<u>Reference Figures</u>
PI	67.6	3.2-3.4
ST-1	41.3	3.2
SM-1	69.3	3.3
SM-2	65.2	3.4

As can be seen from the IAE values reported in Table 3.3, the ST-1 control scheme clearly provided superior control performance compared with that achieved using the other three control schemes. The IAE value of 41.3 for the ST-1 scheme is more than 50% lower than the IAE values for the SM-1, SM-2 or PI control schemes. From the control behavior shown in Figs 3.2 to 3.4, it can be observed that all four control schemes were able to return the bottoms composition,  $X_B$ , to the set point. The bottoms composition

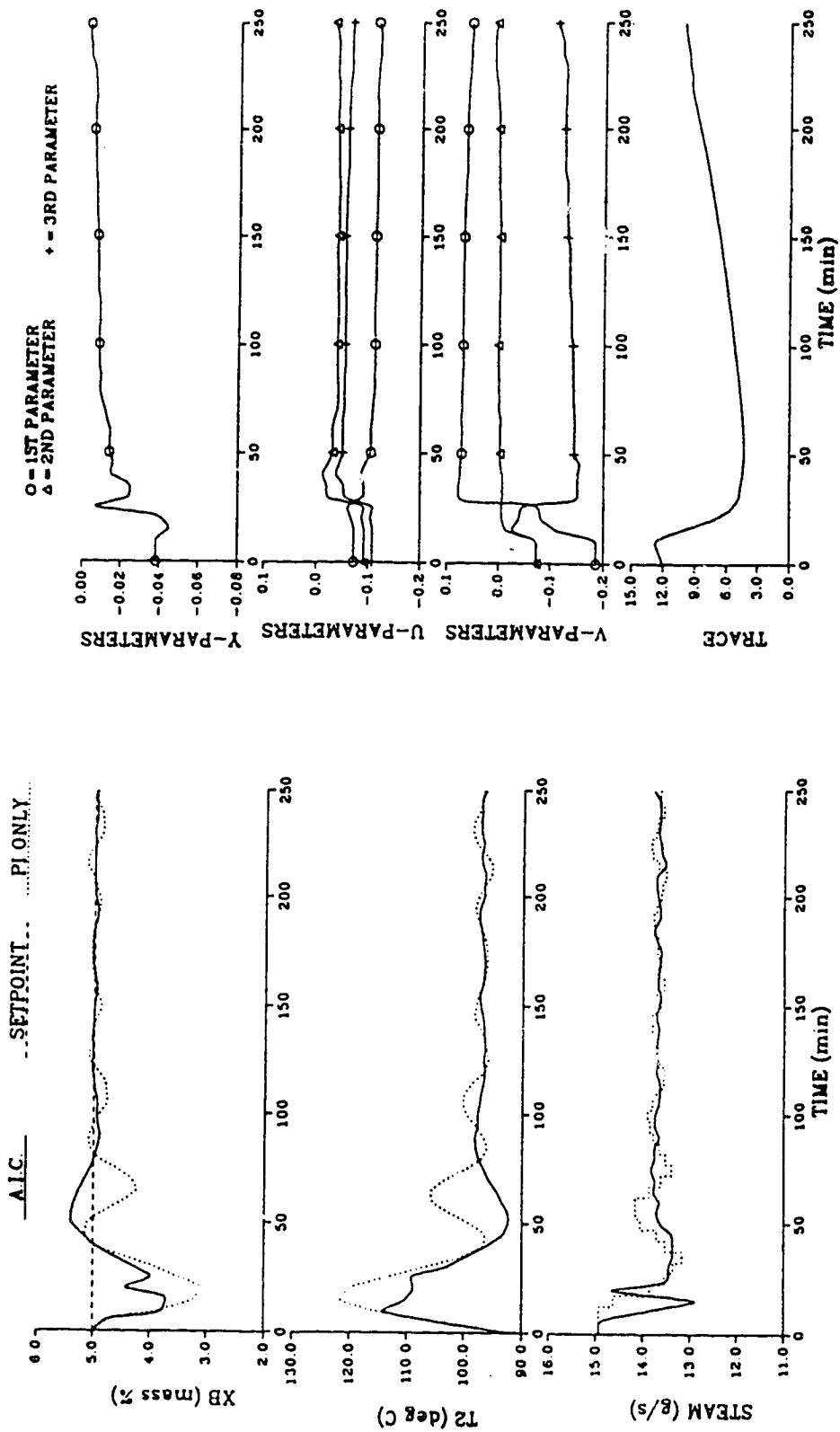


Figure 3.2 Comparison of Conventional PI and ST-1 AIC Control Performance for a -25% Step Change in Feed Rate and AIC Parameter Trajectories

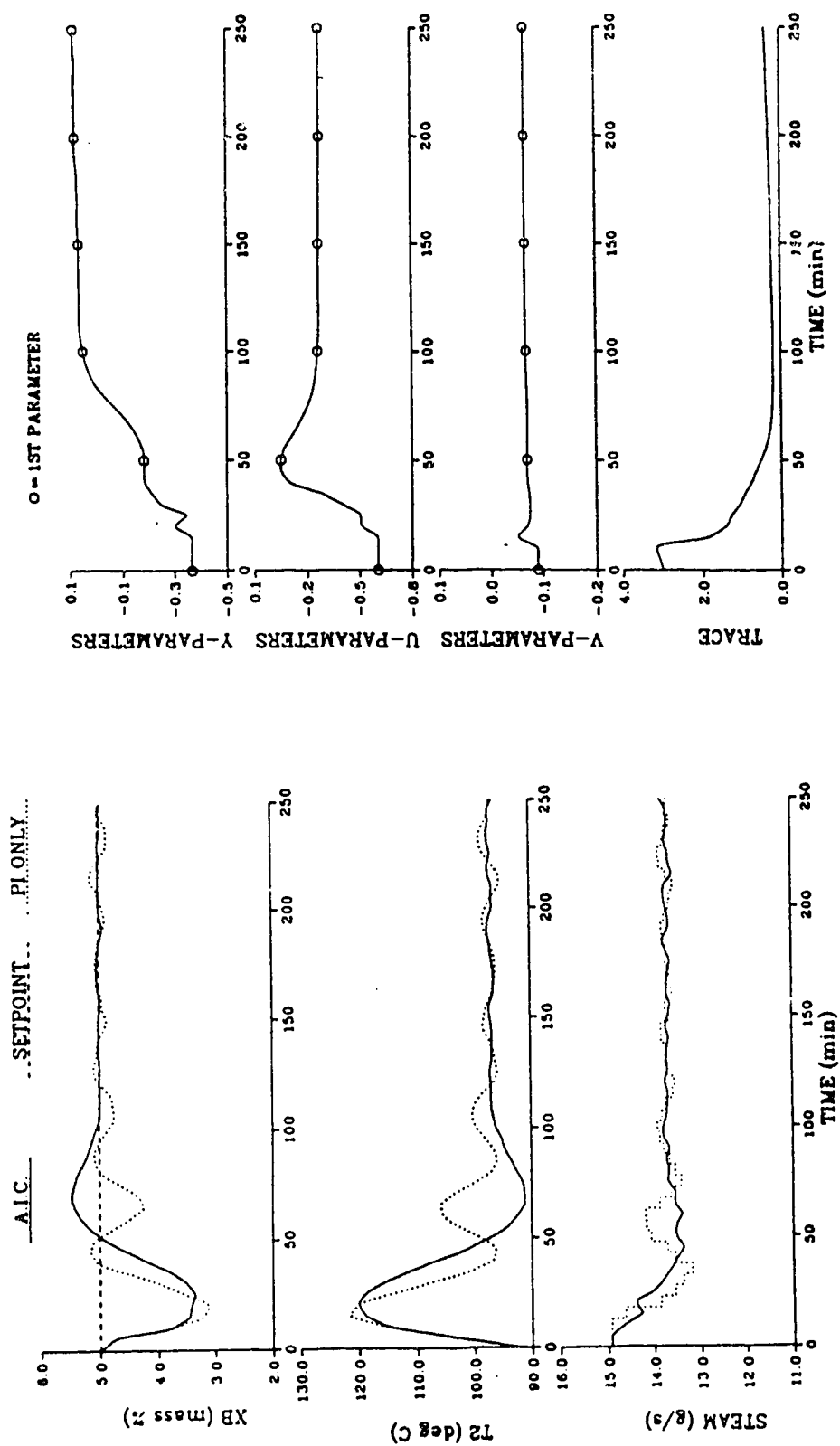


Figure 3.3 Comparison of Conventional PI and SM-1 AIC Control Performance for a -25% Step Change in Feed Rate and AIC Parameter Trajectories

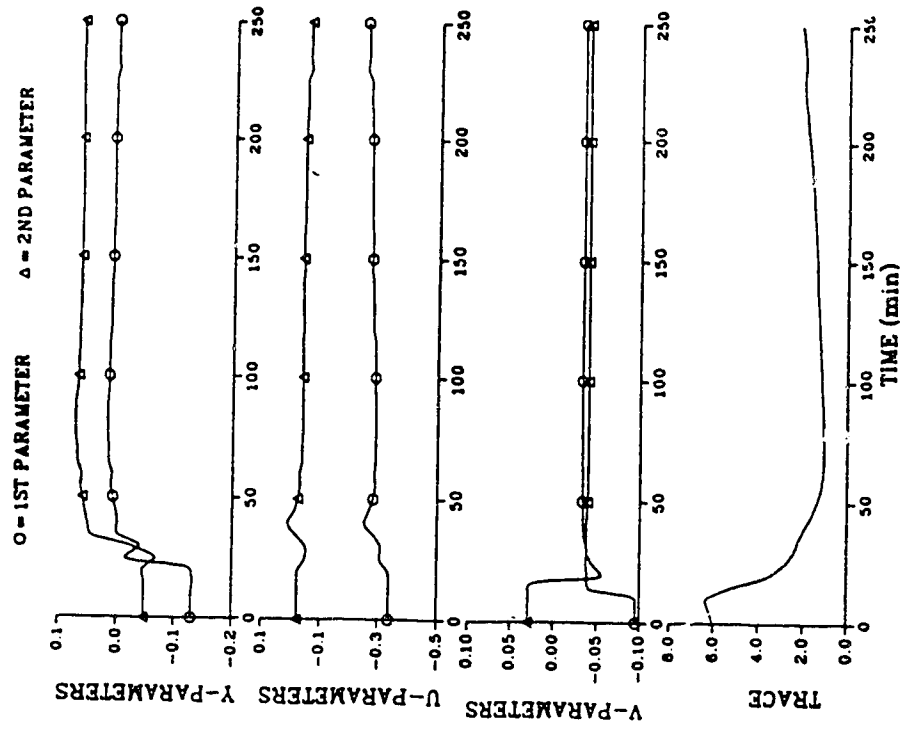
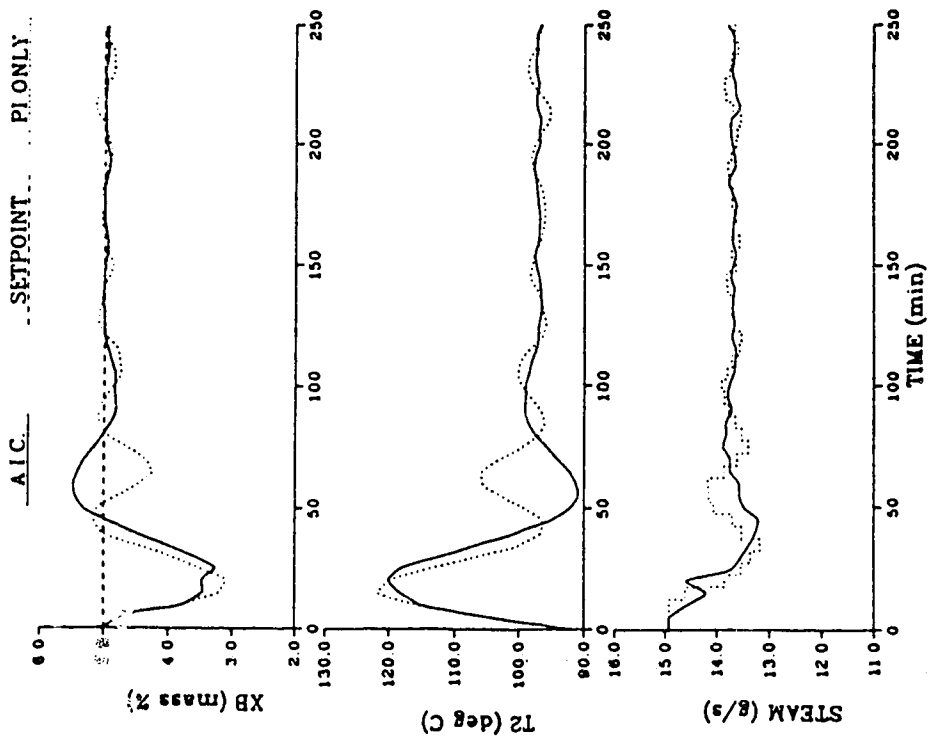


Figure 3.4 Comparison of Conventional PI and SM-2 AIC Control Performance for a -25% Step Change in Feed Rate and AIC Parameter Trajectories



response that resulted when the PI scheme was employed is slightly oscillatory because the controller settings were tuned to obtain a minimum IAE value. If the proportional gain was decreased to remove the small oscillation, slower controlled response resulted, thus leading to a larger IAE value. Similarly, if the proportional gain was increased to give faster response, more oscillatory control behavior was observed and again a larger IAE value was obtained. The rise time is defined in this work as the time required for the controlled variable to reach its set point for the first time after a disturbance or set point change has been introduced. The rise time for the ST-1 scheme was found to be 40 minutes, approximately the same as the rise time resulted from utilizing the PI scheme, but the controlled response is faster than the controlled response obtained by using either SM-1 or SM-2 algorithm. The maximum absolute deviation of  $X_B$  from its set point, when the ST-1 scheme was employed, is about 1.3 mass percent methanol, the smallest excursion obtained from employing any of the four control schemes.

Since the performance of the AIC schemes depends mainly on the accuracy of the predicted values ( $y_e$ ) of the controlled output ( $y$ ), it is useful to compare  $y_e$  with  $y$  to attempt to understand the control behavior obtained using the AIC algorithms. In Fig. 3.5 the predicted bottoms composition is compared with the actual composition for each of the AIC schemes. As can be seen from the top plot of this figure, the estimator of the ST-1 scheme was able to predict the "trend" of the bottoms composition but since the parameters were converging to new values due to the disturbance, the predicted value of  $X_B$ , which reached a minimum value of 0.7 mass percent methanol at time  $t=15$  minutes, was not accurate during the initial transient

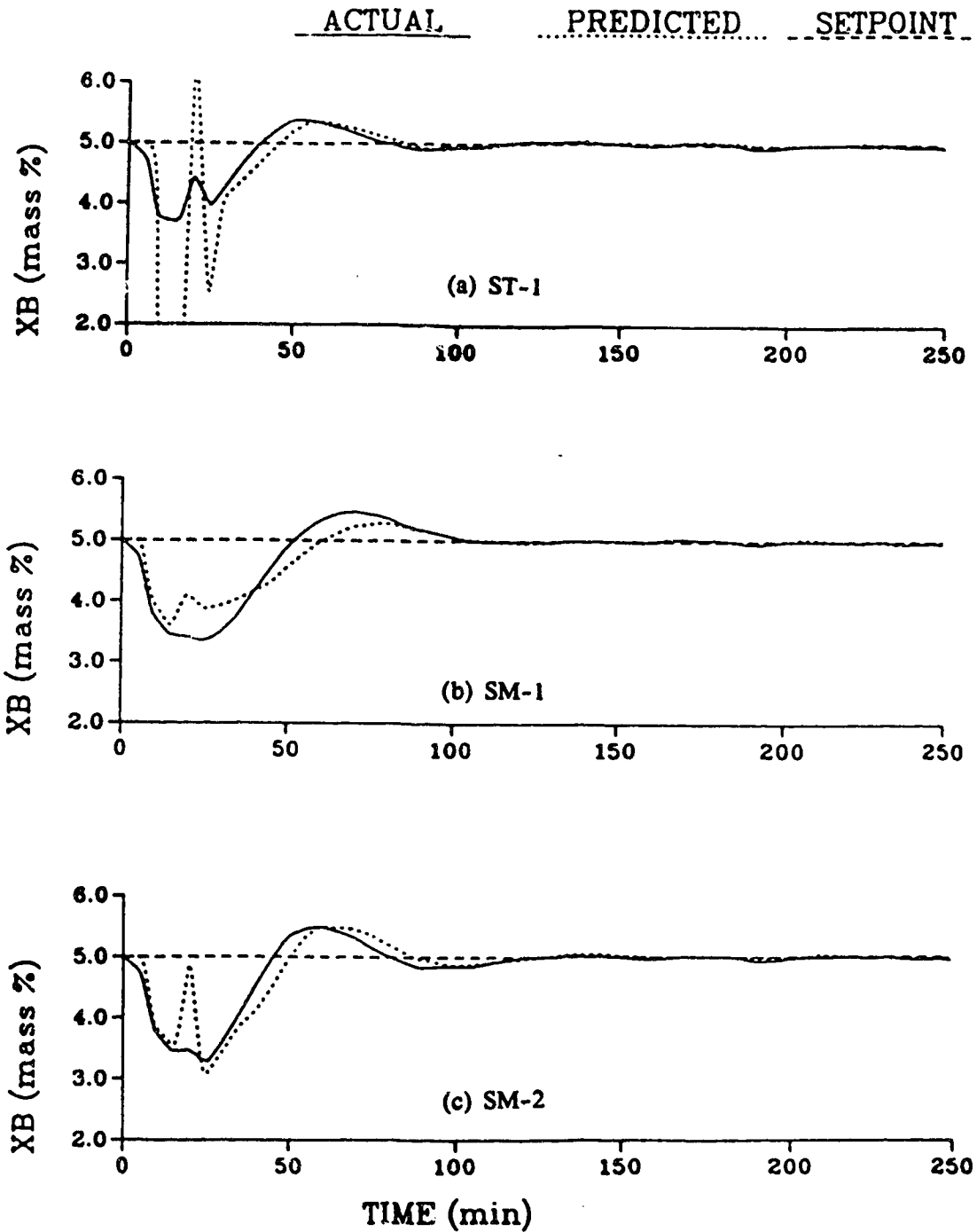


Figure 3.5 Comparison of Predicted Bottoms Composition versus Actual Bottoms Composition for a -25% Step Change in Feed Rate

period. However, because the "trend" of the  $X_B$  was correctly predicted, the ST-1 control scheme was able to take corrective control action faster than the PI control scheme did, as can be seen from the changes in steam rate, the manipulated variable, shown in Fig. 3.2. Because of the "over-prediction" of the changes in  $X_B$ , the control action applied by the ST-1 control scheme resulted in the composition deviating significantly from the set point during the initial 25 minutes following the disturbance. The minimum value of  $X_B$  obtained is 3.7 mass percent methanol. Nevertheless, despite the pronounced change in steam rate (c.f. Fig. 3.2), this control action in turn resulted in a smaller excursion of  $X_B$  from the set point than the other three control schemes. The sudden changes in the parameters shown in Fig. 3.2 illustrate the adaptation during the initial transient period. After the parameters had converged to new values, the predicted output eventually matched the actual output. Almost perfect prediction of the bottoms composition resulted from using the ST-1 scheme after 60 minutes of operation. It can be observed by comparing the parameter trajectories shown in Figs 3.2 to 3.4 that the parameter adaptation patterns of the ST-1 and SM-2 schemes are quite similar while the changes in the parameters of the SM-1 scheme are more gradual. Therefore, the predicted bottoms composition obtained using the SM-1 algorithm was not as oscillatory as that obtained using either the ST-1 or SM-2 scheme during the initial period (c.f. Fig. 3.5). Consequently, the changes in steam rate were initially not as pronounced when the SM-1 algorithm was employed. It should be noted that despite the "over-prediction" of  $X_B$  by the standard algorithm during the initial transient period, the ST-1 scheme provided the best control performance of any of the four control schemes. Because the process model

is a combination of first order plus time delay transfer functions, the "over-prediction" did not lead to stability and robustness problems. It is also to be noted that the ST-1 scheme which required the identification of 12 parameters encountered no problem of parameter convergence. However, it will be shown in Chapter 4 that when the process is highly nonlinear, the ST-1 scheme will not provide satisfactory control performance because of the poor initial prediction of the controlled variable. The problems of employing the standard algorithm in practice will also be demonstrated by the experimental results to be presented in Chapter 5.

(ii) Effect of a Poor Choice of Secondary Output

To investigate the effect of a poor choice of secondary output on the control performance of the AIC schemes, one series of simulations were performed using the liquid temperature at tray 6 ( $T_6$ ) as the secondary output for each of the AIC schemes.  $T_6$  was chosen in this case because from the values of the parameters of the transfer functions for tray liquid temperatures (c.f. Eq. 3.2) tabulated in Table 3.1,  $T_6$  is the least sensitive to changes in feed and steam rates, as indicated by the small magnitudes of the gains  $K_4$  and  $K_5$ . This insensitivity is not surprising as tray 6 is above the feed tray, tray 4. The IAE values that resulted for a -25% step change in feed rate are given in Table 3.4 and the corresponding transient responses are displayed in Figs. 3.6 to 3.8. Although each AIC algorithm was able to regulate the bottoms composition to its set point, the control performance that resulted from using  $T_6$  as the secondary output of the AIC schemes is inferior to the control performance obtained by using  $T_2$  as the secondary output, as would be expected, because  $T_2$  is the most sensitive temperature to changes in feed and steam rates. By comparing the

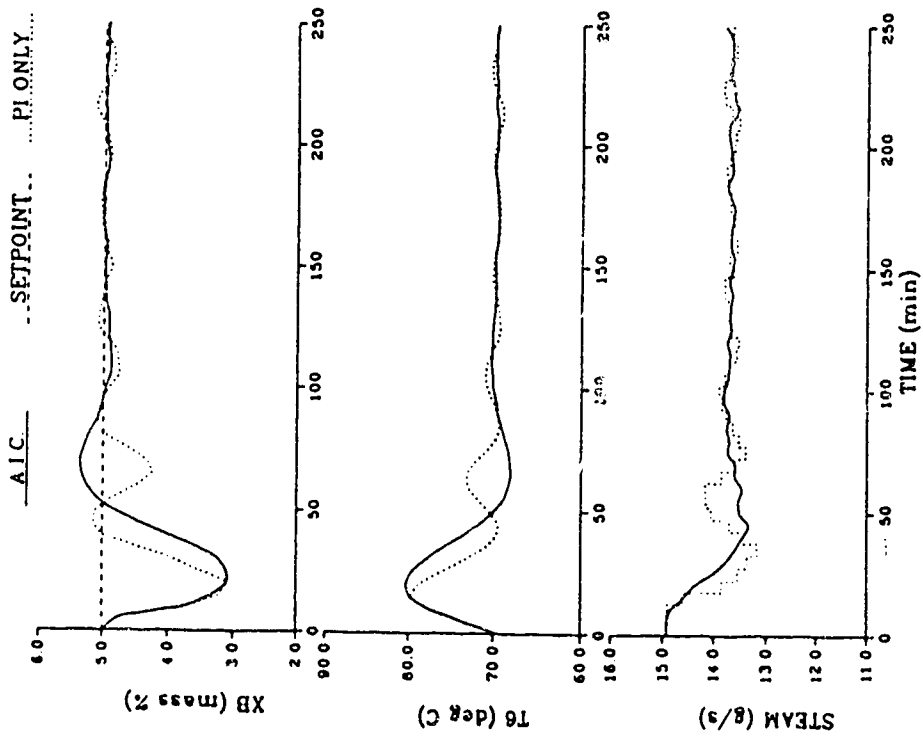
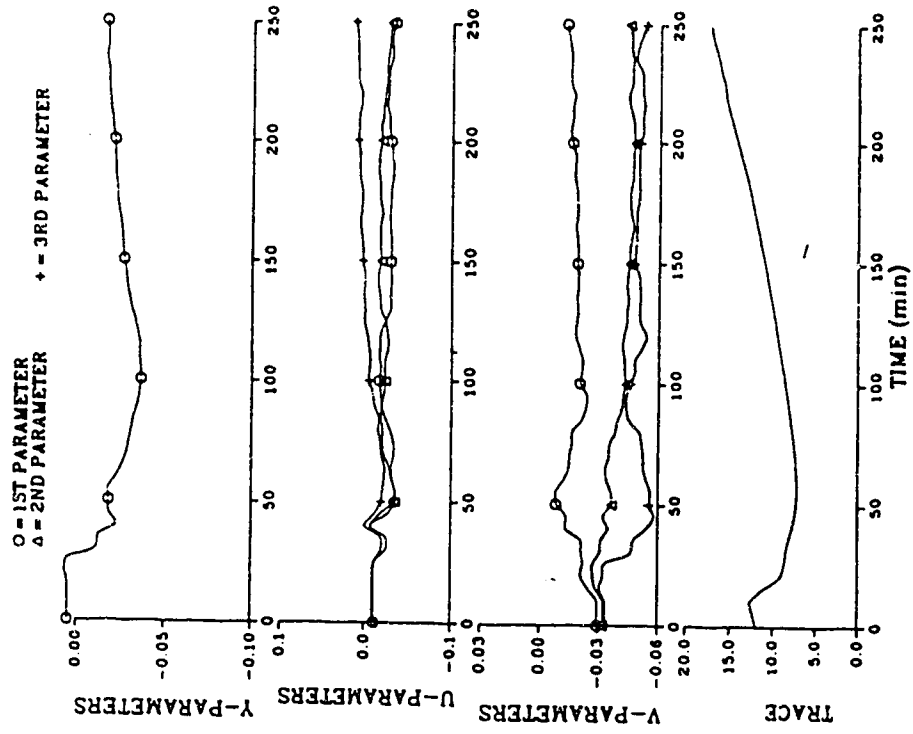


Figure 3.6 Control Performance of the ST-1 AIC Scheme Using Tray 6  
Liquid Temperature as the Secondary Output for a -25% Step  
Change in Feed Rate and AIC Parameter Trajectories



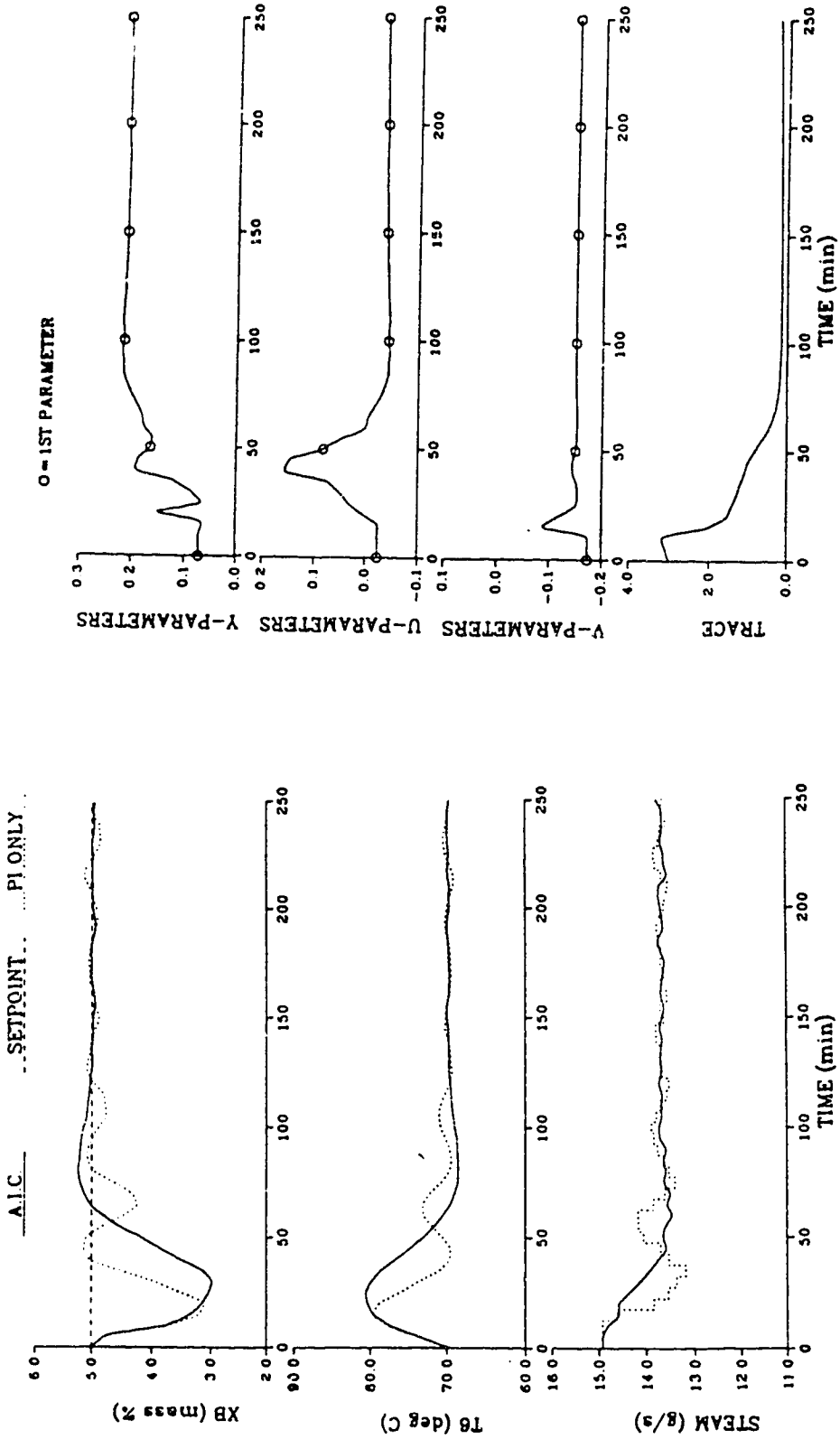


Figure 3.7 Control Performance of the SM-1 AIC Scheme Using Tray 6  
 Liquid Temperature as the Secondary Output for a -25% Step  
 Change in Feed Rate and AIC Parameter Trajectories

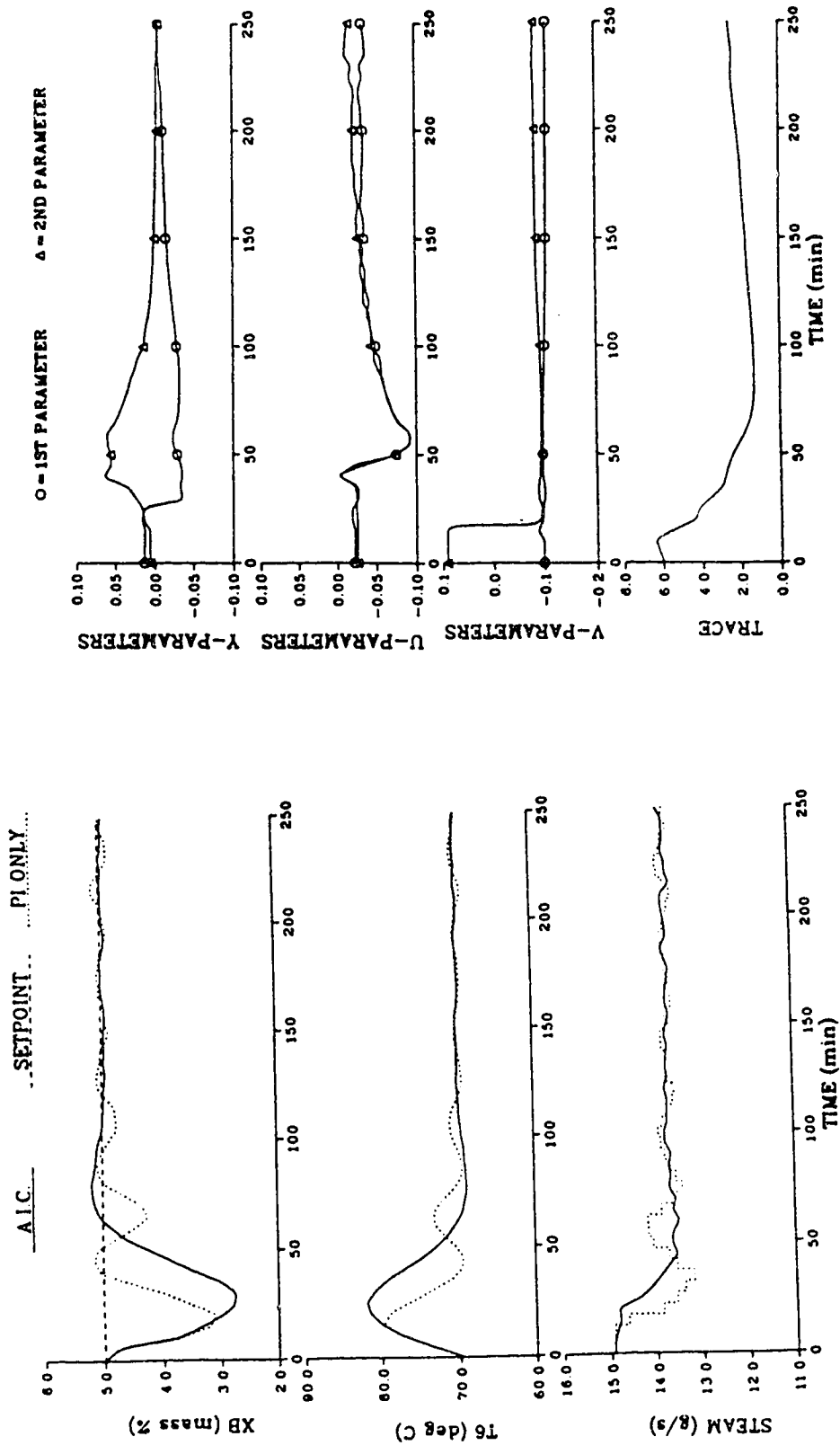


Figure 3.8 Control Performance of the SM-2 AIC Scheme Using Tray 6  
 Liquid Temperature as the Secondary Output for a -25% Step  
 Change in Feed Rate and AIC Parameter Trajectories

control behavior for the case when  $T_2$  was used (c.f. Figs. 3.2 to 3.4) to the corresponding control behavior when  $T_6$  was used (c.f. Figs. 3.6 to 3.8), it is obvious that because  $T_6$  is insensitive to changes in feed and steam rates, the AIC schemes were not able to take corrective control action as rapidly as when  $T_2$  was used as the secondary output. The AIC schemes rely heavily on the information available through the changes in the secondary output to generate good intersample predictions of the controlled output. Since  $T_6$  was not as sensitive to changes in feed and steam rates as  $T_2$ , the information available to the AIC schemes was not as "rich" as in the case  $T_2$  used as the secondary output. This resulted in slower speed of convergence of the parameters of the AIC algorithms, as can be observed by comparing the parameter trajectories shown in Figs. 3.2 to 3.4, for the case where  $T_2$  was used as the secondary output, to the corresponding parameter trajectories displayed in Figs. 3.6 to 3.8 that resulted when  $T_6$  was the secondary output.

Table 3.4  
Summary of Control Performance for a -25% Step Change in  
Feed Rate with Liquid Temperature on Tray 6 Used as the  
Secondary Output for the AIC Schemes

<u>Control Scheme</u>	<u>IAE (mass %-minute)</u>	<u>Reference Figures</u>
PI	67.6	3.6-3.8
ST-1	74.9	3.6
SM-1	85.8	3.7
SM-2	68.4	3.8

The degradation in control performance when  $T_6$  was used as the secondary output instead of  $T_2$  was most significant when the ST-1 scheme was



employed, with the IAE value increasing from 41.3 (c.f. Table 3.3) to 74.9, an increase of over 75%. The IAE values for SM-1 and SM-2 schemes increased by approximately 20% in each case. The significant effect of a poor choice of the secondary output on the control performance of the standard algorithm can be attributed to the large number of parameters that need to be identified when the ST-1 scheme is used. Since the ST-1 algorithm requires that 12 parameters be identified, "rich" information or excitation is required to avoid the problem of slow convergence of the parameters. When  $T_6$  was used as the secondary output instead of  $T_2$ , the "richness" of the information available through this secondary output was reduced. In other words, the system is "more observable" from  $T_2$  than from  $T_6$ . The more profound effect on the rate of convergence of the parameters of the ST-1 algorithm can be readily observed by comparing the parameter trajectories shown in Fig. 3.6 for the ST-1 schemes to the parameter trajectories displayed in Figs 3.7 and 3.8 for SM-1 and SM-2 schemes. It is also noticeable that the parameters for the simplified algorithms converge in a "smoother" manner than the parameters for the standard algorithm.

### (iii) Servo Control Performance

The control performance of the AIC schemes for a step change of 20% in set point of methanol concentration to 6.0 mass percent at time  $t=0$  is compared with the performance achieved using the PI scheme in Figs. 3.9 to 3.11. The best control performance, with an IAE value of 33.5, resulted from using the standard ST-1 scheme while the largest IAE value (42.5) resulted when the SM-1 algorithm was employed. The IAE values for the SM-2 and PI schemes were calculated to be 37.3 and 39.2 respectively. It can be seen from the control behavior shown in Figs. 3.9 to 3.11 that the PI scheme

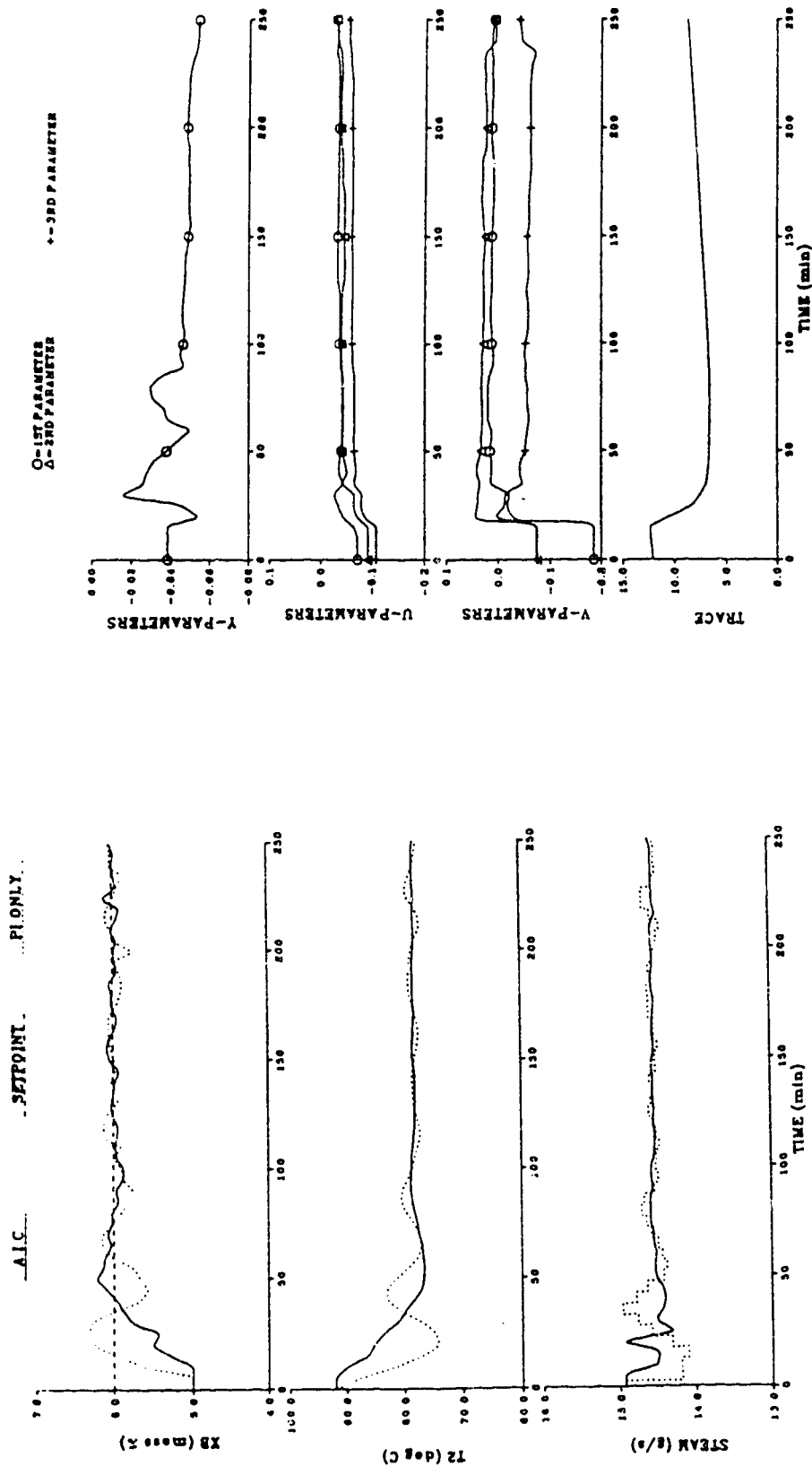


Figure 3.9 Comparison of Conventional PI and ST-1 AIC Control Performance for a Step Increase of One Mass Percent Methanol Concentration in the Bottoms Composition Set Point and AIC Parameter Trajectories

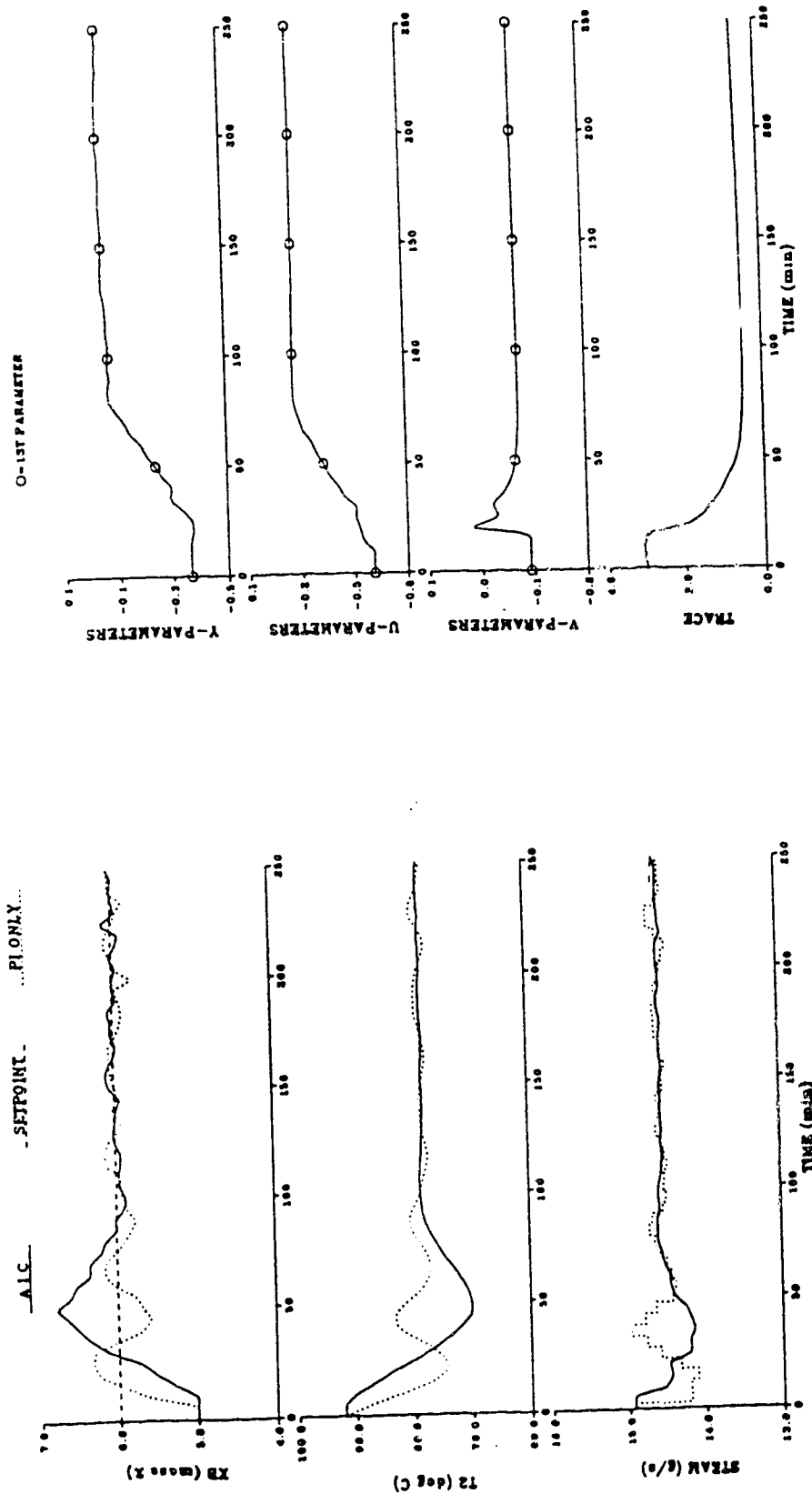


Figure 3.10 Comparison of Conventional PI and SM-1 AIC Control Performance for a Step Increase of One Mass Percent Methanol Concentration in the Bottoms Composition Set Point and AIC Parameter Trajectories

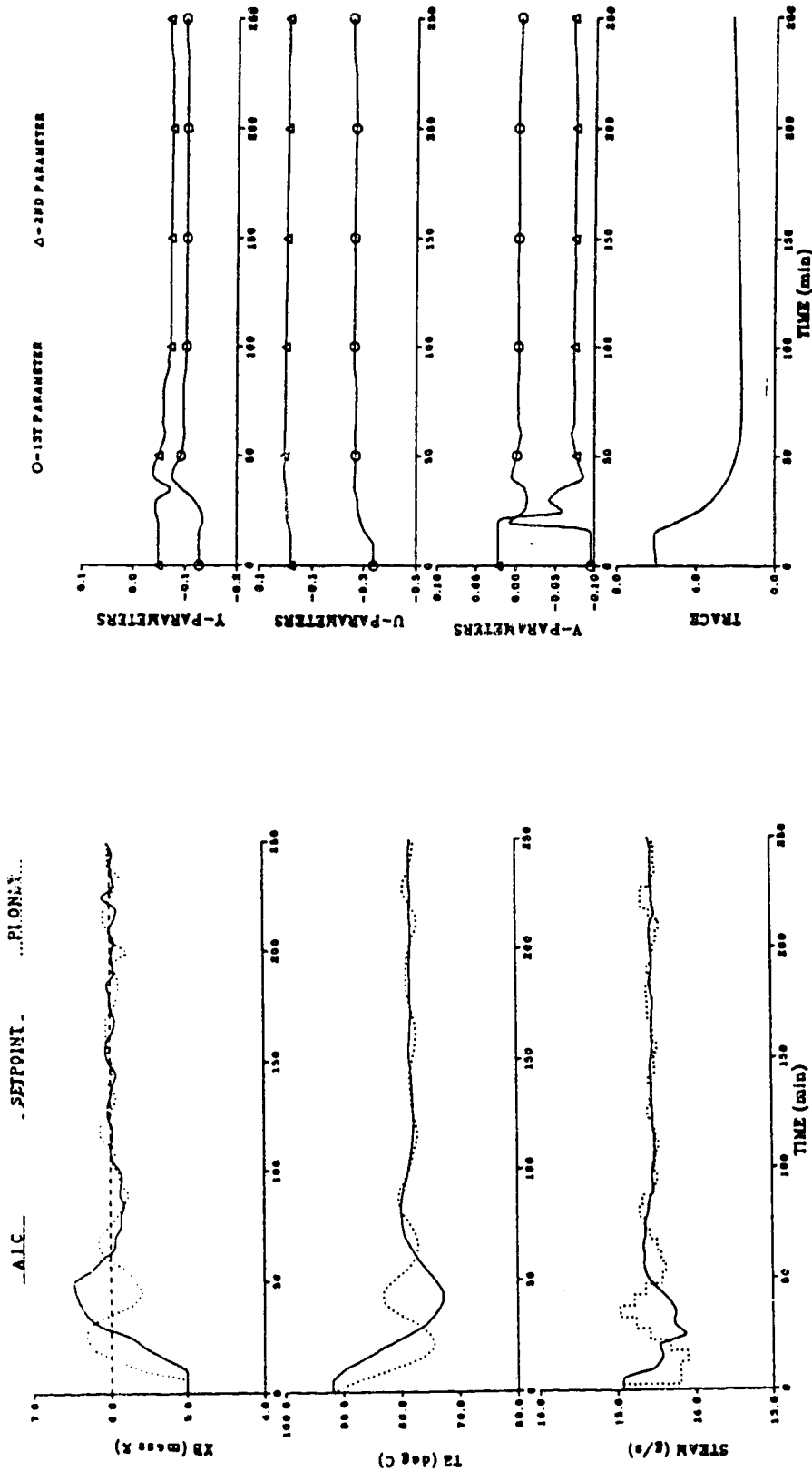


Figure 3.11 Comparison of Conventional PI and SM-2 AIC Control Performance for a Step Increase of One Mass Percent Methanol Concentration in the Bottoms Composition Set Point and AIC Parameter Trajectories

reacted to the set point change much faster than the AIC schemes, as indicated by the short rise time that resulted when the PI scheme was used. This observation is not surprising because a change in set point would not lead to significant change in the secondary output ( $T_2$  in this case) initially. Thus, during the initial transient period, unlike the case when there was a large feed disturbance, the regressor of the adaptive algorithm was not supplied with "rich" information. The initial corrective control action was due to the set point change only and so not until the effect of the corrective control action caused  $T_2$  to deviate from its steady state value did the AIC schemes benefit from the secondary information for intersample prediction. This explanation is supported by the parameter trajectories shown in Figs. 3.9 to 3.11. There are no changes in the "c" parameters, which operate on the secondary output, during the first 20 minutes for the AIC schemes, unlike the behavior of the parameters for the feed flow rate disturbance. In the case of the feed disturbance, the corresponding parameters started changing within 10 minutes of the introduction the disturbance and furthermore, the "a" and "b" parameters, related to  $y_e$  and  $u$ , also changed more quickly.

#### 3.4.2 Control of a Time-Variant Process

Since in practice it is unlikely that exact process models will be available, it will often be necessary to select controller settings based on approximate models. To investigate the robustness of the AIC schemes versus conventional feedback PI control, the performance of the different algorithms for a 25% decrease in feed rate was studied for a variety of combined changes in the gains, time constants and delays of the column

transfer function model. The observed control performance for the case of increasing the gain  $K_2$  to 0.745 and time delay  $\tau_{d1}$  to 4 minutes, and decreasing the gain  $K_1$  to -2.18 and time delay  $\tau_{d2}$  to 2 minutes are summarized in Table 3.5. The closed loop responses obtained using the ST-1, SM-1 and SM-2 control schemes are compared with the controlled response obtained by employing the PI scheme in Figs. 3.12 to 3.14 respectively. Changes of the gains and time delays were introduced at time  $t=0$ . This is a severe test of the robustness of the control algorithms because of the nature of the changes in the process parameters. The changes are such that the time before the effect of the feed disturbance affects the bottoms composition,  $X_B$ , is reduced and the delay for the manipulated variable to take corrective action is increased while the magnitude of the effect of the feed disturbance on  $X_B$  is increased and the magnitude of the effect of the manipulated variable on  $X_B$  is decreased.

Table 3.5

Summary of Control Performance for a -25% Step Change in Feed Rate with Changes in Process Gains and Time Delays

<u>Control Scheme</u>	<u>IAE (mass %-minute)</u>	<u>Reference Figures</u>
PI	81.8	3.12-3.14
ST-1	68.3	3.12
SM-1	88.1	3.13
SM-2	83.8	3.14

As can be appreciated from the IAE values listed in Table 3.5, the ST-1 scheme provided the best control performance, yielding an IAE value of 68.3. The IAE performance index that resulted from employing either the SM-1 or

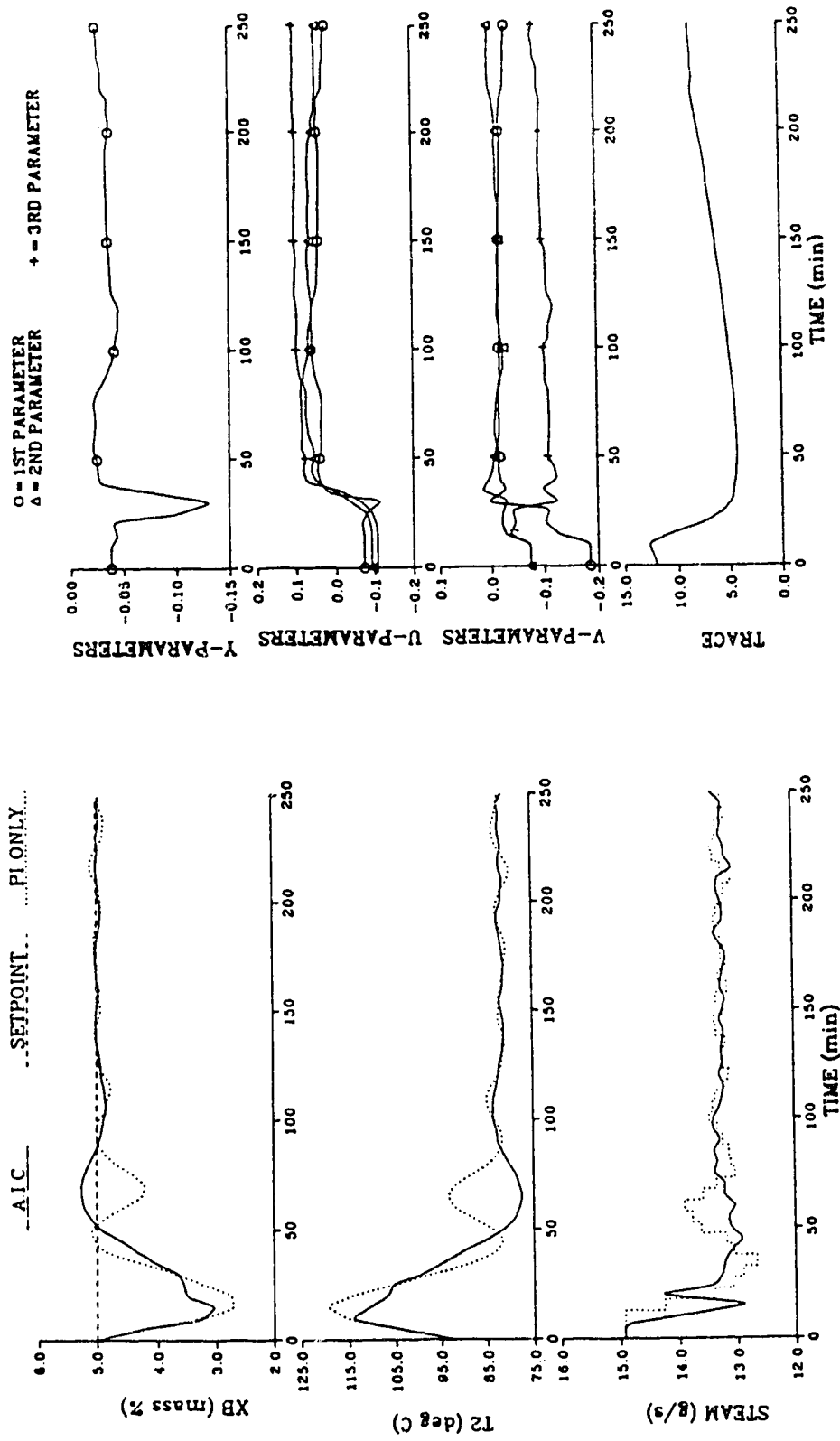


Figure 3.12 Comparison of Conventional PI and ST-1 AIC Control Performance for Changes in the Transfer Function Gains and Time Delays and AIC Parameter Trajectories

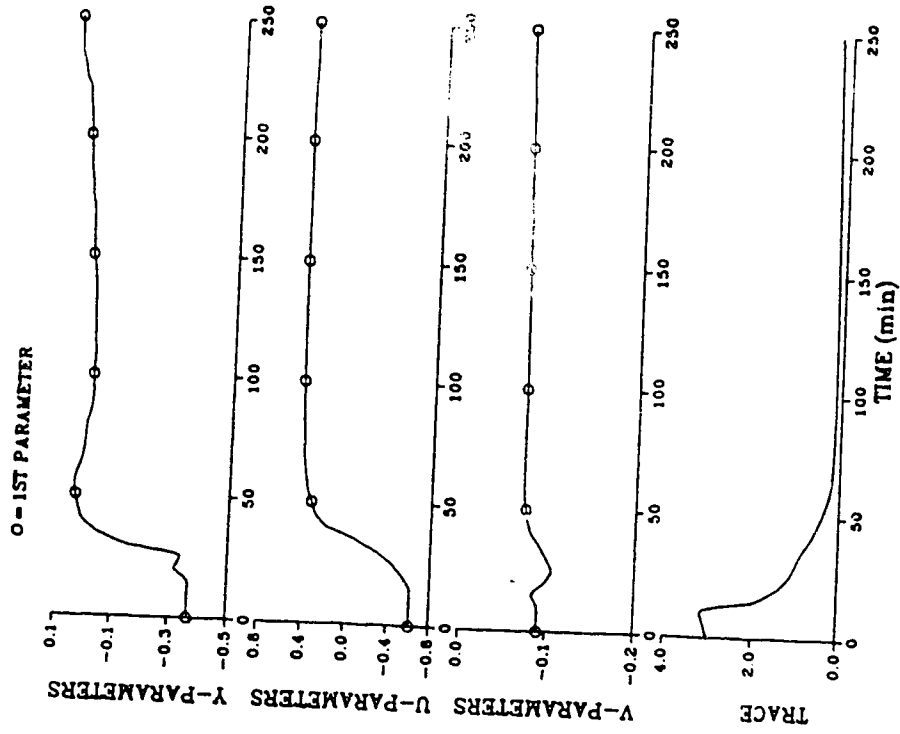
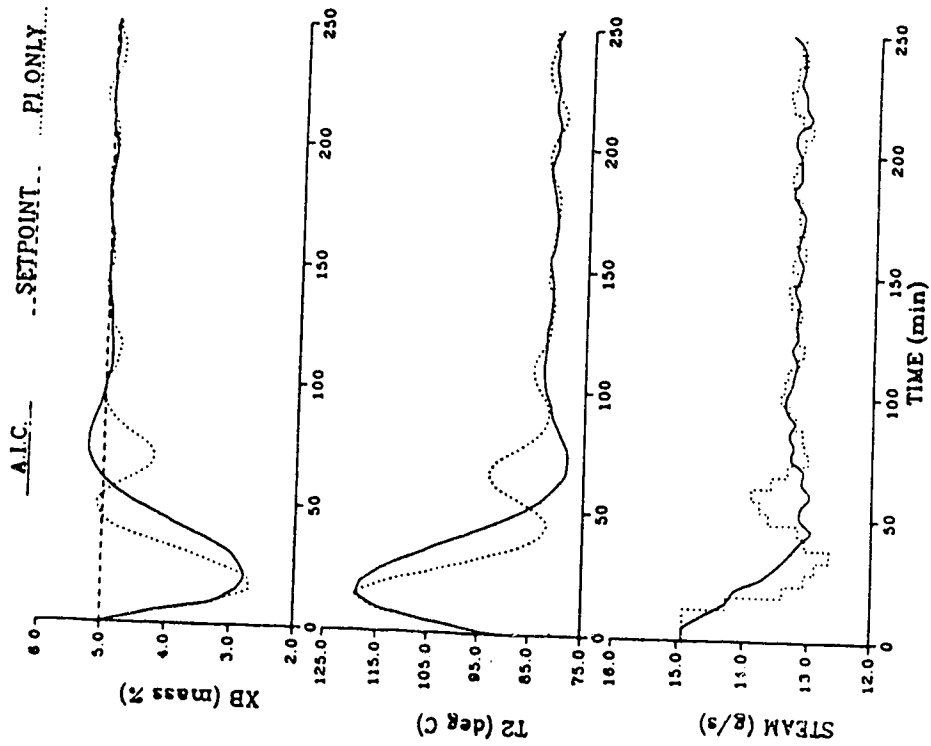


Figure 3.13 Comparison of Conventional PI and SM-1 AIC Control Performance for Changes in the Transfer Function Gains and Time Delays and AIC Parameter Trajectories



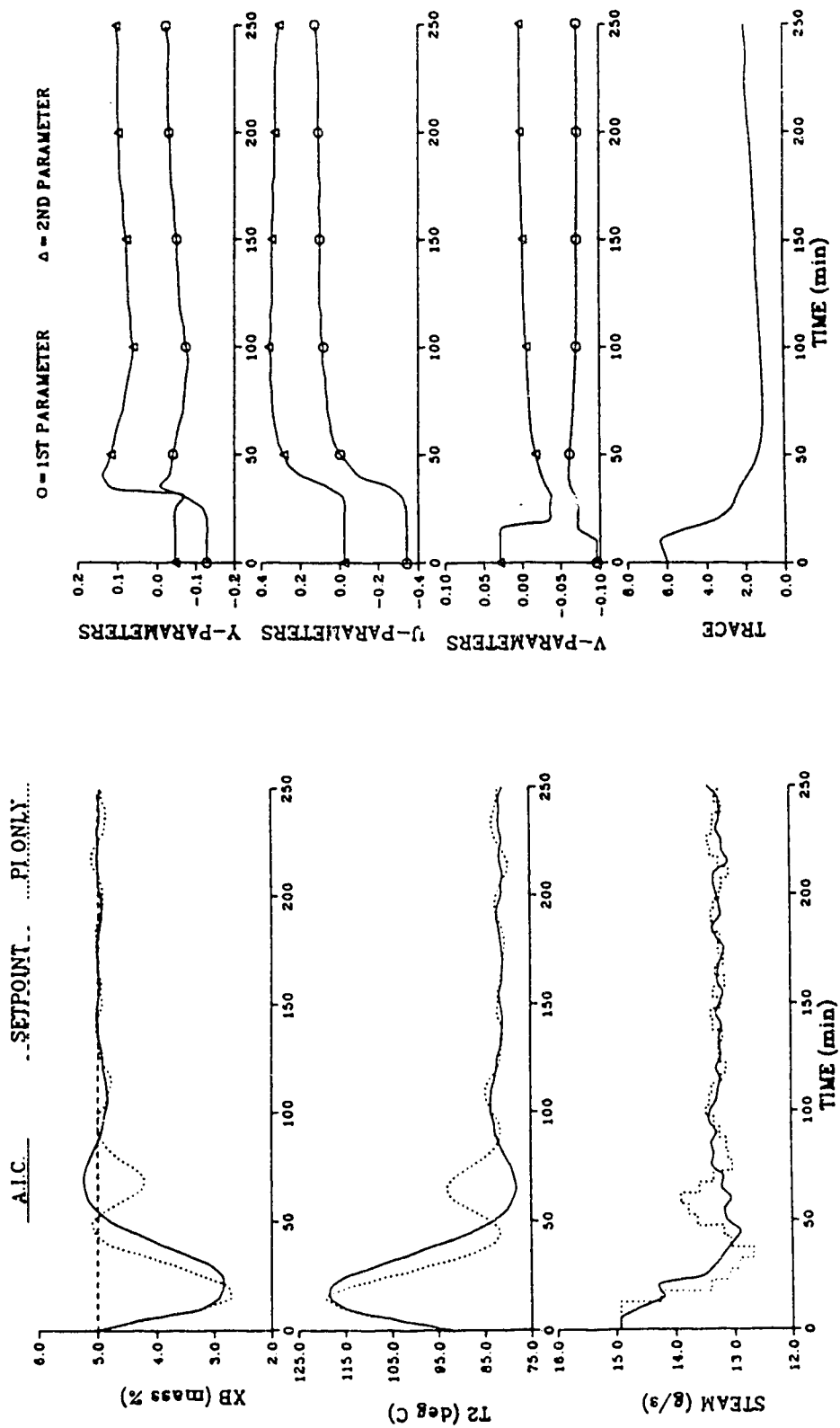


Figure 3.14 Comparison of Conventional PI and SM-2 AIC Control Performance for Changes in the Transfer Function Gains and Time Delays and AIC Parameter Trajectories

SM-2 algorithm was comparable to the value that resulted from using the PI scheme. It should be noted that these changes in process gains and time delays had the most profound effect on the control performance of the standard algorithm, with the IAE value having increased by 65% compared to the base case (c.f. Table 3.3). The effect of the changes in gains and time delays on the control performance using the PI scheme is minimal (IAE value increased by 21%) as is the increase in the IAE value for either the SM-1 or SM-2 scheme of about 28%. When an AIC algorithm is employed, the identification algorithm needs time to adapt the parameters due to the changed process characteristics in order to generate good prediction of the actual controlled output. Since the ST-1 scheme requires the identification of 12 parameters, as compared to 3 for the SM-1 scheme and 6 for the SM-2 scheme, it is understandable that it will take the standard algorithm longer for the parameters to converge to new values and so it is not surprising that the effect of the changes in process gains and time delays on control performance is most significant when the ST-1 algorithm is used. The basis for this explanation can be appreciated by comparison of the controlled responses and parameter trajectories shown in Figs. 3.12 to 3.14 with the corresponding base case closed loop control behavior displayed in Figs. 3.2 to 3.4. By comparing the  $X_B$  trajectory shown in Fig. 3.2 to that in Fig. 3.12, it can be observed that the rise time increased by about 10 minutes and the maximum excursion of  $X_B$  from the set point increased by approximately 0.7 mass percent methanol when the changes in process gains and time delays was introduced. The parameter trajectories displayed in these two figures reveal that for the base case, the parameters changed in a "smoother" manner than was the case when the process parameters changed. When the parameter

trajectories for the SM-1 and SM-2 schemes, shown in Figs. 3.13 and 3.14 respectively, are examined, the robustness of the simplified algorithms can be readily appreciated because even in this case with changes in process parameters, the adaptation of the parameters was almost as "smooth" as in the base case (c.f. Figs. 3.3 and 3.4). The effect of the time-variant nature of the process on the control performance of the simplified algorithms was not very significant.

### 3.5 Summary

Simulation to determine the effectiveness of the three AIC algorithms (ST-1, SM-1 and SM-2) for controlling the bottoms composition of a binary column, characterized by a transfer function model compared with the control response achieved using the conventional feedback PI control scheme shows that the standard algorithm (ST-1) provided the best control performance. This was found to be the case for both the step changes in feed rate and set point.

All three AIC schemes were found to be sensitive to the choice of the secondary output. Selection of the liquid temperature on tray 6,  $T_6$ , instead of  $T_2$  caused the control performance to deteriorate as  $T_6$  is not as sensitive to changes in feed and steam rates as  $T_2$ . Because a large number of parameters (12 in this case) had to be identified, the effect of a poor choice of the secondary output on control behavior was most profound when the standard algorithm was employed.

The robustness of the AIC schemes has also been investigated by changing some process parameters (gains and time delays) when a step disturbance in feed rate was introduced into the process. The standard

algorithm again provided the best control performance. However, as in the case where an insensitive secondary output was used, the degradation in control performance, compared to the base case where the process parameters were not changed, was most significant when the standard algorithm was used because of the large number of parameters that had to be identified. These results indicate that a potential problem of the convergence of parameters may arise when the standard algorithm is applied to control a highly nonlinear and/or time-varying process.

## Chapter 4 : Multirate Adaptive Inferential Control of a Nonlinear System

### 4.1 Introduction

The evaluation of the control performance of the AIC schemes for control of linear systems is extended to the control of a nonlinear system in this chapter. Control of a five component depropanizer is studied using DYCONDIST, a general purpose digital dynamic simulator of multicomponent distillation columns (Wong and Wood, 1985; Carling and Wood, 1986; Yiu *et al.*, 1989). In Section 4.2, the DYCONDIST program is briefly described and the depropanizer example used in this work is introduced in Section 4.3. The four schemes evaluated in Chapter 3 (PI, ST-1, SM-1 and SM-2) were employed to regulate the composition of the light key (LK) in the bottoms product of the depropanizer to its set point when the process was subjected to changes in feed rate, feed compositions, and set point. The robustness of the AIC algorithms was also investigated by increasing the cycle time of the composition analyzer. The sensitivity of the AIC schemes to selection of tray temperature was also examined. The control performance for regulation of bottoms composition using the truncated first order standard algorithm, presented in Chapter 2, was compared with the performance obtained using the other AIC algorithms.

### 4.2 The DYCONDIST Simulator

The DYCONDIST simulator was originally developed by Wong (1985) and further enhanced by Carling (1986). The program has been developed using a modular program structure and so the user can easily extend the program to incorporate modifications to the column model (e.g. new type of tray) or add

additional control strategies and algorithms for evaluation.

The multicomponent distillation column model employed consists of a collection of ordinary differential and algebraic equations. These equations, based on rigorous material and energy balances, are expressed in a general form so that the behavior of towers with multiple feed streams as well as columns with sidestream draw-offs can be simulated. The material and energy balance differential equations are based on a general stage representation (Carling, 1986; Carling and Wood, 1986). The C+1 material balance differential equations employed in the simulator are based on the following assumptions :

- (1) nonreactive mixture
- (2) perfect mixing in the stage
- (3) negligible material holdup in the vapor phase and of liquid in the tray downcomers

while the general energy balance for the  $j$ th stage is obtained by assuming

- (1) negligible energy and material holdup in the vapor phase
- (2) negligible energy storage in the stage metal
- (3) negligible energy storage in the liquid contained in tray downcomers
- (4) negligible heat of mixing among species

Thermodynamic properties/data for either ideal or nonideal species can be easily employed with the simulator because of its modular nature. Column dynamic behavior is predicted by the solution of these material and energy balance differential equations in conjunction with user specified ideal or nonideal vapor-liquid equilibrium functional relationships. Solution of this set of  $N(2C+3)$  equations, known as the "MESH" equations (Henley and

Seader, 1981), for unsteady state operation involves their solution at each time step with the liquid composition and flow rate determined first. The integration algorithm utilized in DYCONDIST is the adaptive semi-implicit Runge-Kutta (ASIRK) method proposed by Prokopakis and Seider (1981). This algorithm and the step size control strategy, adopted from the work of Ballard *et al.* (1978), have been discussed in detail by Wong (1985).

The stage temperatures and vapor compositions are solved for using an iterative procedure based on Newton's method using the stage liquid compositions in conjunction with the vapor-liquid equilibrium specifications. Finally, the stage vapor flow rates are solved from the energy balance differential equation of each stage. The procedure adopted from Ballard *et al.* (1978) is discussed in detail by Carling (1986).

In this work, the DYCONDIST simulator has been enhanced to make it more suitable for evaluating control algorithms by allowing for :

- (1) up to twenty separate input disturbances applied to the column at different times;
- (2) feed stream data (temperature, flow rate, compositions), reboiler duty, and reflux rate to be read from a data file;
- (3) a sampled-data process analyzer, with user specified cycle time, to be implemented for every control loop (except for level control).

In addition, the AIC algorithms examined in this work have also been incorporated into the library of control algorithms of the DYCONDIST program. The AIC algorithms have been written in such a way to make the schemes very general while making minimum modifications to the original program. The user can control the liquid composition at any tray using the

liquid temperature at any stage as a secondary output in conjunction with a manipulated variable (e.g. reboiler duty, reflux rate). The time at which to initiate identification of the model parameters and the time to activate the AIC algorithm for product composition control can also be specified. Furthermore, data conditioning can be performed by specifying nominal values and scaling factors used in forming the regressor vector (c.f. Section 4.4.2). The algorithm also allows the user to specify a dead-band when performing the identification and for using the predicted output from an AIC scheme for control calculation.

#### 4.3 Description of the Depropanizer Column

The depropanizer column used in this work has been studied by Carling and Wood (1986). The operating conditions for this five component column are based on those presented by Cook (1980) and Carling et al. (1978) and subsequently modified by Wong (1985). The column has 29 trays, a total condenser and a total reboiler. Stages are numbered from top to bottom, with stage 1 being the condenser and stage 31 being the reboiler. There is a single saturated liquid feed consisting of ethane, propylene, propane, isobutane and cis-2-butene entering at stage 13 (tray 12). Operating conditions for the 31 ideal stage column are presented in Table 4.1. The control objective in this study is control of the concentration ( $X_B$ ) of propane, the light key (LK), in the bottoms to its set point by manipulating the reboiler duty,  $Q_R$ . It is assumed that an on-line composition analyzer (e.g. gas chromatograph), which has a cycle time of 5 minutes, measures bottoms composition. Liquid temperature at a user specified stage is sampled at a 1 minute interval. The details on the polynomial functions



Table 4.1  
Depropanizer Operating Conditions

Feed :

Temperature	353 K
Pressure	2.6 MPa
Rate	50 kmol/min
Composition (mole fraction)	
ethane	0.03
propylene	0.40
propane (LK)	0.15
isobutane (HK)	0.15
cis-butene	0.27

Column conditions :

Pressure	2.6 MPa
Reflux rate	90 kmol/min
Reboiler duty	584 kJ/min
Accumulator holdup	50 kmol
Column base holdup	50 kmol
Tray holdup	12-22 kmol <sup>(1)</sup>

Product rates and purities :

Distillate rate	28.6 kmol/min
Bottoms rate	21.4 kmol/min
Heavy key in distillate	0.42 mole %
Light key in bottoms	1.63 mole %

(1) See Appendix B for tray holdup profile.

used to characterize the liquid and vapor enthalpies and equilibrium ratios are given in Appendix B.

#### 4.4 Implementation of the AIC Algorithms

##### 4.4.1 Selection of the Secondary Output

The secondary output used in the AIC schemes is the temperature of the liquid on a specified tray. In order to compare the control responses of the proposed algorithm with those of single tray temperature feedback control, the tray liquid temperature used for the adaptive schemes is the same as would be used for conventional single tray temperature feedback control. Many criteria have been suggested for determining the optimum control tray for temperature feedback control (e.g. Boyd, 1948 a,b, 1963, 1967; Rademaker *et al.*, 1975; Shinskey, 1984; Tolliver and McCune, 1978 and 1980). The criterion used in this work is that the selected tray liquid temperature should show the largest temperature deviations for step changes (increases and decreases) for a given magnitude of disturbance, and the temperature deviations should also be symmetrical (Tolliver and McCune, 1978). Fig. 4.1 shows the open loop responses of four stage liquid temperatures to a 10% feed flow rate step decrease at time  $t=0$  followed by a 10% feed rate step increase to a value of 60 kmol/min at  $t=50$  minutes. It can be seen that the liquid temperature on stage 10 (tray 9) in the rectification section is not sensitive to the flow rate disturbances. However, the temperature responses of the liquid at the other three stages (17, 23 and 27) in the stripping section are sensitive. Since the dynamic response of the liquid temperature on stage 23 ( $T_{23}$ ) is the most sensitive to the feed rate changes, this stage is selected as the location for the

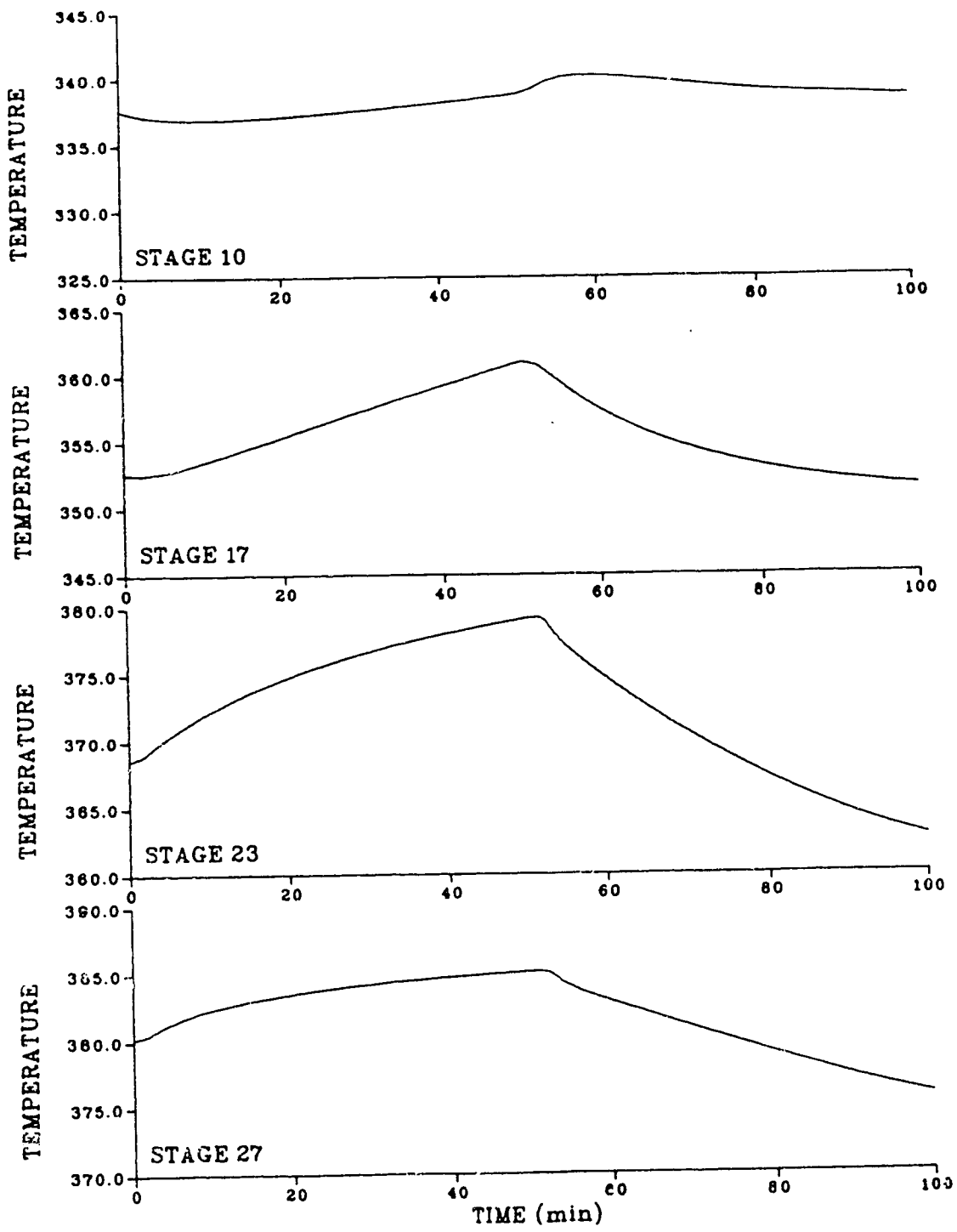


Figure 4.1 Open Loop Responses of Four Tray Liquid Temperatures to Step Changes in Feed Rate (-10% F at t=0 ; +10% F at t=50)

stripping section temperature sensor, i.e.  $T_{23}$  is chosen to be the secondary measured output for use in the adaptive control laws. This same stage liquid temperature was selected by Carling (1986) as the temperature for tray temperature feedback control of bottoms composition.

#### 4.4.2 Estimation Equations, Identification and Initialization

As mentioned earlier, the cycle time of the analyzer was selected to be 5 minutes and the tray liquid temperature was sampled at a 1 minute interval. Thus, the ratio of the larger sampling time to the smaller sampling time, denoted as  $J$  in Chapter 2, is 5. Using a first order plant model for the standard algorithm (ST-1) and first and second order models for the simplified algorithm (SM-1 and SM-2), the three estimator equations obtained are the same as those presented in Chapter 3 (c.f. Eqs. 3.5 to 3.7). As in Chapter 3, each estimator was combined with a fixed parameter proportional plus integral controller (Eq. 3.8) to form an AIC scheme. The control performance obtained using the three AIC schemes is compared with the performance obtained using the conventional PI feedback control scheme.

The initial settings of the proportional plus integral controller, established using the process reaction curve and the Cohen-Coon formulae (Stephanopoulos, 1984), were calculated to be  $K_P = -0.463 \left( \frac{\text{MJ/min}}{\text{mol fract}} \right)$  and  $K_I = -0.116 \left( \frac{\text{MJ/min}}{\text{mol fract-min}} \right)$ . The controller settings for each scheme were tuned for a 5% step decrease in feed flow rate (from steady state) at time  $t=0$  followed by a step increase in feed flow rate to its original steady state value (50 kmol/min) at  $t=100$  minutes. The settings which gave the minimum IAE value were chosen as the final settings. For the PI control scheme, the controller settings are  $K_P = -1.7 \left( \frac{\text{MJ/min}}{\text{mol fract}} \right)$  and

$K_I = -0.425 \left( \frac{\text{MJ/min}}{\text{mol fract} \cdot \text{min}} \right)$ . The controller settings for the AIC schemes are summarized in Table 4.2.

Table 4.2  
Tuned Controller Settings for the AIC Schemes Using Stage 23  
Liquid Temperature as the Secondary Output

Scheme	$K_P \left( \frac{\text{MJ/min}}{\text{mol fract}} \right)$	$K_I \left( \frac{\text{MJ/min}}{\text{mol fract} \cdot \text{min}} \right)$
ST-1	-2.2	-0.176
SM-1	-1.8	-0.180
SM-2	-1.8	-0.180

Since the process is very nonlinear, the RLS identification algorithm that is implemented utilizes a variable forgetting factor to maintain a constant trace of the covariance matrix. This idea, originated from the improved least squares (ILS) algorithm of Sripada and Fisher (1987), has been presented in Chapter 2. The scaling option in the origin ILS algorithm was not implemented. To prevent significant bursting in process parameters when there is a sudden change in the process characteristic, the minimum value of the forgetting factor,  $\lambda$ , is 0.2. If  $\lambda$  drops below this minimum value, the covariance matrix is reset to its initial value. For all simulations presented in this chapter, the covariance matrix was initialized to the identity matrix and the trace of the covariance matrix was maintained constant at its initial value. All the initial parameters in the parameter vector were the final values obtained from the controller tuning runs which used the tuned controller settings listed in Table 4.2. To prevent numerical problems, all the values used in the regressor vector are scaled deviation values, with the scaled deviation value defined as

$$\text{scaled deviation value} = \frac{\text{actual value} - \text{nominal value}}{\text{scaling factor}} \quad (4.1)$$

where the nominal values and scaling factors for  $y$  (the controlled output),  $u$  (the manipulated variable) and  $v$  (the secondary output) are specified by the user. Thus, the scaled deviation value of  $y$ , denoted as  $\tilde{y}$ , is given by

$$\tilde{y}(t) = \frac{y(t) - y_{\text{nom}}}{y_{\text{sca}}}$$

The scaled deviation values of  $u$  and  $v$  are defined in the same manner.

Since scaled deviation values are used in the regressor, the predicted  $y$  is also a scaled deviation value. The value of  $y_e(t)$  is then obtained by

$$y_e(t) = y_{\text{sca}} * y_{e_{\text{sca}}}(t) + y_{\text{nom}}$$

where  $y_{e_{\text{sca}}}$  is the scaled deviation value of  $y_e$ .

In this work, the nominal values for  $y$ ,  $u$  and  $v$  were set to the initial steady state values. In other words, the nominal values, neglecting the units for convenience, for  $y$ ,  $u$  and  $v$  were 0.0163, 0.5 and 368.56 (if  $T_{23}$  was used as the secondary output). The scaling factors were chosen to scale each of the deviation values to the same order of magnitude. Based on closed loop response obtained when the PI scheme was employed, the magnitudes of the deviation values (i.e. actual value - nominal value) for  $y$ ,  $u$  and  $v$  were in the order of  $10^{-2}$ ,  $10^{-2}$  and  $10^1$  respectively. The scaling factors for  $y$ ,  $u$  and  $v$  selected were 0.001, 0.001 and 1.0 so that the resulting magnitudes of the scaled deviation values used in the regressor were all in the order of  $10^1$ .

## 4.5 Simulation Results

The four control schemes (PI, ST-1, SM-1 and SM-2) were evaluated for changes in feed rate, feed compositions, set point and cycle time of the composition analyzer. The specific details of these tests are summarized in Table 4.3. It should be noted that test MD4 is a very severe test of the robustness of the control algorithms since it involves a large disturbance in feed rate in addition to an increase of 3 minute in the analyzer cycle time.

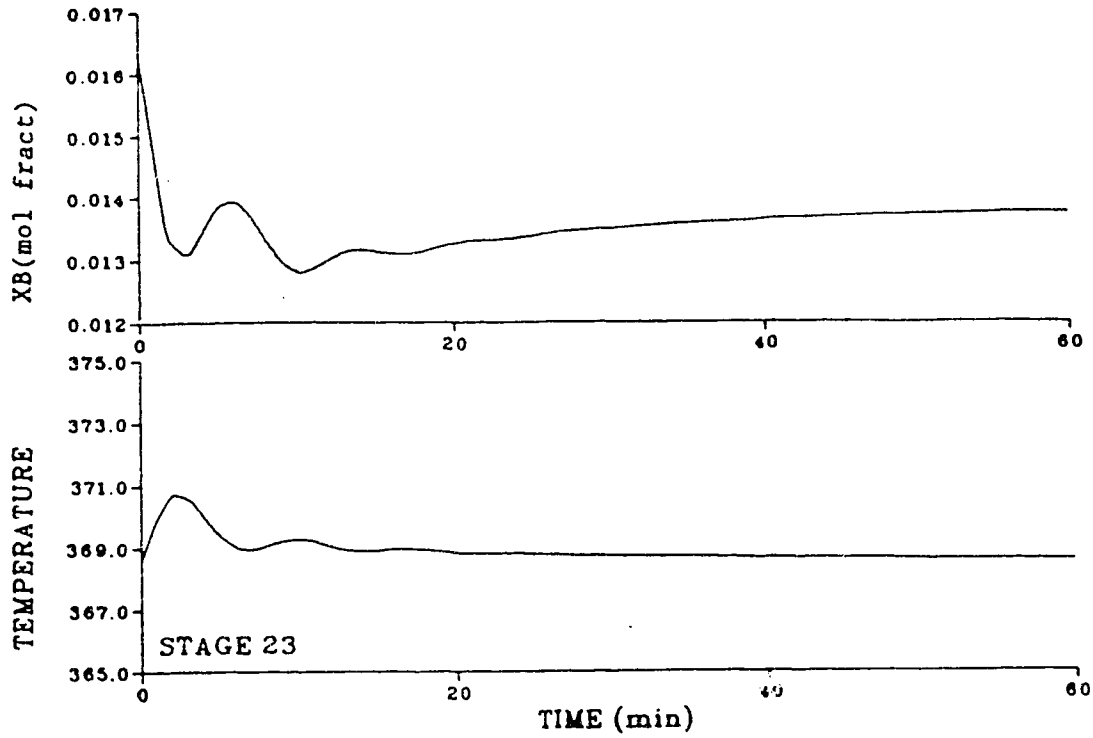
### 4.5.1 Single Tray Temperature Feedback Control

As mentioned in Chapter 1, the most commonly used composition estimation technique is the measurement of the liquid temperature on a single stage in the column. Use of tray temperature feedback control for regulating product quality will result in steady state offset (Pakte *et al.*, 1982). This drawback is exemplified by the control behavior shown in Fig. 4.2 for feedback control of the liquid temperature at stage 23. The proportional plus integral controller settings, established by Carling (1986), employed are  $K_p=0.012 \left( \frac{\text{MJ}/\text{min}}{\text{K}} \right)$  and  $K_i=0.10 \left( \frac{\text{MJ}/\text{min}}{\text{K}-\text{min}} \right)$ . It is obvious from Fig. 4.2 that controlling  $T_{23}$  to its original steady state value of 386.56 K leads to a large offset in  $X_B$  for step increases and decreases in feed rate.

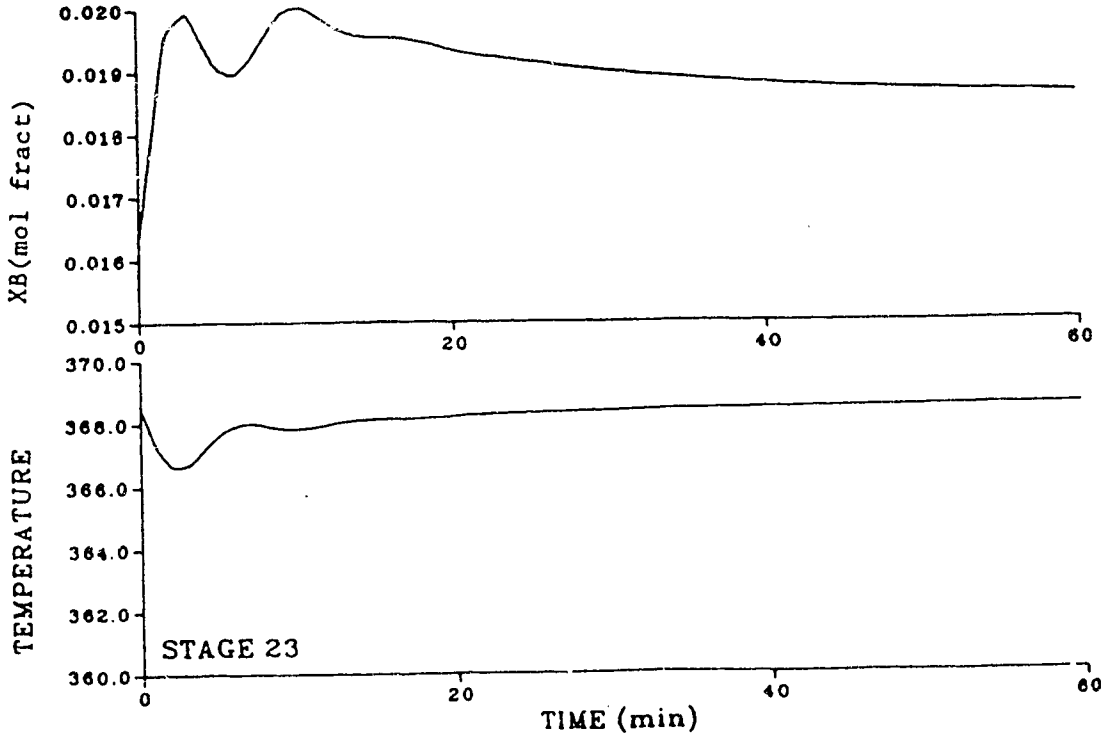
Table 4.3  
Description of the Tests Used in Simulation of  
Control of the Depropanizer

Test	Magnitude and type of change	Duration (minutes)	Cycle time of analyzer (minutes)
MD1	-20% feed rate	0-150	5
MD2	+20% feed rate	0-150	5
MD3	Feed composition change. New feed concentrations are : $z_1=0.03$ $z_2=0.37$ ( $\downarrow$ 7.5%) $z_3=0.18$ (LK, $\uparrow$ 20%) $z_4=0.12$ (HK, $\downarrow$ 20%) $z_5=0.30$ ( $\uparrow$ 11%)	10-150	5
MD4	+20% feed rate	0-200	8
MSP1	-20% set point	0-150	5





(a) -20% F (test MD1)



(b) +20% F (test MD2)

Figure 4.2 Single Tray Temperature Feedback Control of Bottoms Composition for +20% and -20% Step Changes in Feed Rate

#### 4.5.2 Control Performance of the Adaptive Inferential Control Scheme Using a Sensitive Secondary Output

##### (i) 20% Step Decrease in Feed Rate

Table 4.4 provides a summary of the IAE performance value for each AIC scheme and the conventional feedback PI control scheme when a -20% step change in feed rate (MD1 test) was introduced into the process. The closed loop responses obtained using the ST-1, SM-1 and SM-2 control strategies are compared in Figs. 4.3 to 4.5 with the controlled response obtained by utilizing the PI scheme. As mentioned in Chapter 3, for the sake of clarity, only seven of the twelve parameters of the ST-1 scheme will be shown in the parameter trajectories presented in this chapter. As can be seen from the IAE values reported in Table 4.4, the SM-1 algorithm provided the best control performance, yielding an IAE value of 0.268. The IAE performance index resulted from utilizing either ST-1 or SM-2 scheme is comparable to the value that resulted from using the PI scheme. It should be noted that all of the AIC schemes provided superior control performance to that obtained using the PI scheme. From the controlled responses shown in Figs. 4.3 to 4.5, it can be observed that all four control schemes were able to bring the composition ( $X_B$ ) of the light key component in the bottoms product to its set point. However, the controlled response of  $X_B$  that resulted when the PI scheme was employed is more oscillatory than the controlled behavior achieved using the AIC algorithms. The maximum absolute excursion of  $X_B$  from its set point is about the same for all four control schemes.

Since the performance of the AIC schemes depends mainly on the accuracy of the predicted values of  $X_B$ , it is necessary to compare the predicted  $X_B$

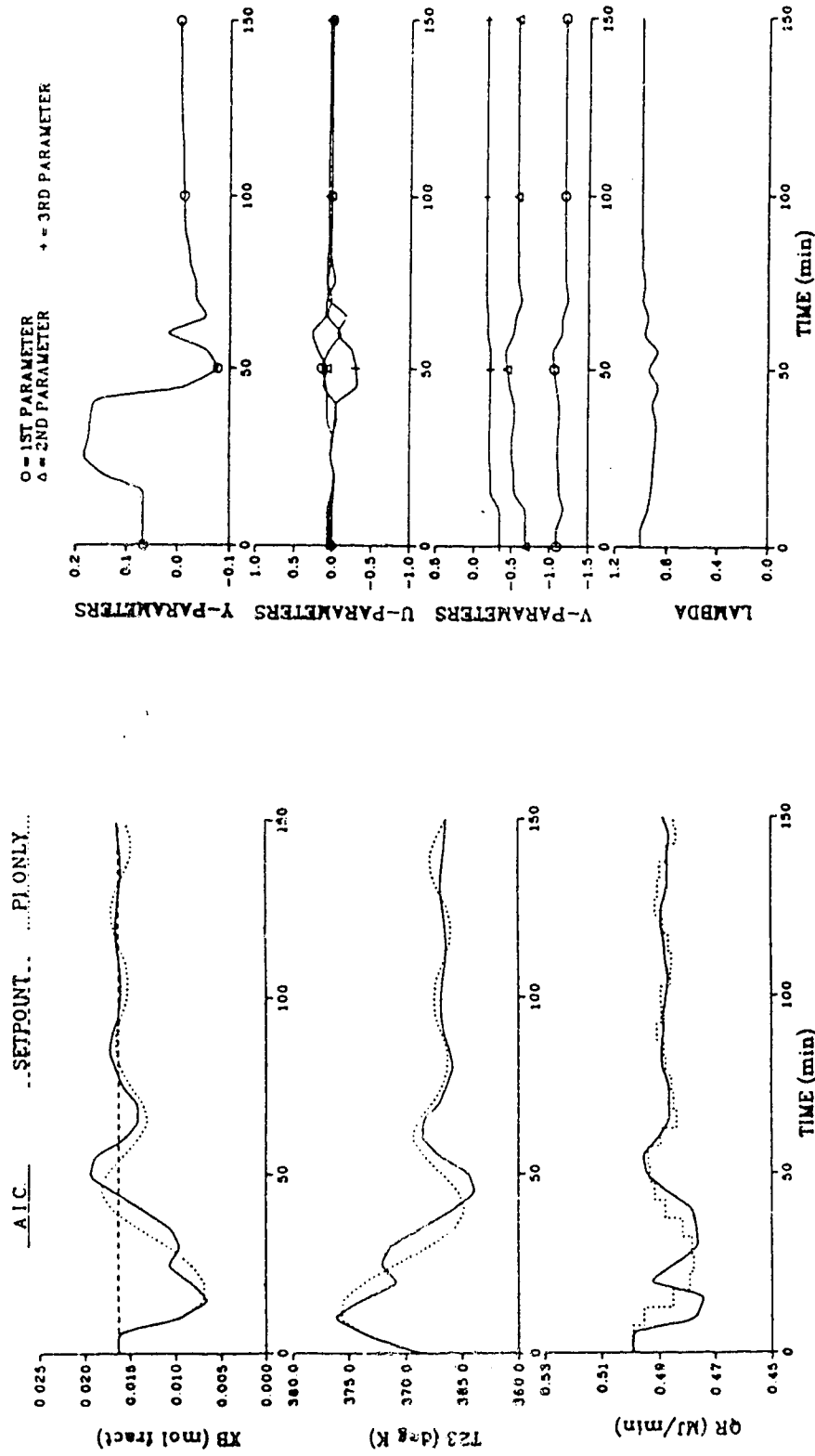


Figure 4.3 Comparison of Conventional PI and ST-1 AIC Control Performance for a -20% Step Change in Feed Rate and AIC Parameter Trajectories (No Dead-band with AIC)

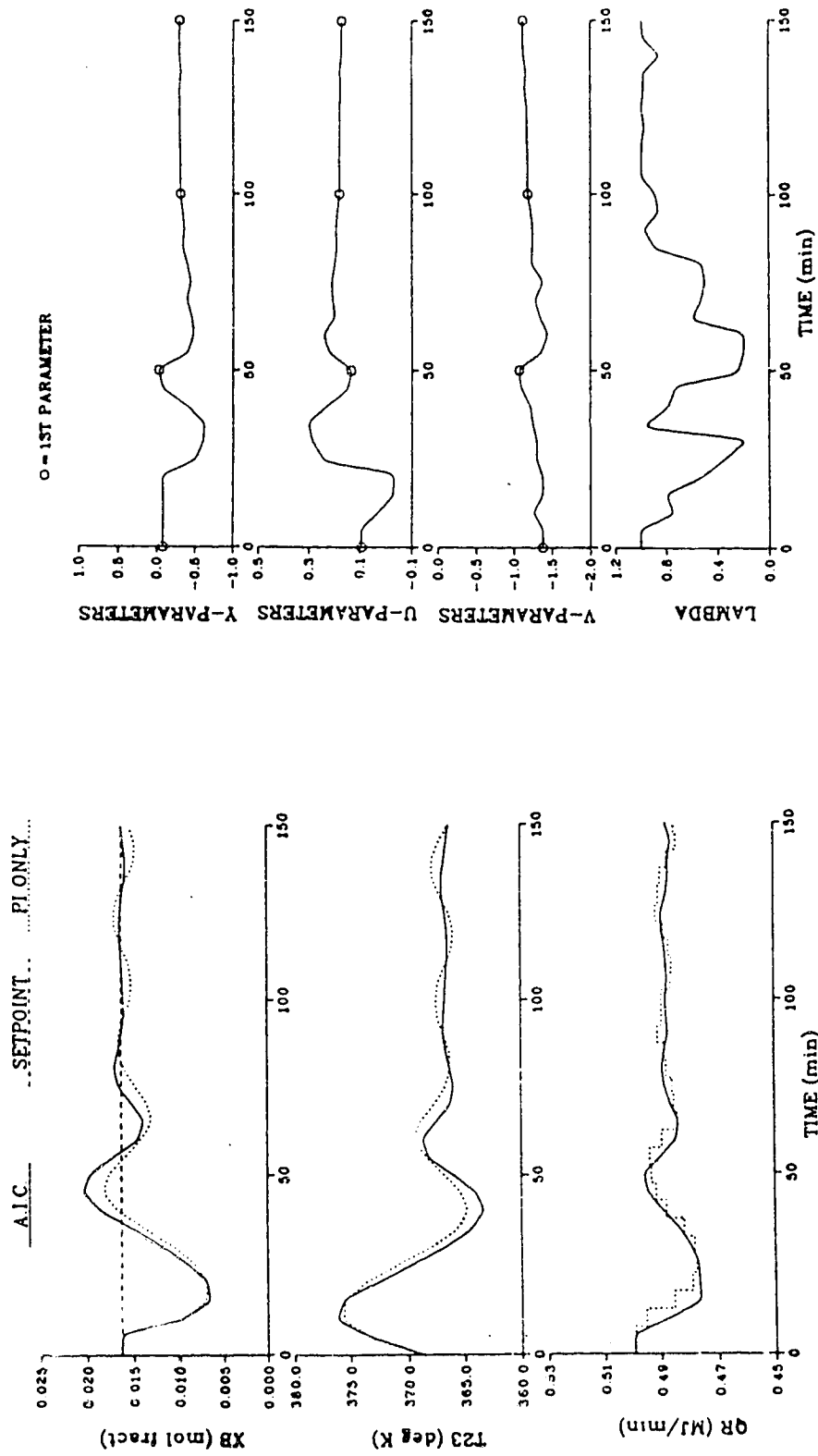


Figure 4.4 Comparison of Conventional PI and SM-1 AIC Control Performance for a -20% Step Change in Feed Rate and AIC Parameter Trajectories (No Dead-band with AIC)

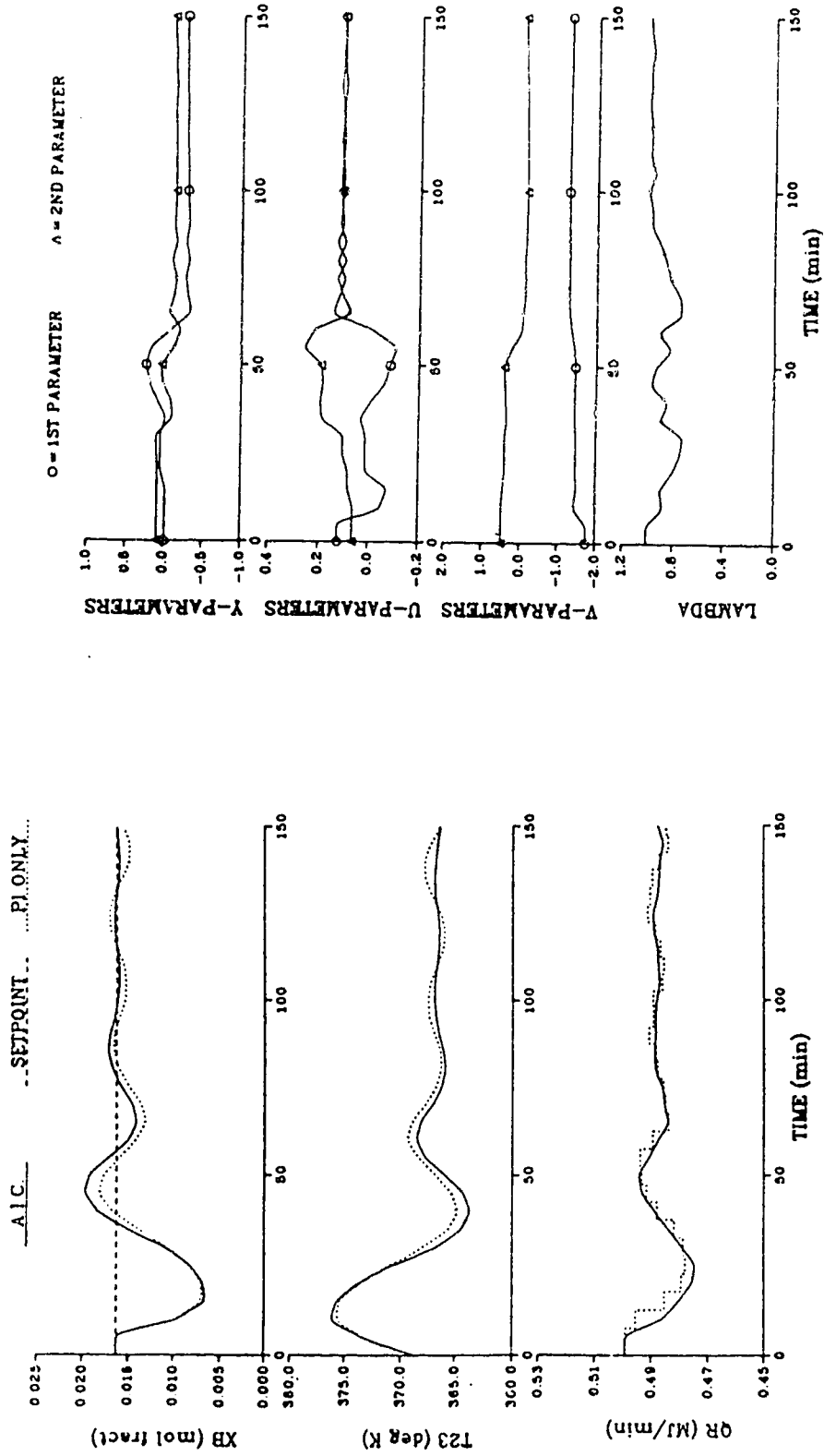


Figure 4.5 Comparison of Conventional PI and SM-2 AIC Control Performance for a -20% Step Change in Feed Rate and AIC Parameter Trajectories (No Dead-band with AIC)

with actual  $X_B$  to explain the control behavior obtained using the AIC schemes. In Fig. 4.6, the predicted  $X_B$  is compared with the actual  $X_B$  for each of the AIC schemes. As can be observed from the top plot in Fig. 4.6, the predicted  $X_B$  generated by the ST-1 algorithm was very erratic during the initial transient period when the feed disturbance was introduced but the prediction matched the actual controlled output after 30 minutes of operation. However, the plots of predicted  $X_B$  for the simplified algorithms reveal that the SM-1 and SM-2 schemes were able to generate quite accurate predictions of the controlled output during the initial transient period. As no dead-band (c.f. Section 2.5) was employed with the AIC schemes, the predicted  $X_B$  was used for calculating the reboiler duty  $Q_R$ , the manipulated variable, every 1 minute. Therefore, the erratic prediction generated by the ST-1 scheme resulted in inappropriate and more oscillatory changes in  $Q_R$  during the initial transient period, as can be seen from the trajectories in the reboiler duty shown in Fig. 4.3. Consequently, poorer control performance resulted when the ST-1 scheme was employed.

Table 4.4  
Summary of Control Performance for a -20% Step Change in Feed Rate

<u>Control Scheme</u>	<u>IAE (mol fract-min)</u>	<u>Reference Figures</u>
PI	0.429	4.22-4.24
ST-1	0.312	4.22
SM-1	0.228	4.23
SM-2	0.223	4.24

The fast speed of convergence of the predicted value of  $X_B$  to the actual  $X_B$  when the simplified algorithms were employed could be attributed

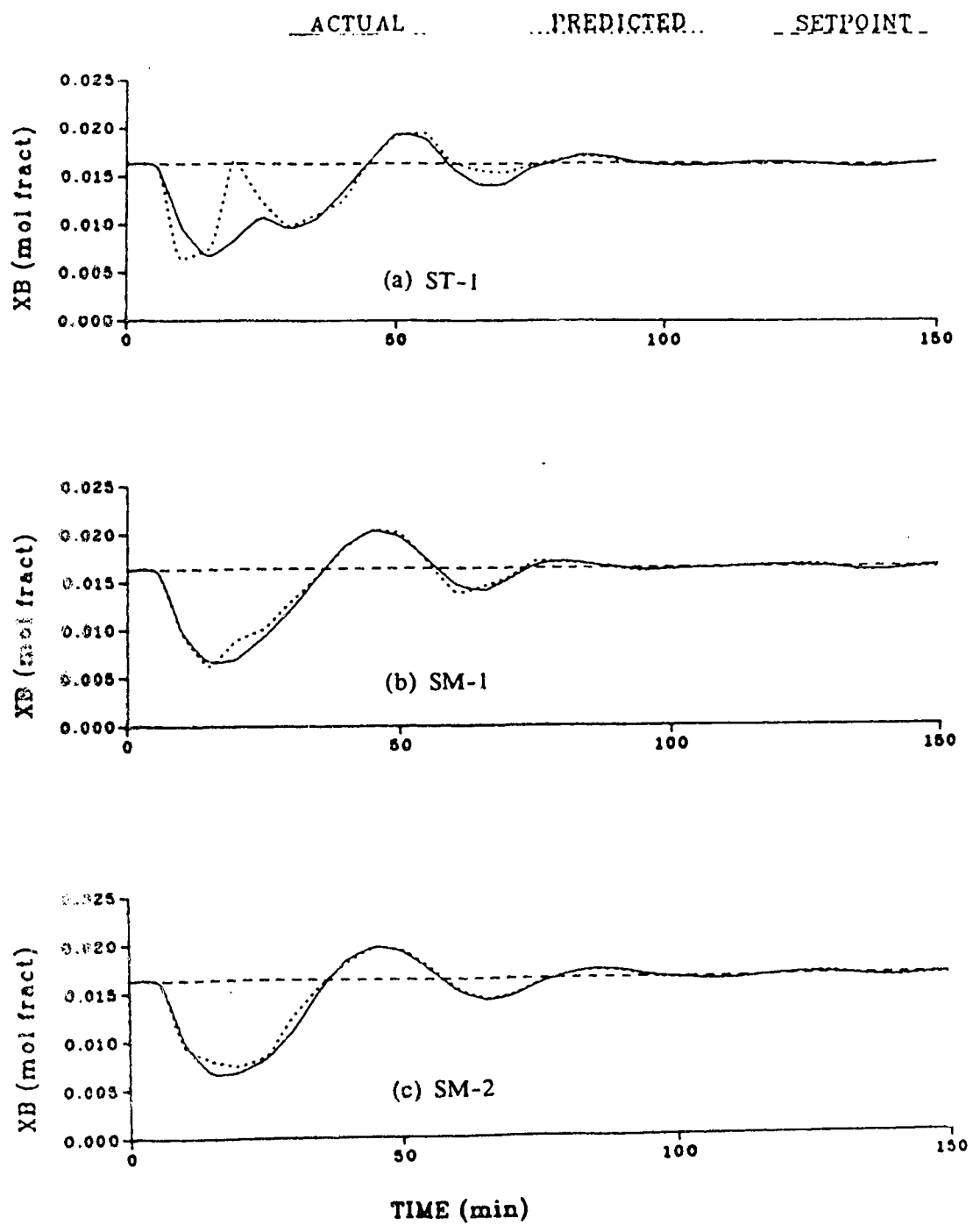


Figure 4.6 Comparison of Predicted Bottoms Composition versus Actual Bottoms Composition for a -20% Step Change in Feed Rate (No Dead-band with AIC)

to the small number of parameters that had to be identified. The SM-1 scheme only has 3 parameters while the SM-2 algorithm has 6 but the ST-1 scheme has 12 parameters and thus it should take longer for the parameters of the ST-1 scheme to converge to new values, resulting in slow convergence of the prediction to the actual controlled output. It can be seen from the parameter trajectories presented in Figs. 4.3 to 4.5 that the parameters of the simplified algorithms converged to new values after only 60 minutes of operation while the parameters of the ST-1 scheme did not converge until  $t=100$  minutes. Since the ST-1 scheme has 12 parameters, it requires "richer" information from the regressor than the simplified algorithms so as to achieve fast parameter convergence. From the trajectories of the variable forgetting factor (designed as  $\lambda$  trajectories hereafter) presented in these figures, it can be observed that there was very slow adaptation when the ST-1 scheme was employed since the variable forgetting factor,  $\lambda$ , changed very slowly compared with the pattern of change observed for either of the simplified algorithms.

(ii) 20% Step Increase in Feed Rate

The control behavior obtained using the ST-1, SM-1 and SM-2 control schemes is compared with that obtained by employing the PI scheme in Figs 4.7 to 4.9 when a +20% step change in feed rate (test MD2) was introduced into the process. The best control performance, with an IAE performance index of 0.320, resulted from using the SM-1 algorithm while the largest IAE value (1.950) resulted when the ST-1 strategy was employed. The IAE values for the SM-2 and PI schemes were calculated to be 0.372 and 0.429 respectively. Due to the highly nonlinear characteristic of the process, the IAE values obtained for this test MD2 are significantly different from



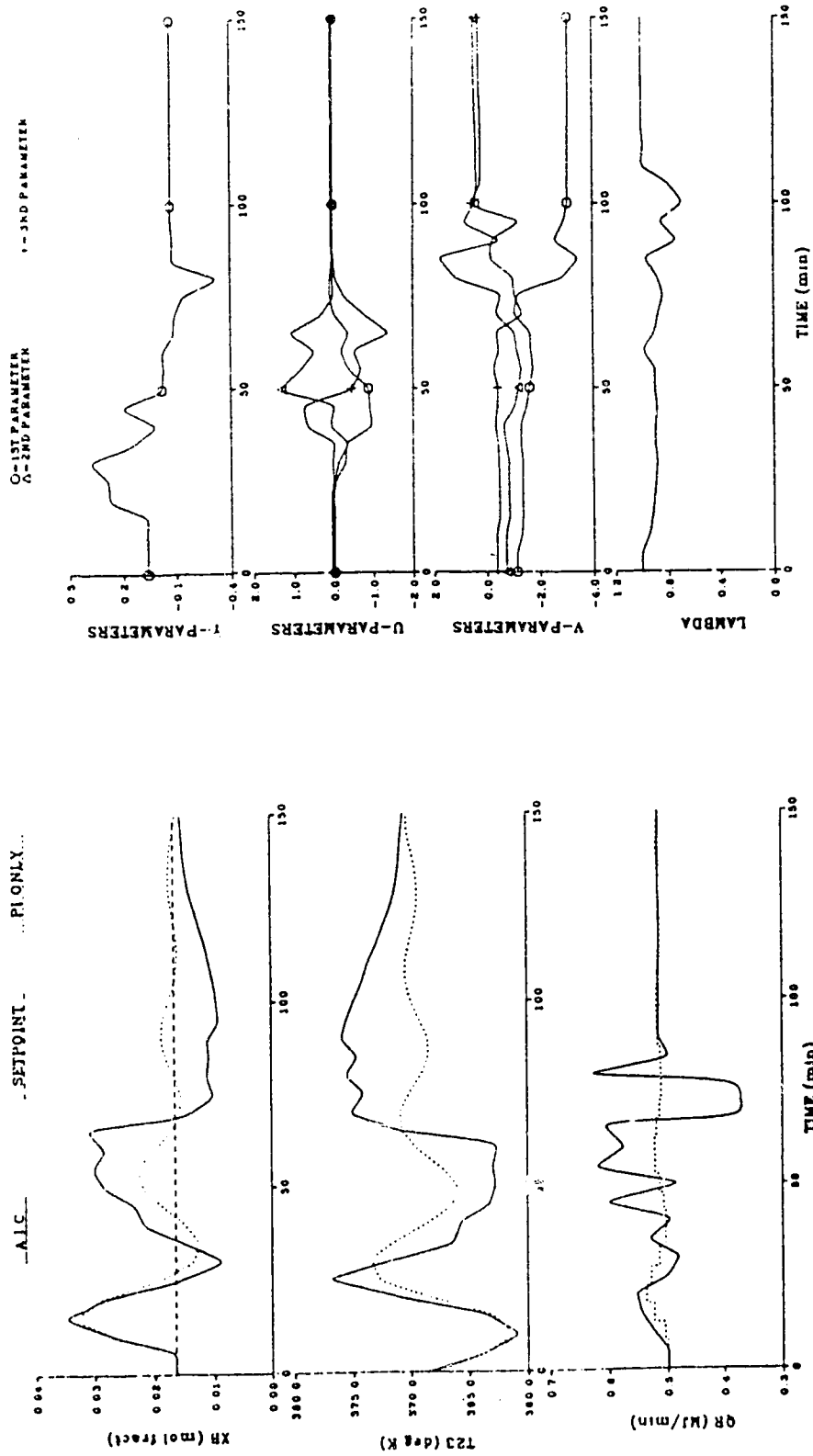


Figure 4.7 Comparison of Conventional PI and ST-1 AIC Control Performance for a +20% Step Change in Feed Rate and AIC Parameter Trajectories (No Dead-band with AIC)

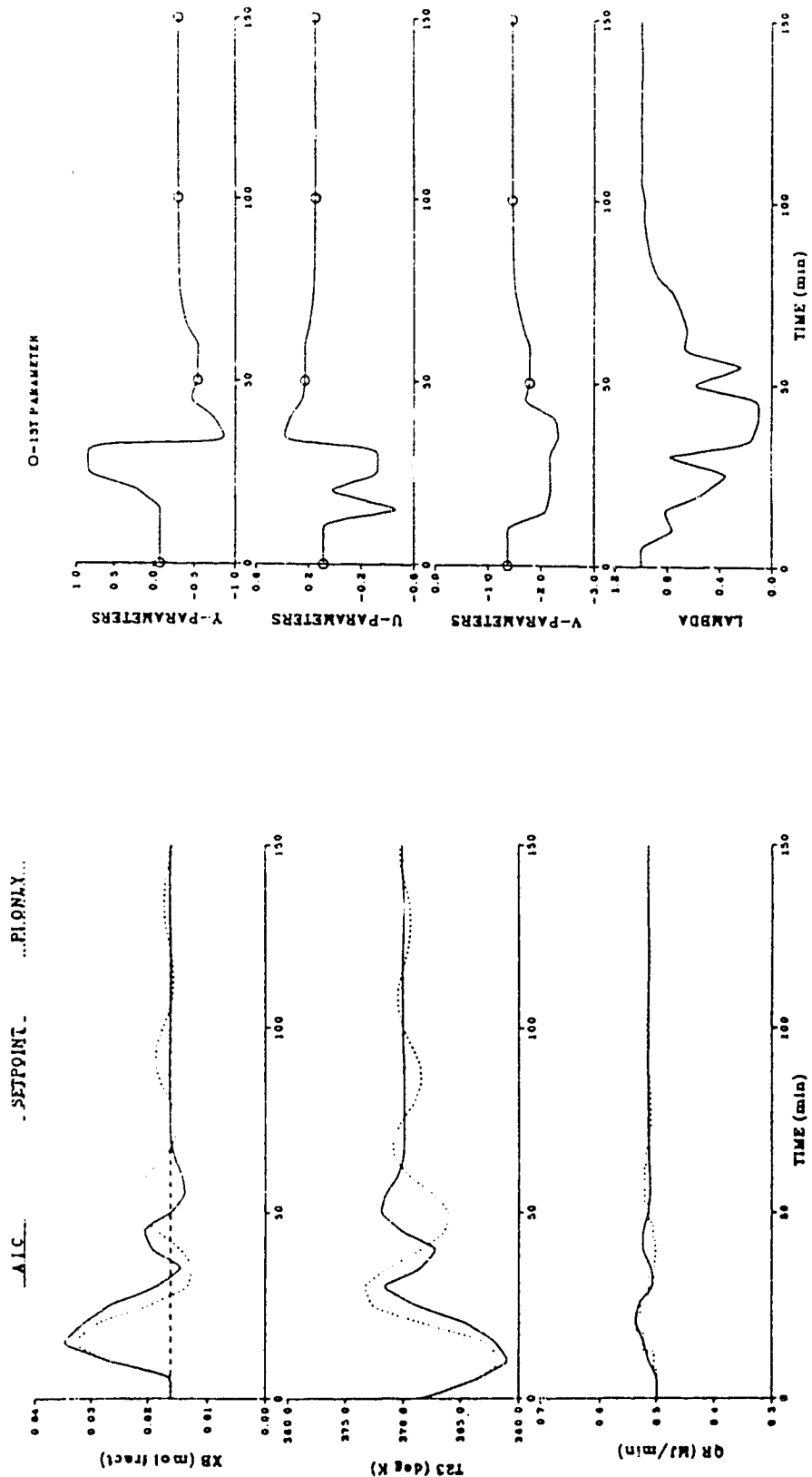


Figure 4.8 Comparison of Conventional PI and SM-1 AIC Control Performance for a +20% Step Change in Feed Rate and AIC Parameter Trajectories (No Dead-band with AIC)

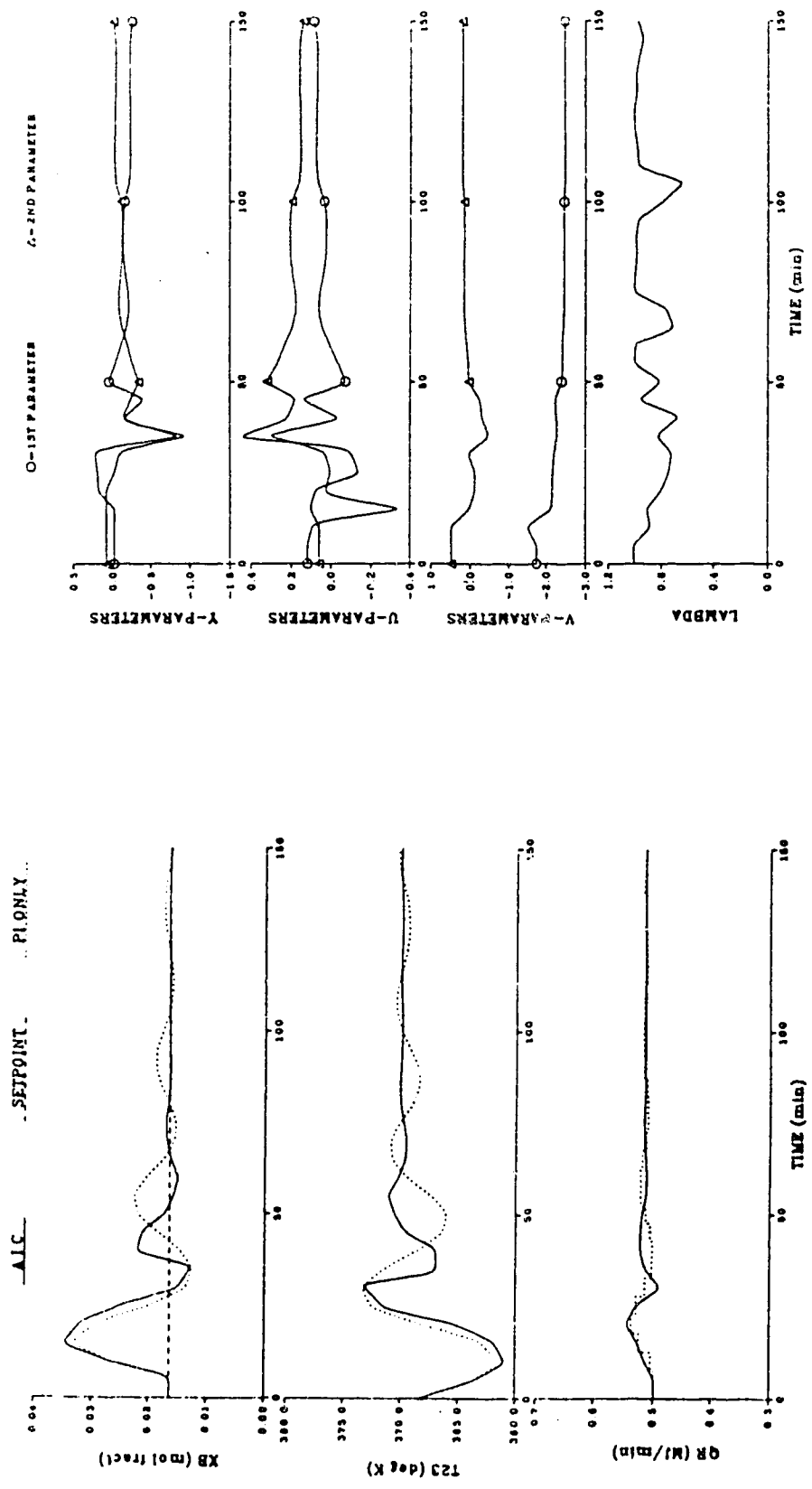


Figure 4.9 Comparison of Conventional PI and SM-2 AIC Control Performance for a +20% Step Change in Feed Rate and AIC Parameter Trajectories (No Dead-band with AIC)

those values obtained for the MDI test. The large number of parameters that needed to be identified when the ST-1 scheme was employed resulted in unsatisfactory control behavior. From the parameter trajectories presented in Fig. 4.7, it can be seen that the parameters of ST-1 changed drastically from  $t=20$  to  $t=100$  minutes. This slow speed of parameter convergence caused oscillatory changes in the reboiler duty from  $t=10$  to  $t=80$  minutes, resulting in the oscillatory controlled response of  $X_B$  during the initial 100 minutes. Since the parameters did not converge until  $t=100$  minutes, the response of  $X_B$  was sluggish and did not return to its set point even after 150 minutes of operation. The parameter adaptation patterns shown in Figs. 4.8 and 4.9 for SM-1 and SM-2 schemes are similar to the patterns observed for the MDI test (c.f. Figs. 4.4 and 4.5). In this case, since the parameters of the SM-1 scheme converged to new values faster than those of the SM-2 scheme, the SM-1 provided better control performance than the SM-2 strategy. It should also be noted that the controlled response was slightly oscillatory when the PI scheme was employed. The  $\lambda$  trajectories of SM-1 and SM-2 are also similar to the corresponding trajectories for the MDI test. The value of  $\lambda$  for the ST-1 scheme, however, changed more frequently than was observed with test MDI, indicating more adaptation of parameters.

(iii) Effect of Using a Dead-band with AIC Scheme on Control Performance

As discussed in Section 2.5, for the proposed AIC schemes, the prediction ( $y_p$ ) of the controlled variable will obviously not be reliable during the initial adaptation period. In addition, since the parameters can only be updated at the cycle time of the analyzer and the AIC schemes utilize the value of  $y_p$  for calculating the control action during the

intersample interval of the primary output, it is important to incorporate a dead-band on the AIC schemes so that the controller output will not be calculated based on a poor predicted value of  $y$ . The effect of the use of a dead-band on control performance of the AIC schemes was studied for a -20% step change in feed rate (test MD2) with the dead-band implemented as discussed in Section 2.5. The magnitude of the dead-band which provided the best performance was selected by trial and error method selected from values of 20%, 15% and 10%. It was found that when a 20% dead-band was used, the AIC scheme was not "switched off" frequently enough to eliminate the effect of initial adaptation dynamics on the control performance, and yet for a 10% dead-band the AIC scheme was "switched off" too often to give robust control response. Consequently, a 15% dead-band provided the best results, in terms of dynamic response as well as IAE value, and so it was used for the MD2 test of the AIC schemes.

The IAE values that resulted when a 15% dead-band was used with the AIC schemes are compared with the IAE performance indices achieved without a dead-band in Table 4.5 and the controlled responses obtained when the dead-band was employed are presented in Figs. 4.10 to 4.12. As can be seen from the IAE values reported, the most significant improvement resulted when the dead-band was employed with the ST-1 scheme, with the IAE value having decreased by 33%. Only slight improvement in control performance was achieved when a dead-band was utilized with the simplified algorithms, with IAE values for the SM-1 and SM-2 schemes having decreased by less than 10%.

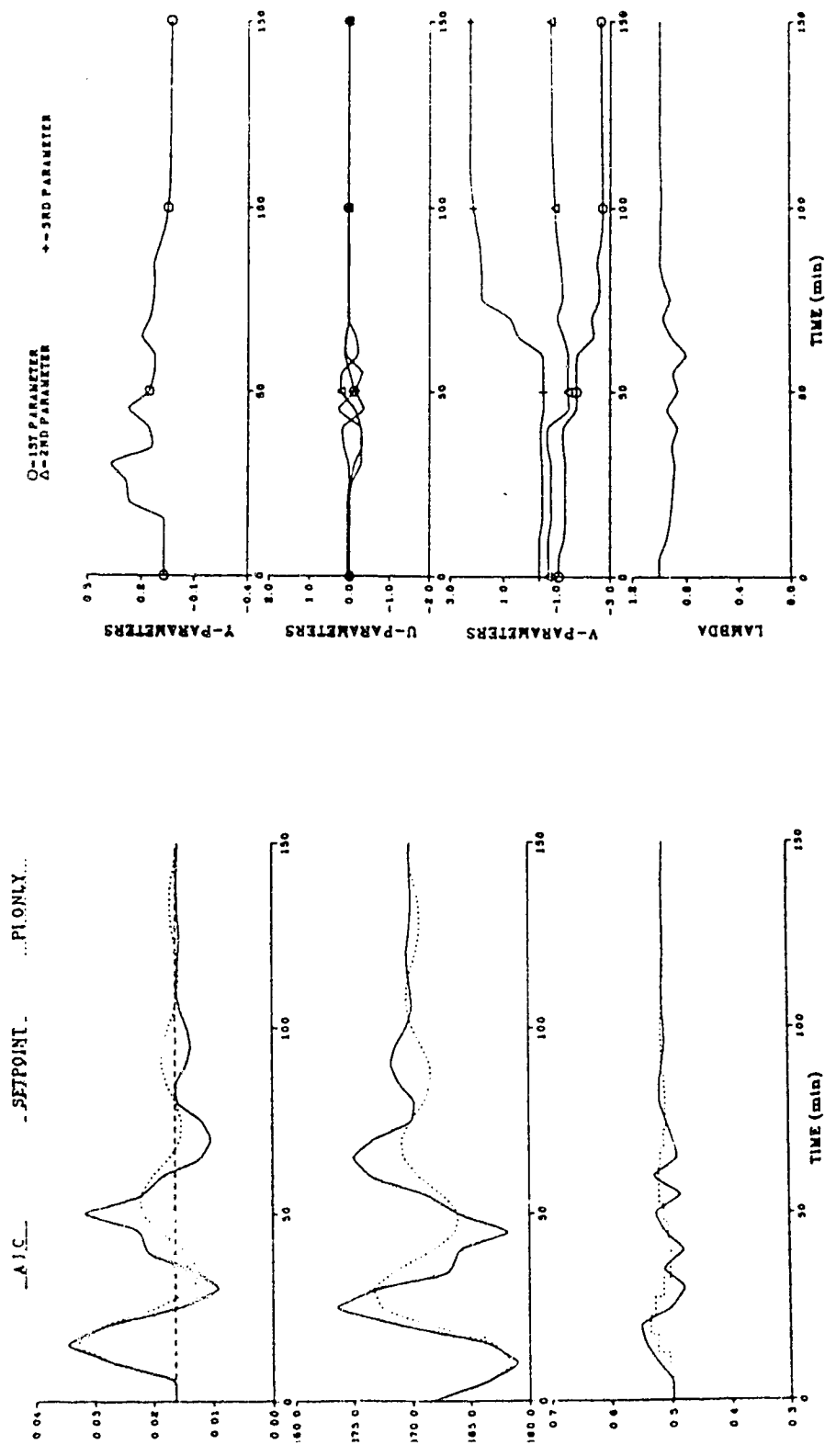


Figure 4.10 Comparison of Conventional PI and ST-1 AIC Control Performance for a +20% Step Change in Feed Rate and AIC Parameter Trajectories (15% Dead-band with AIC)

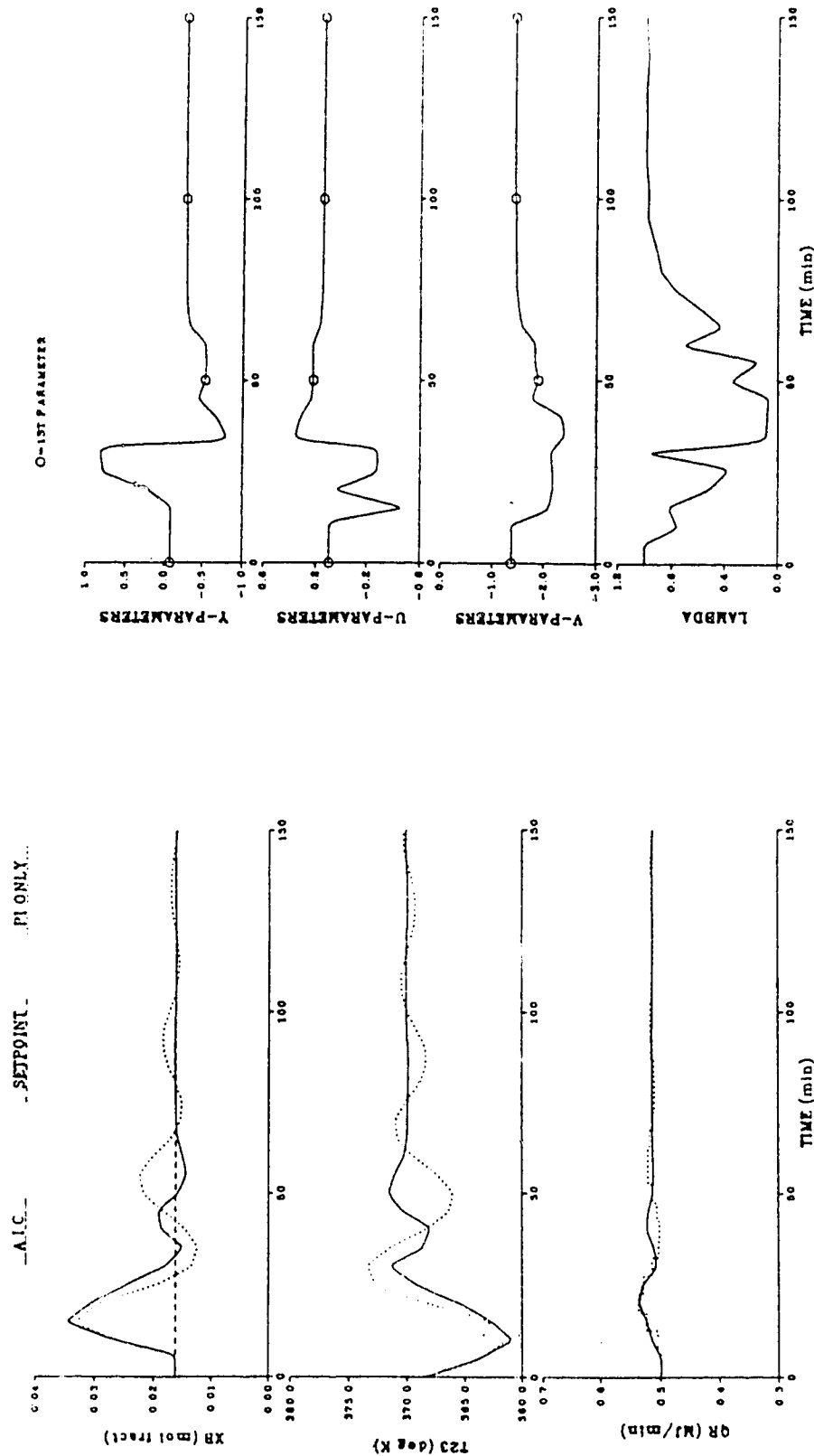


Figure 4.11 Comparison of Conventional PI and SM-1 AIC Control Performance for a +20% Step Change in Feed Rate and AIC Parameter Trajectories (15% Dead-band with AIC)

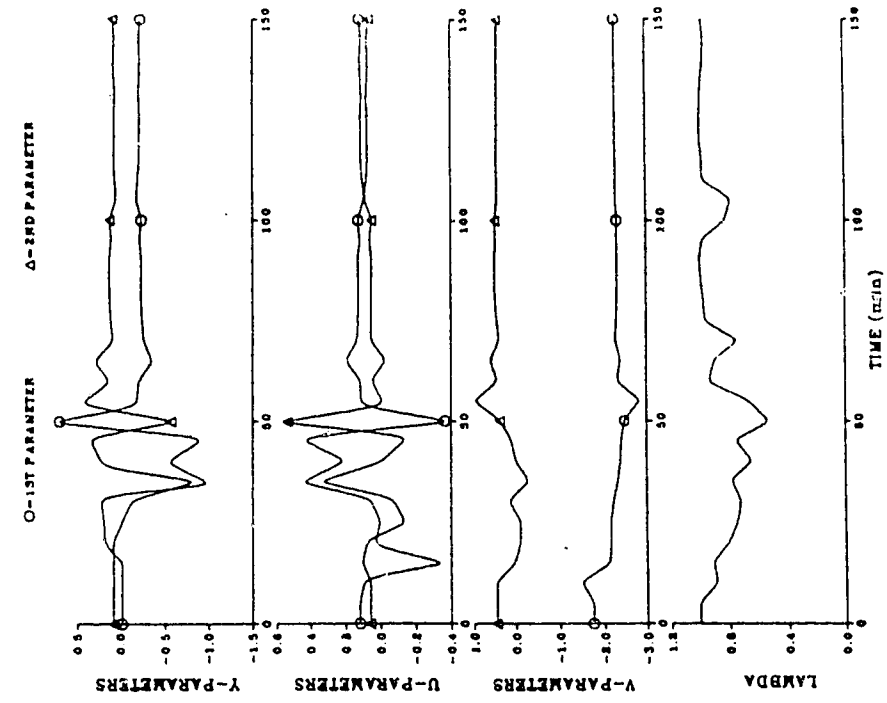
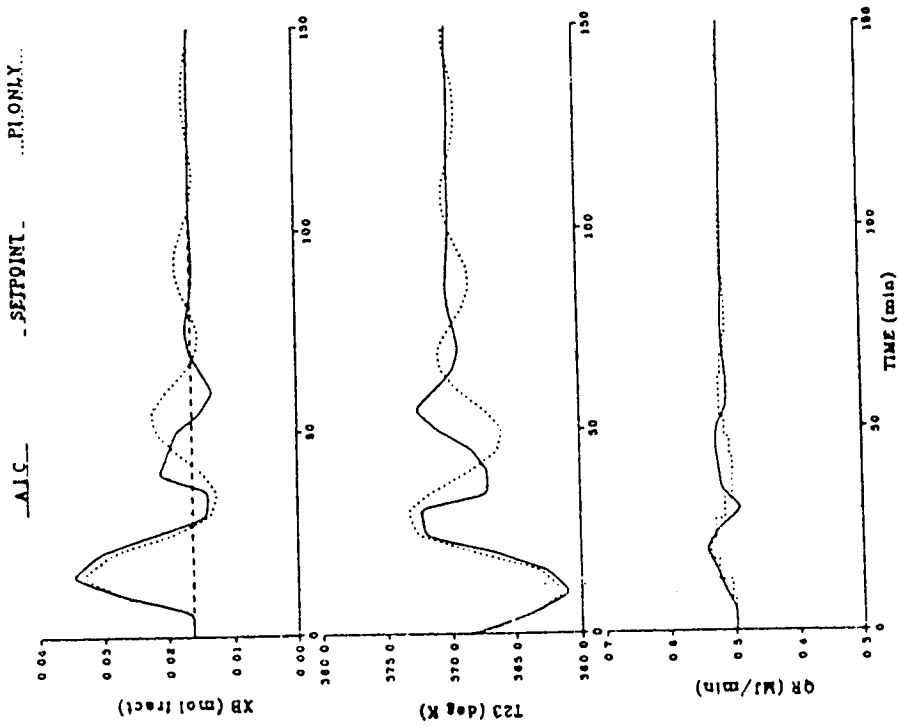


Figure 4.12 Comparison of Conventional PI and SM-2 AIC Control Performance for a +20% Step Change in Feed Rate and AIC Parameter Trajectories (15% Dead-band with AIC)



Table 4.5

Effect of Employing a 15% Dead-band on Control Performance of the AIC Schemes for a 20% Step Increase in Feed Rate

Control Scheme	IAE with 15% Dead-band (mol fract-min)	IAE with No Dead-band (mol frac-min)
ST-1	0.626	1.950
SM-1	0.293	0.320
SM-2	0.223	0.372

The profound improvement observed when a dead-band was employed with the ST-1 scheme can be explained by the slow speed of parameter convergence when the ST-1 algorithm was employed. Since 12 parameters had to be identified, the predicted  $X_B$  was very erratic during the initial transient period as the parameters had not converged to new values. When no dead-band was employed, the ST-1 algorithm used the erratic predicted value of  $X_B$  to calculate the control action,  $Q_R$ , thus resulting in unsatisfactory control behavior. The "safety check" incorporated through the use of a dead-band enhanced the control performance.

In Fig. 4.13, the predicted  $X_B$  obtained when no dead-band was used with the ST-1 scheme is compared with the case when a 15% dead-band was employed. It can be seen that the prediction was very inaccurate during the initial 100 minutes when no dead-band was used but the prediction almost matched the actual controlled output after only 80 minutes of operation when a dead-band was applied. This improved prediction of the primary output caused the large decrease in the IAE performance index. The stabilizing effect of the dead-band can also be observed by comparing the parameter adaptation patterns shown in Fig. 4.10 with the parameter trajectories presented in

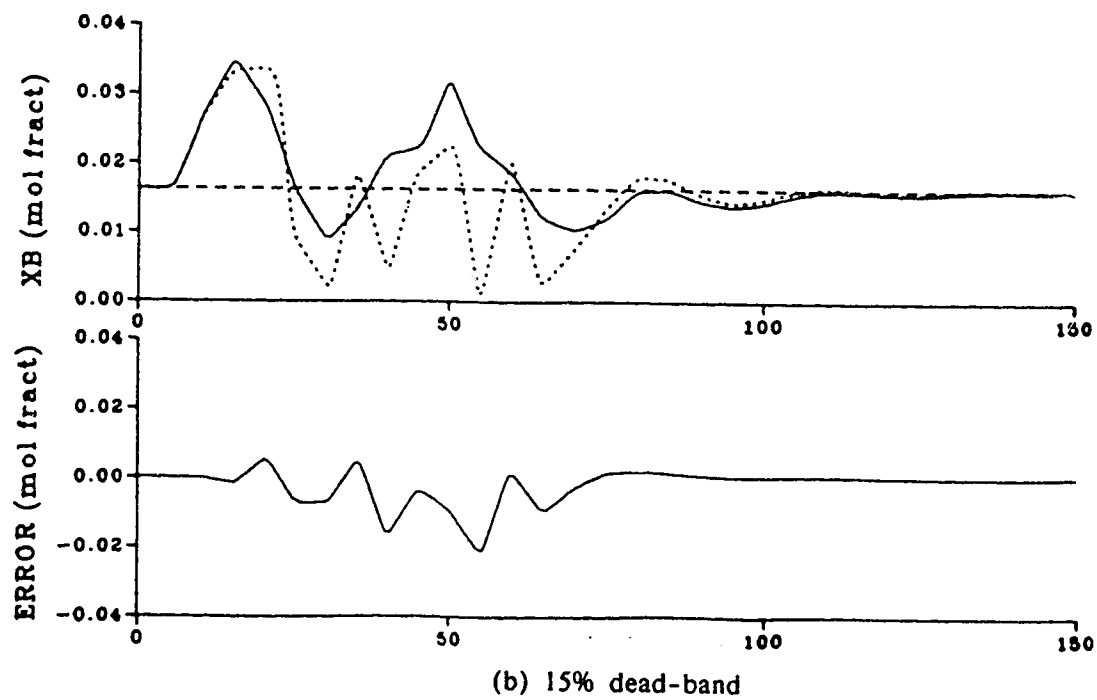
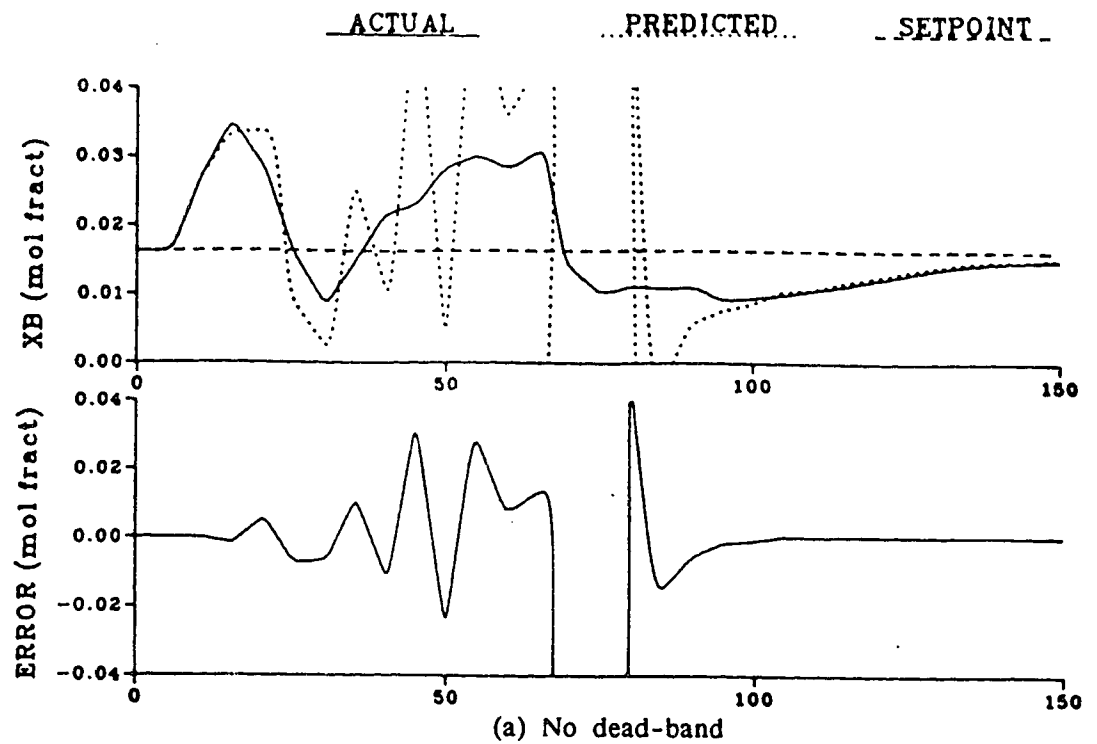


Figure 4.13 Effect of Using a Dead-band with ST-1 AIC on Control Performance for a +20% Step Change in Feed Rate

Fig. 4.7 which shows that the parameter trajectories were much "smoother" when a dead-band was used. Since the simplified algorithms are very robust, only a small improvement in control performance was achieved when a dead-band was used with the SM-1 and SM-2 schemes. As can be appreciated by comparing the parameter and  $\lambda$  trajectories of the simplified algorithms displayed in Figs. 4.11 and 4.12 with the corresponding trajectories shown in Figs. 4.8 and 4.9, the effect of incorporating a dead-band on the parameter adaptation was quite minimal. Nevertheless, since in practice it would be advisable to employ a dead-band for all AIC schemes, a 15% dead-band has been employed in all subsequent performance evaluations of the AIC schemes.

(iv) Step Changes in the Concentrations of the Components in the Feed Stream

The control performance of the AIC schemes for step changes in the concentrations of components 2 to 5 (propylene, propane, isobutane and cis-butene respectively) in the feed stream at  $t=15$  minutes (test MD3 in Table 4.3) are compared with the performance achieved using the PI scheme in Figs. 4.14 to 4.16 and the IAE indices for the four control schemes are summarized in Table 4.6. From the calculated IAE values, it is obvious that the control performance achieved using any of the AIC algorithms is superior to that obtained by utilizing the PI scheme. Similar to the simulation results presented earlier in this chapter, the SM-1 algorithm provided the best control behavior, with an IAE value more than 50% lower than that obtained using the PI scheme while the controlled response that resulted from utilizing the SM-2 scheme was comparable to that of the SM-1 algorithm. Although the ST-1 algorithm did not provide excellent control behavior, it

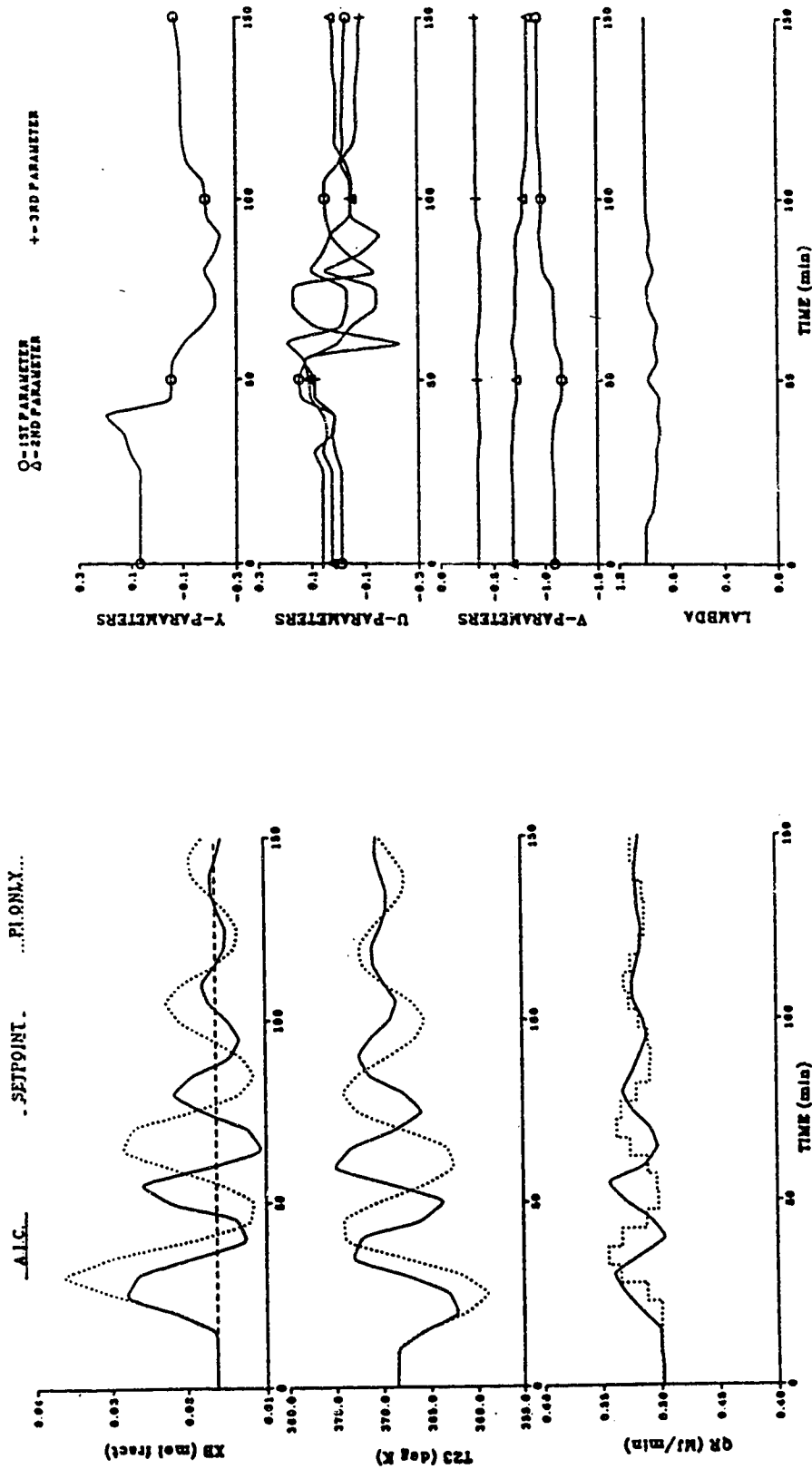


Figure 4.14 Comparison of Conventional PI and ST-1 AIC Control Performance for Step Changes in the Concentrations of the Components in the Feed Stream and AIC Parameter Trajectories (15% Dead-band with AIC)

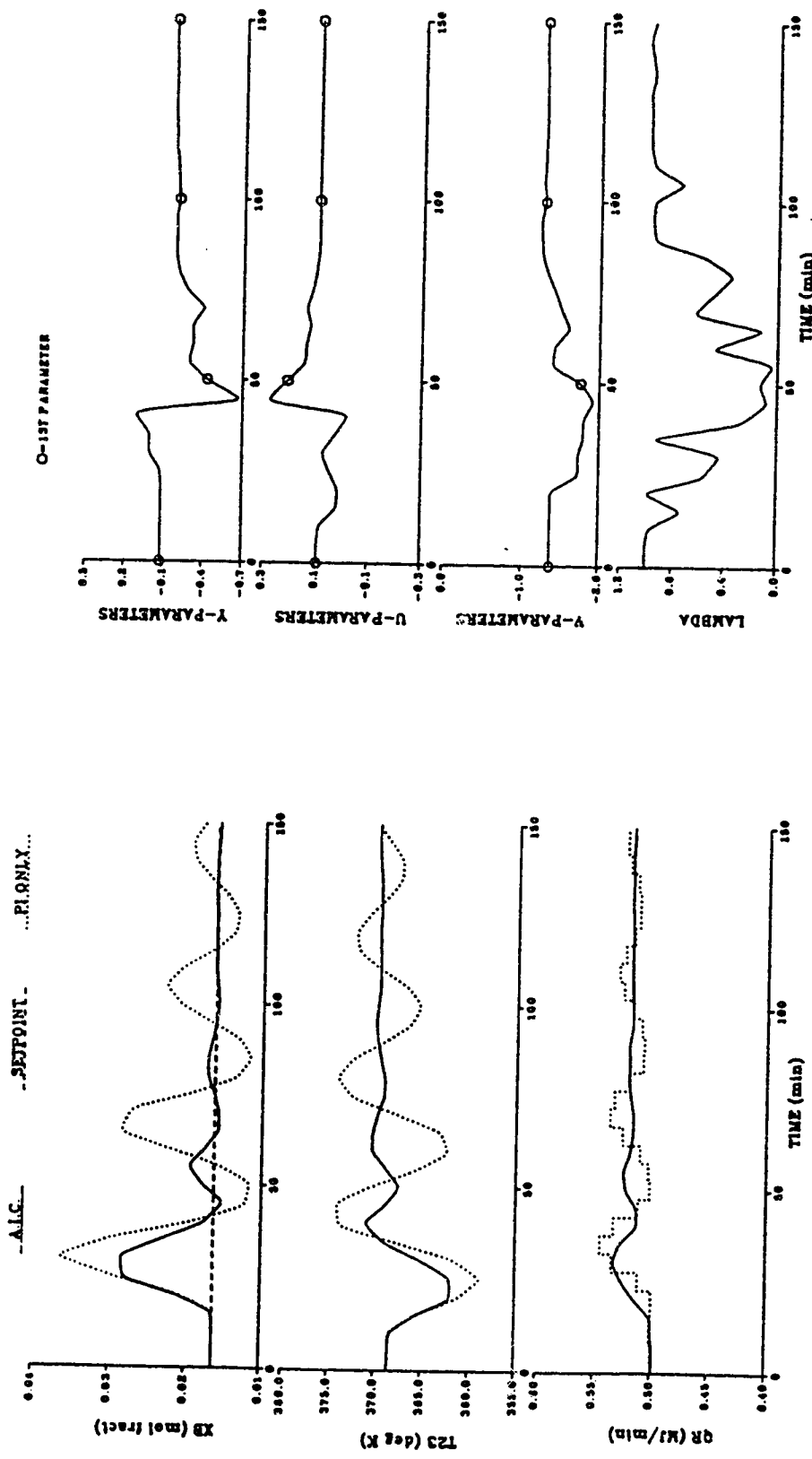


Figure 4.15 Comparison of Conventional PI and SM-1 AIC Control Performance for Step Changes in the Concentrations of the Components in the Feed Stream and AIC Parameter Trajectories (15% Dead-band with AIC)

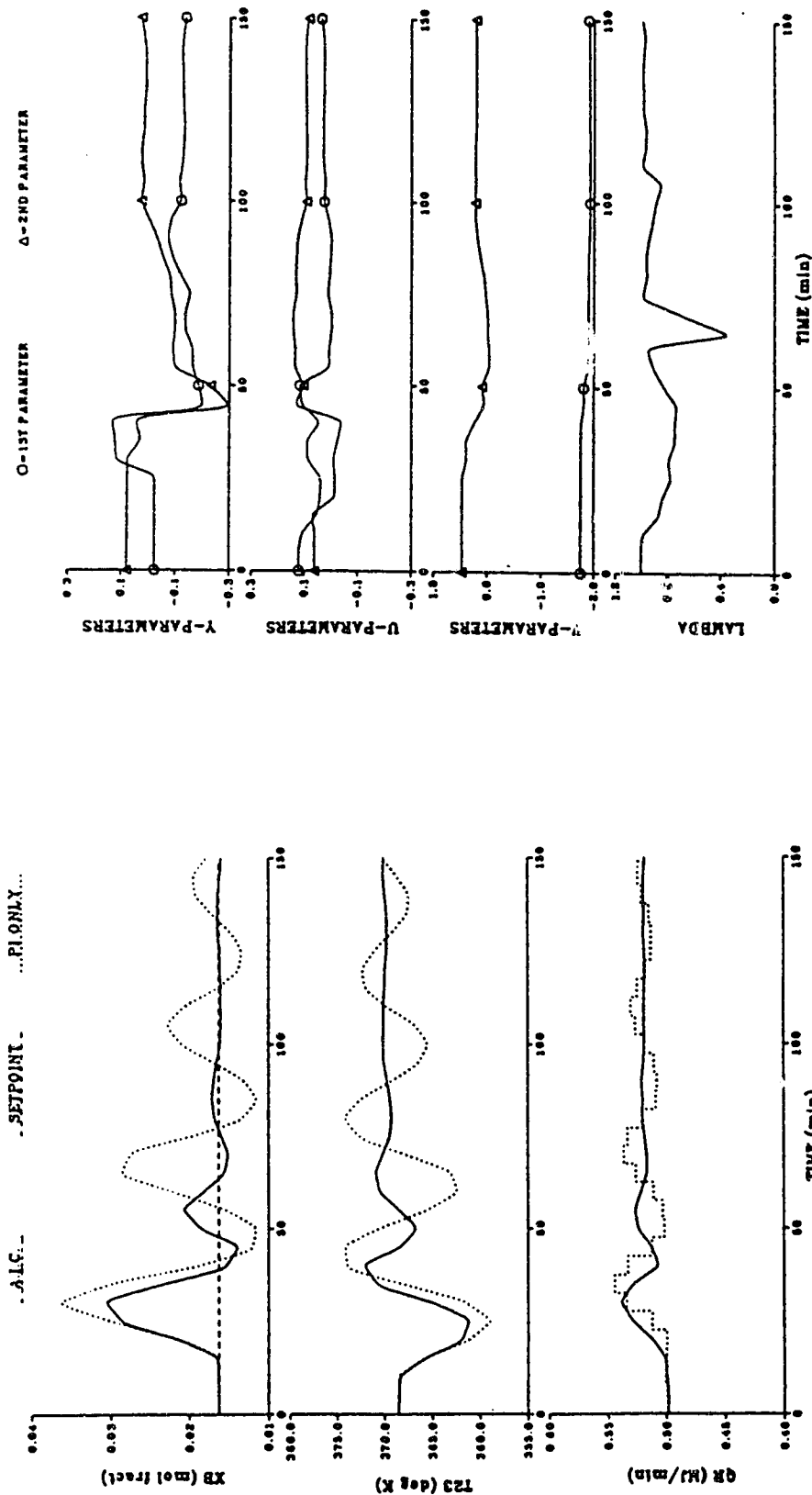


Figure 4.16 Comparison of Conventional PI and SM-2 AIC Control Performance for Step Changes in the Concentrations of the Components in the Feed Stream and AIC Parameter Trajectories (15% Dead-band with AIC)

outperformed the PI scheme. From the responses of  $X_B$  displayed in Fig. 4.14 to 4.16, it can be observed that the simplified algorithms were able to return  $X_B$  to its set point value of 1.63 mole percent after 100 minutes of operation. The controlled response that resulted when the PI scheme was used was more oscillatory and inferior to that achieved using any of the AIC schemes. The outstanding performance of the simplified algorithm can again be explained by the robust and fast parameter adaptation displayed in Figs. 4.15 and 4.16. As in the case for the feed disturbance, the parameters of SM-1 converged in the shortest time (80 minutes) while the parameters of SM-2 converged to new values approximately 20 minutes later. The rigorous changes in the parameters of the ST-1 scheme during  $t=50$  to  $t=100$  minutes (c.f. Fig. 4.14) resulted in slow parameter convergence, thus resulting in inferior control performance compared with that achieved using the simplified algorithms.

Table 4.6  
Summary of Control Performance for Step Changes in the Concentrations of the Components in the Feed Stream

<u>Control Scheme</u>	<u>IAE (mol fract-min)</u>	<u>Reference Figures</u>
PI	0.429	4.14-4.16
ST-1	0.312	4.14
SM-1	0.228	4.15
SM-2	0.223	4.16

(v) Simultaneous Increase in Feed Rate and Analyzer Cycle Time

To investigate the robustness of the AIC schemes versus the PI scheme, the performance of the different algorithms for a 20% step increase in feed

rate was studied when the cycle time of the analyzer was increased from 5 minutes to 8 minutes. This MD4 test is a very severe test of the robustness of the control algorithms because each control scheme, without re-tuning any parameters of the parameter vector and/or controller, has to cope with the situation where the measurement of the controlled output is available less frequently and simultaneously a feed disturbance is introduced. This test was used to evaluate the robustness of the AIC schemes under the condition of model-plant-mismatch since the model-prediction equations employed were the same as those used for the case where the analyzer cycle time was 5 minutes (c.f. Eqs. 3.5 to 3.7). The simulation results showed that the standard algorithm could not handle this severe change in operating conditions and, consequently, unstable behavior resulted. No closed loop responses or parameter trajectories are presented because the present design of the DYCONDIST simulator does not provide for output of transient values if the program is terminated due to stability and/or convergence problems. From the execution run summary produced by DYCONDIST, the simulation terminated after 73 minutes of simulated operation when the concentration ( $X_B$ ) of propane in the bottoms product reached 21 mole percent versus the desired set point value of 1.63 mole percent. The performance achieved using the SM-1 scheme, which has only 3 parameters, resulted in a minimum IAE value of 0.502, almost half of the IAE value of 0.983 obtained using the SM-2 scheme and less than one third of the IAE value of 1.528 that resulted when the PI scheme was used. The controlled responses presented in Figs. 4.17 to 4.18 show that use of either of the simplified AIC algorithms produced control behavior that was superior to that achieved using the PI scheme. The propane concentration was controlled to within 10 percent of



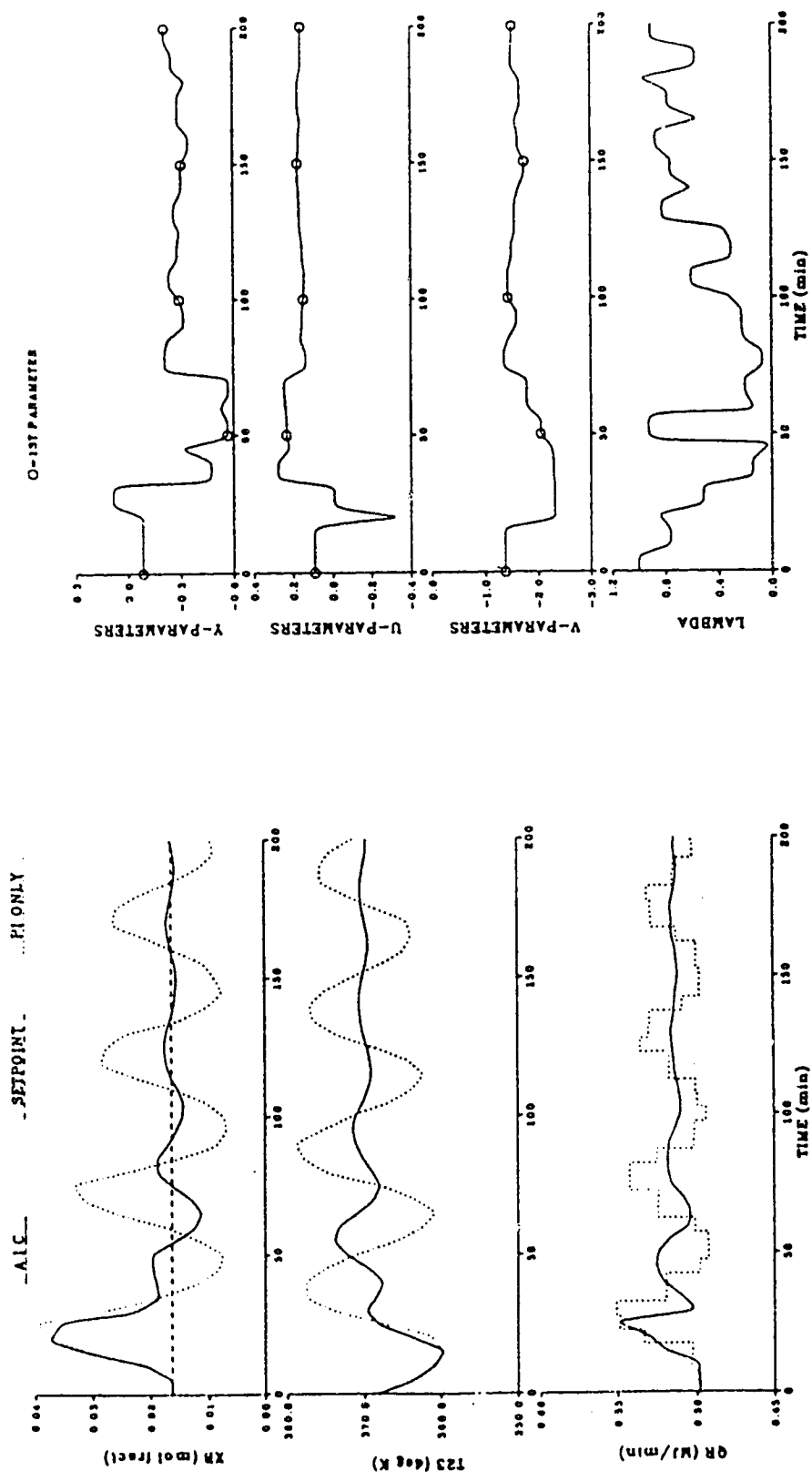


Figure 4.17 Comparison of Conventional PI and SM-1 AIC Control Performance for Simultaneous Increases in Feed Rate and Analyzer Cycle Time and AIC Parameter Trajectories (15% Dead-band with AIC)

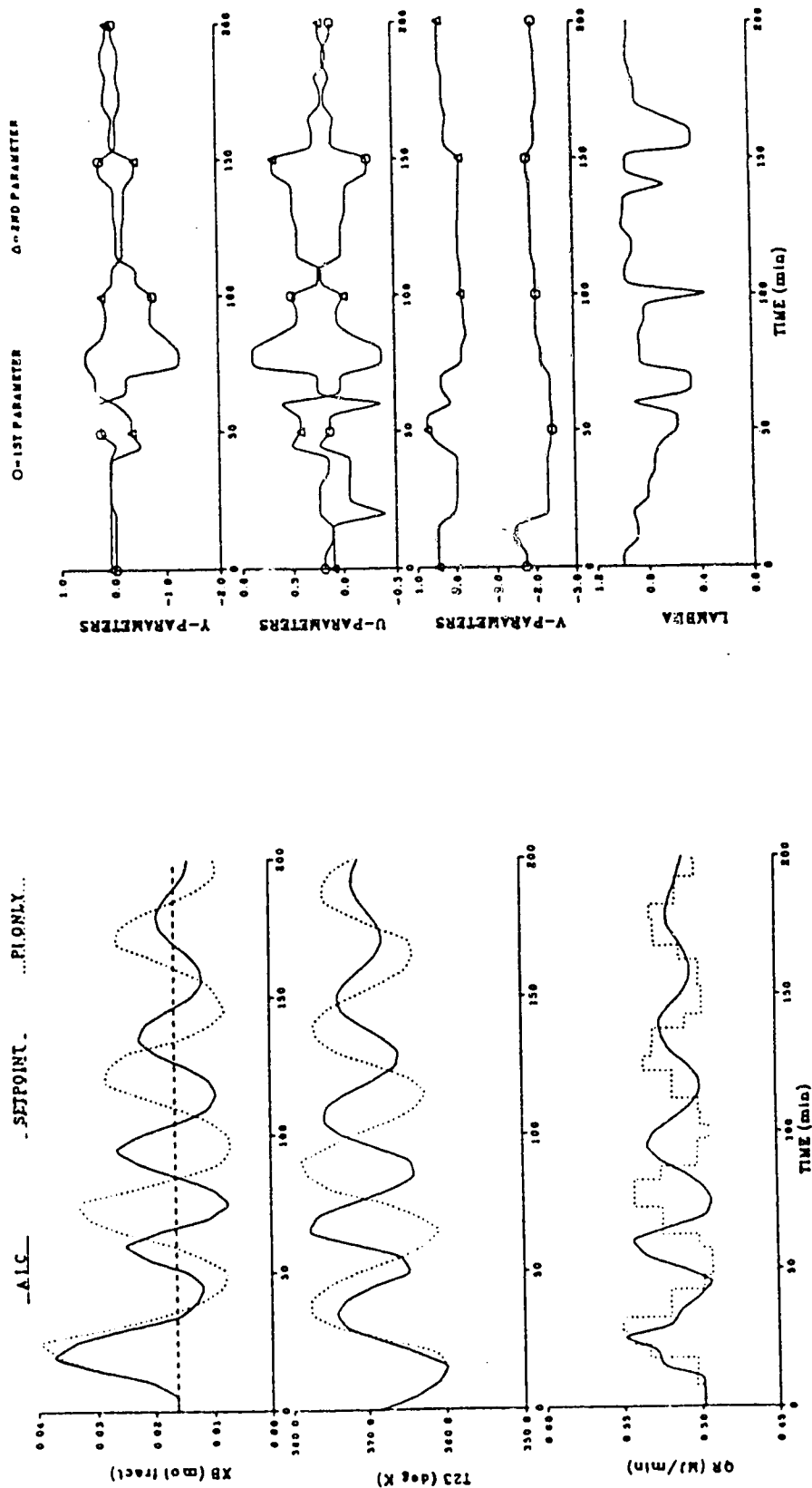


Figure 4.18 Comparison of Conventional PI and SM-2 AIC Control Performance for Simultaneous Increases in Feed Rate and Analyzer Cycle Time and AIC Parameter Trajectories (15% Dead-band with AIC)

its set point after only 110 minutes of operation when the SM-1 scheme was employed while neither the SM-2 nor the PI scheme was able to achieve this excellent control behavior after 200 minutes of operation. The superior performance of the SM-1 algorithm is attributed to the fast parameter convergence, as can be observed by examining the parameter trajectories of the two simplified algorithms displayed in Figs. 4.17 and 4.18. It is obvious from these trajectories that the parameters of the SM-1 scheme converged much faster and "smoother" than those of the SM-2 scheme.

(vi) Servo Control Performance

The servo control responses of the four control schemes for a -20% step change in set point to a value of 1.30 mole percent are displayed in Figs. 4.19 to 4.21 and the corresponding IAE values are reported in Table 4.7. The best control performance, with an IAE value of 0.043, resulted from employing the ST-1 scheme. This IAE value is more than 50 percent lower than the IAE value achieved using the PI scheme while the IAE indices obtained for the SM-1 and SM-2 algorithms are more than 40 percent lower than the IAE value for the PI scheme. As can be seen from the controlled responses presented in Figs. 4.19 to 4.21, the ST-1 scheme provided the best control performance while the control behavior that resulted from utilizing either of the simplified AIC algorithms was comparable to that obtained using the standard ST-1 scheme. The controlled response that resulted when the PI scheme was employed was found to be more oscillatory and inferior to the behavior obtained using any of the AIC algorithms. Similar to the servo control responses reported in Section 3.4.1(iii) for a linear process, the PI scheme reacted to the set point change faster than the AIC schemes, as indicated by the short rise time. The explanation for this observation has

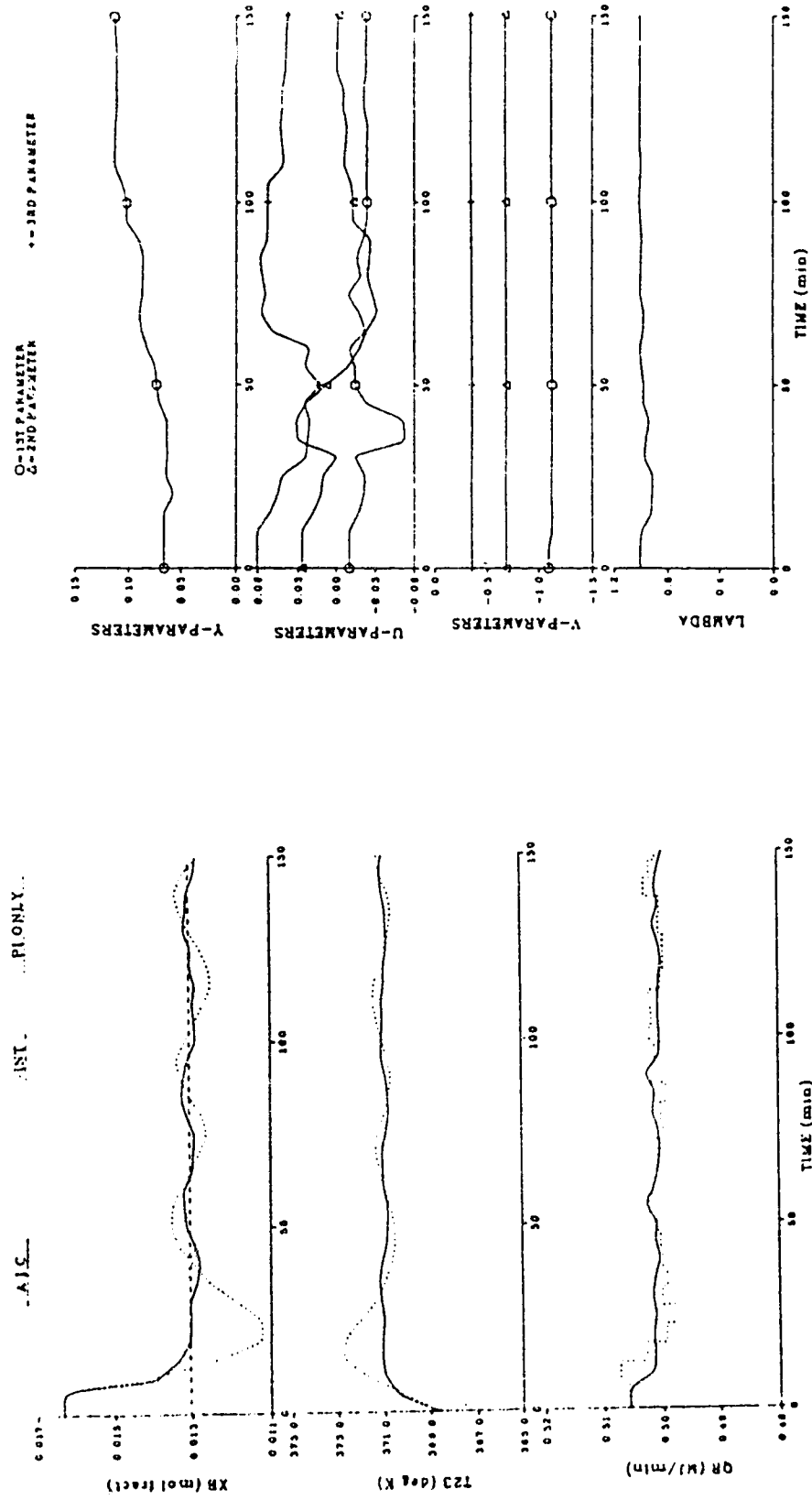


Figure 4.19 Comparison of Conventional PI and ST-1 AIC Control Performance for a -20% Step Change in Bottoms Composition Set Point and AIC Parameter Trajectories (15% Dead-band with AIC)

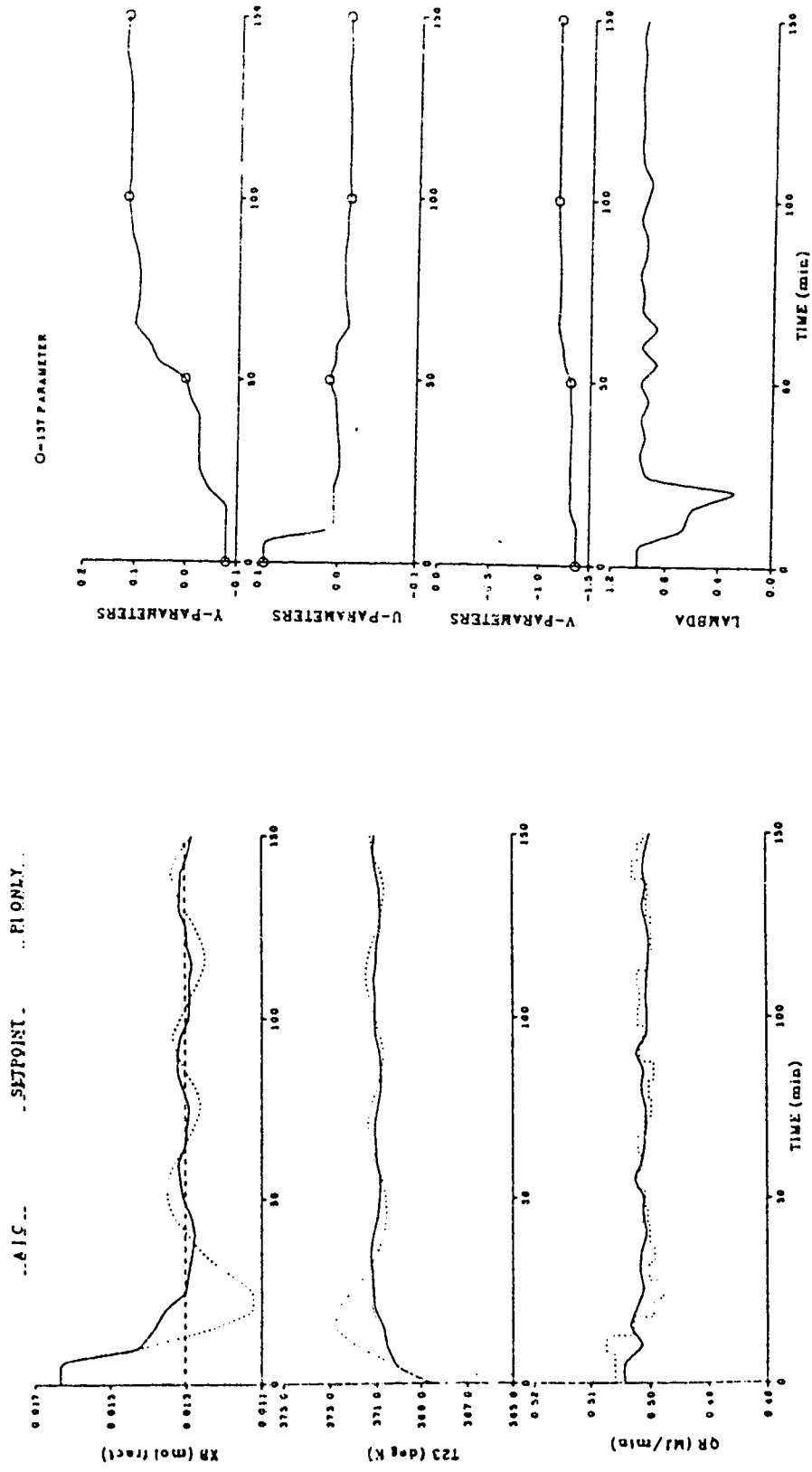


Figure 4.20 Comparison of Conventional PI and SM-1 AIC Control Performance for a -20% Step Change in Bottoms Composition Set Point and AIC Parameter Trajectories (15% Dead-band with AIC)

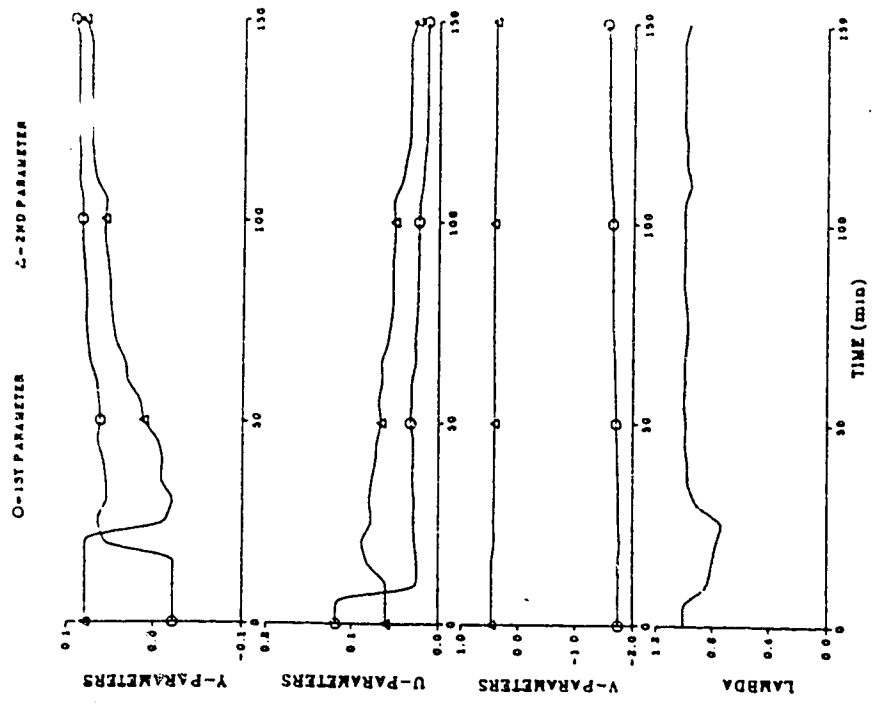
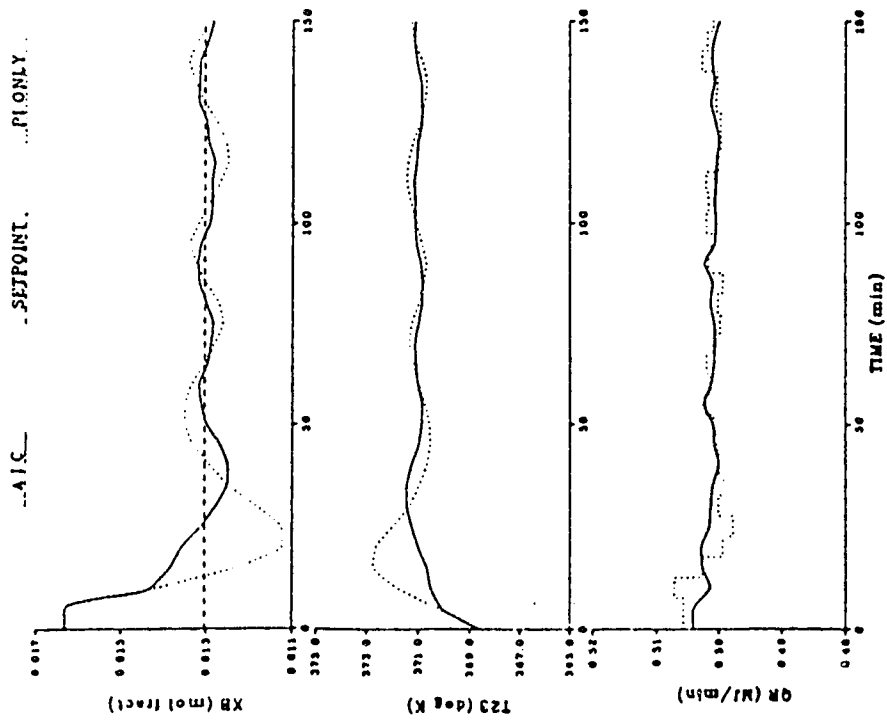


Figure 4.21 Comparison of Conventional PI and SM-2 AIC Control Performance for a -20% Step Change in Bottoms Composition Set Point and AIC Parameter Trajectories (15% Dead-band with AIC)

been presented in Section 3.4.1(iii) and will not be repeated here. The ST-1 scheme provided slightly better control performance than either of the simplified algorithms. A possible reason is that the process did not exhibit strong nonlinear behavior for a step change in set point compared with the behavior for a disturbance in feed flow rate. This is not unexpected since, as shown by the results obtained for the control of the binary column presented in Chapter 3, use of the standard algorithm is to be preferred for control of linear systems. The parameter and  $\lambda$  trajectories shown in Figs. 4.9 to 4.21 also support this explanation that the set point change introduced did not cause the column to exhibit as much nonlinear behavior since the parameter and  $\lambda$  trajectories obtained in this case are "smoother" than the corresponding trajectories that resulted for the disturbance in feed flow rate (c.f. Figs. 4.10 to 4.12).

Table 4.7  
Summary of Control Performance for a -20% Step Change in Set Point

<u>Control Scheme</u>	<u>IAE (mol fract-min)</u>	<u>Reference Figures</u>
PI	0.096	4.19-4.21
ST-1	0.043	4.19
SM-1	0.051	4.20
SM-2	0.056	4.21

#### 4.5.3 Sensitivity of Control Performance of the Adaptive Inferential Control Schemes to Selection of the Secondary Output

As shown in Fig. 4.1,  $T_{23}$  is very sensitive to a feed rate disturbance.

To investigate the sensitivity of the AIC algorithms to secondary output selection, the liquid temperature at stage 27 ( $T_{27}$ ) has been used in the AIC schemes to perform closed loop control of  $X_B$ . The tests used to evaluate performance are MD2 and MD4 (c.f. Table 4.3) with the initial parameter values and controller settings selected in the same manner as described in Section 4.4.2. It was observed from these simulations that the controller settings presented in Table 4.2 for each of the AIC schemes also resulted in minimum IAE values for use of  $T_{27}$  and so the controller settings used were those listed in Table 4.2. The IAE values obtained with the AIC schemes using  $T_{27}$  as the secondary output are compared with the values obtained using  $T_{23}$  as the secondary output in Table 4.8. The responses that resulted when  $T_{27}$  was used are presented in Figs. 4.22 to 4.26. As mentioned Section 4.5.2(iii), a 15% dead-band was used with the AIC schemes.

Table 4.8  
Effect of Using Stage 27 Liquid Temperature as the Secondary Output  
on Control Performance of the AIC Schemes

<u>Test Code</u>	<u>Control scheme</u>	<u>IAE Using <math>T_{27}</math> (mol fract-min)</u>	<u>IAE Using <math>T_{23}</math> (mol frac-min)</u>
MD2	PI	0.429	0.429
	ST-1	0.312	0.626
	SM-1	0.228	0.293
	SM-2	0.223	0.365
MD4	PI	1.528	1.528
	ST-1	unstable	unstable
	SM-1	0.518	0.502
	SM-2	0.600	1.983



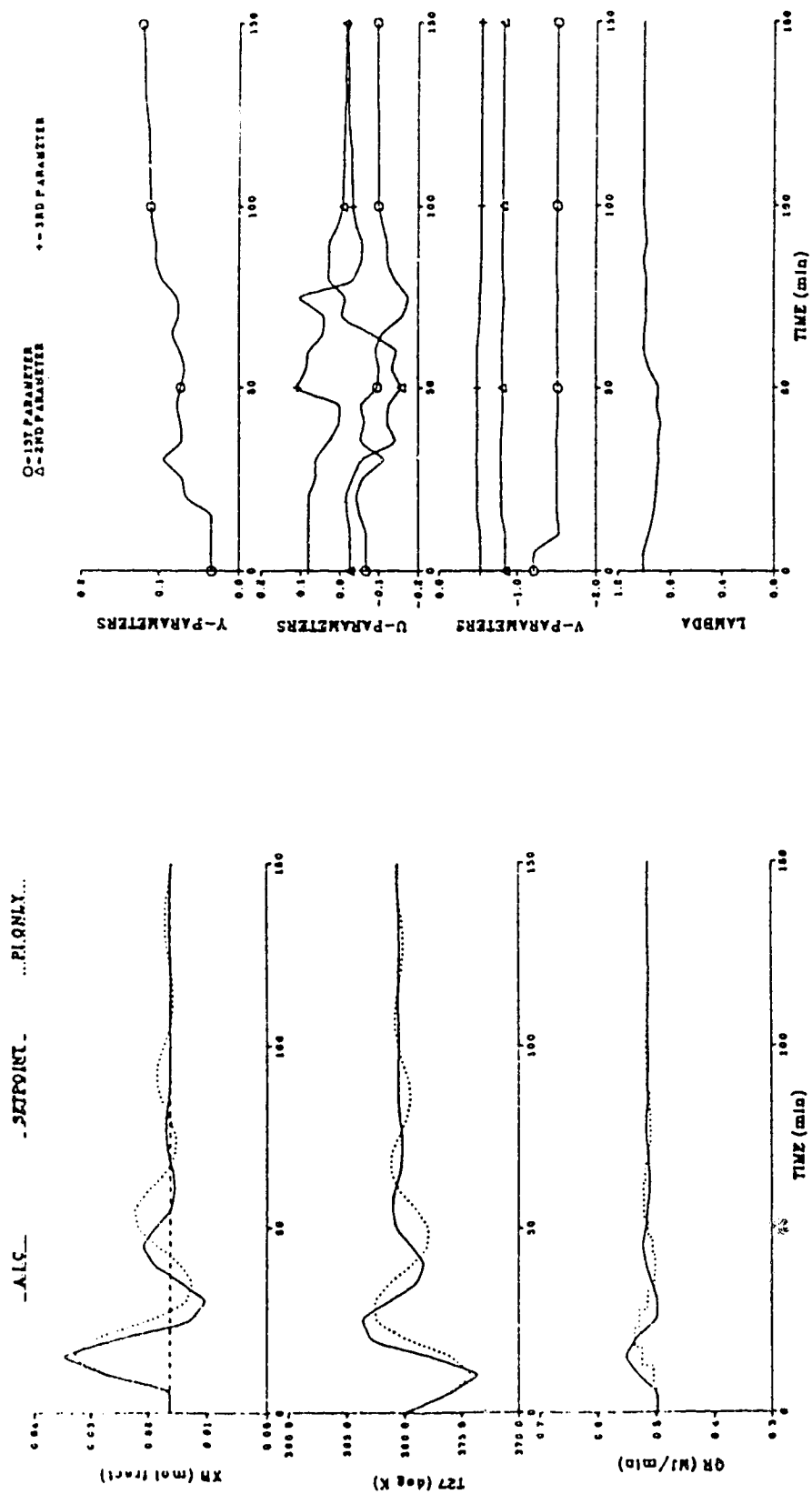


Figure 4.22 Control Performance of ST-1 AIC Scheme Using Stage 27 Liquid Temperature as Secondary Output and AIC Parameter Trajectories for a +20% Step Change in Feed Rate (15% Dead-band with AIC)

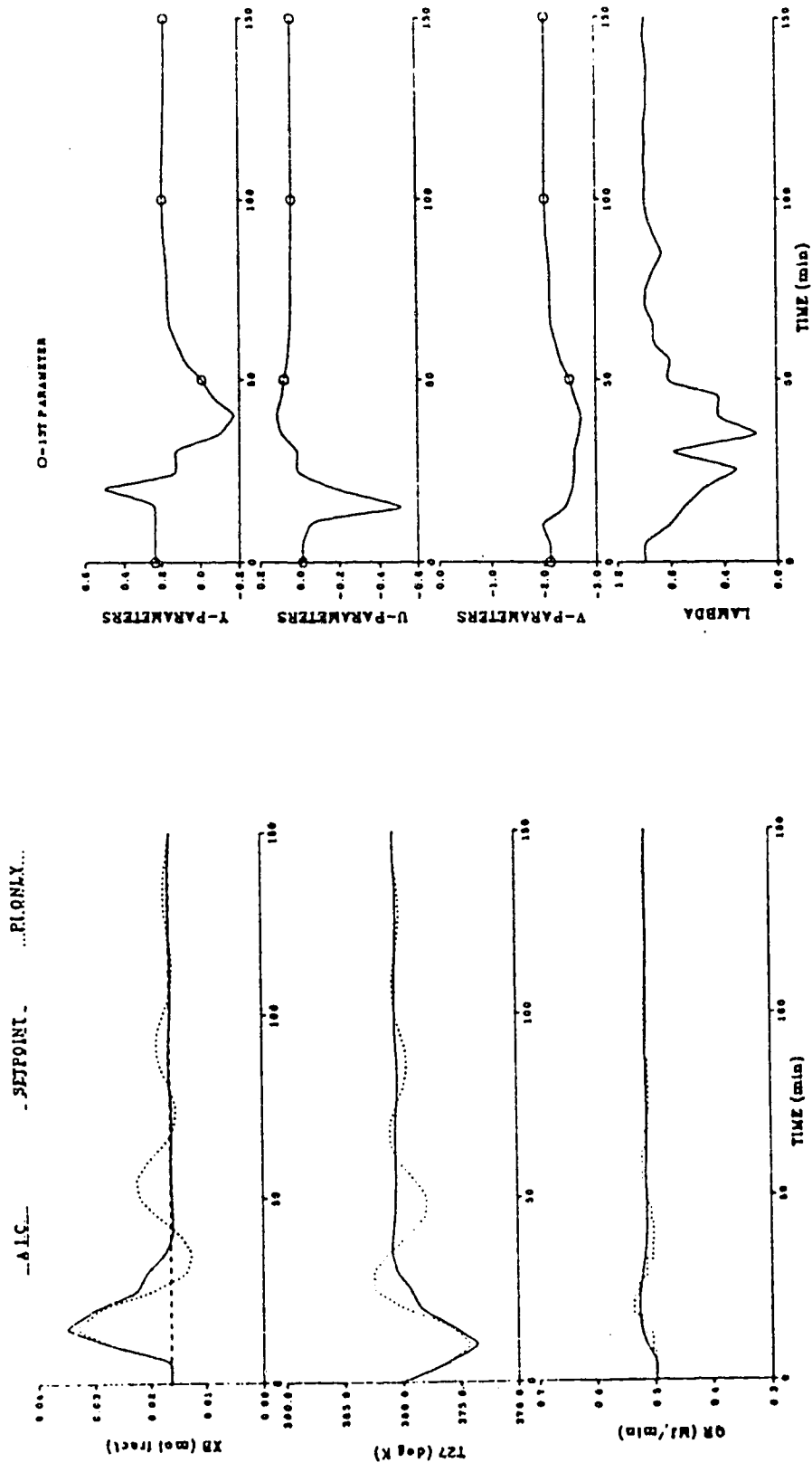


Figure 4.23 Control Performance of SM-1 AIC Scheme Using Stage 27 Liquid Temperature as Secondary Output and AIC Parameter Trajectories for a +20% Step Change in Feed Rate (15% Dead-band with AIC)

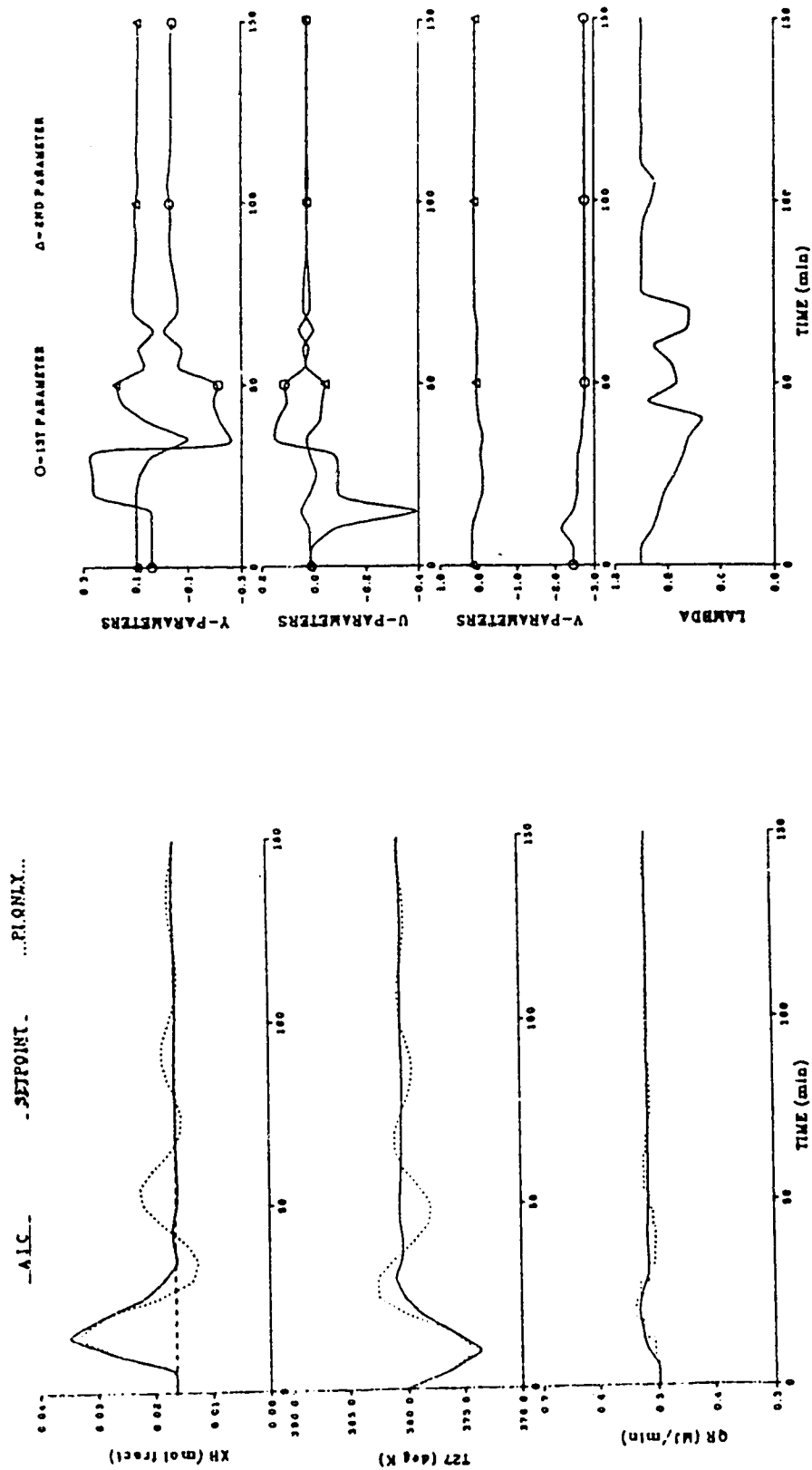


Figure 4.24 Control Performance of SM-2 AIC Scheme Using Stage 27 Liquid Temperature as Secondary Output and AIC Parameter Trajectories for a +20% Step Change in Feed Rate (15% Dead-band with AIC)

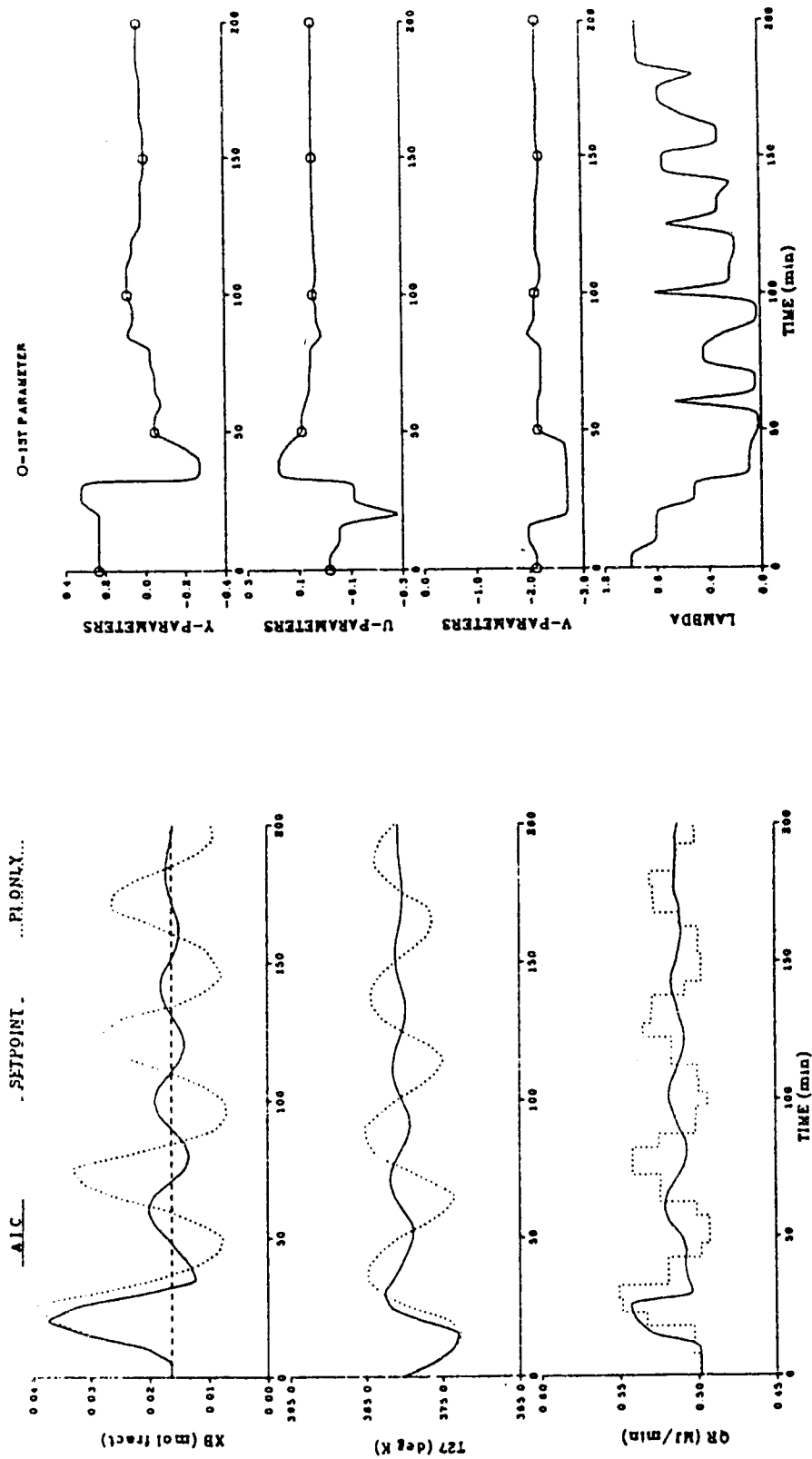


Figure 4.25 Control Performance of SM-1 AIC Scheme Using Stage 27 Liquid Temperature as Secondary Output and AIC Parameter Trajectories for Simultaneous Increases in Feed Rate and Analyzer Cycle Time (15% Dead-band with AIC)

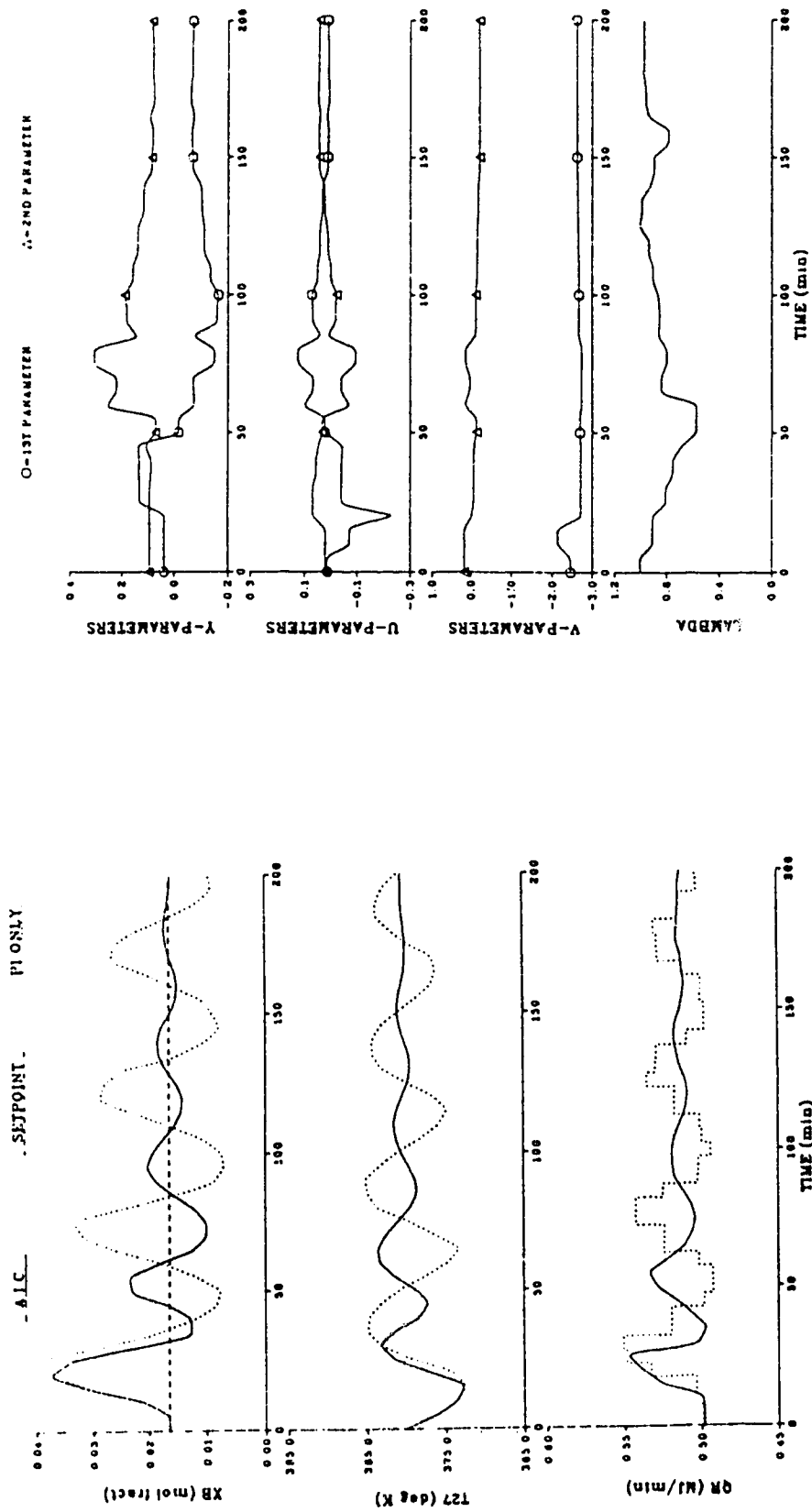


Figure 4.26 Control Performance of SM-2 AIC Scheme Using Stage 27 Liquid Temperature as Secondary Output and AIC Parameter Trajectories for Simultaneous Increases in Feed Rate and Analyzer Cycle Time (15% Dead-band with AIC)

For the MD2 test, the control responses achieved by using  $T_{27}$  as secondary output were superior to those obtained using  $T_{23}$ . The most significant improvement was obtained when the ST-1 scheme was used, with the IAE value having decreased from 0.626 to 0.312, a decrease of over 50 percent, while the IAE values for the SM-1 and SM-2 decreased by 22% and 39% respectively. In this case, all AIC schemes provided better control behavior than that achieved using the PI scheme, as can be seen from the controlled responses shown in Figs 4.22 to 4.24.

The MD4 test of the ST-1 algorithm, using  $T_{27}$ , showed that control with this scheme was not possible due to the strong nonlinear behavior, as previously observed using  $T_{23}$ . The test of the SM-1 algorithm showed that although the IAE value is slightly larger when  $T_{27}$  was used rather than  $T_{23}$  (0.518 vs. 0.502), the transient responses and parameter trajectories for both cases were quite similar (c.f. Figs 4.17 and 4.25). However, use of  $T_{27}$  with the SM-2 algorithm shows that  $T_{27}$  was a better choice of secondary output than  $T_{23}$ , as can be observed from the significant decrease in the IAE value from 0.983 to 0.600 reported in Table 4.8 and the improved control behavior shown in Fig. 4.26.

One explanation for the improvement in control behavior when  $T_{27}$  was used is that  $T_{23}$  might be too sensitive to feed disturbance. This higher sensitivity of  $T_{23}$  caused more drifting of the  $v$ -parameters, as can be observed by comparing the trajectories of  $v$ -parameters shown in Figs. 4.10 to 4.12 with the corresponding plots in Figs. 4.22 to 4.24 for the MD2 test. A similar phenomenon can be observed for the MD4 test (c.f. Figs. 4.17 and 4.18 versus Figs. 4.25 and 4.26). The results obtained also showed that for either choice of stage liquid temperature as the secondary output, the

simplified algorithms provided superior performance than either the ST-1 or PI scheme.

#### 4.5.4 Control Performance of the Truncated Standard Algorithm

As mentioned in Chapter 2, a major concern in using the standard algorithm is the large number of parameters that must be estimated when the ratio ( $J$ ) of the sample time of the primary output to that of the secondary output is large. The results presented in the previous two sections have demonstrated the difficulty that may arise in the use of the AIC schemes to control a nonlinear system. The simplified algorithm discussed in Chapter 2 is an extreme case of reducing the number of parameters of the standard algorithm (Lu and Fisher, 1989). However, if the value of  $J$  is large and the process being controlled has slow dynamics, application of the simplified algorithm may not provide satisfactory control. An alternate approach, called the truncated standard algorithm (TST), has been proposed in Chapter 2. In this section, the ST-1 algorithm, which has 12 parameters, is truncated to a 5 parameter algorithm that employs 1  $y$ -parameter, 2  $u$ -parameters and 2  $v$ -parameters (i.e.  $\hat{a}_1$ ,  $\hat{b}_1$ ,  $\hat{b}_2$ ,  $\hat{c}_0$ , and  $\hat{c}_1$ ). The corresponding estimation scheme, when combined with a fixed parameter proportional plus integral controller, is denoted as control scheme TST-2. Performance of the TST-2 algorithm for control of bottoms composition of the depropanizer tower using  $T_{23}$  as secondary output was evaluated for the MD2 and MD4 tests. All initial parameters and controller settings were obtained in the same manner as described in Section 4.4.2, with the tuned controller settings found to be  $K_P = -1.7 \left( \frac{\text{MJ/min}}{\text{mol fract}} \right)$  and  $K_I = -0.136 \left( \frac{\text{MJ/min}}{\text{mol fract-min}} \right)$ . A 15% dead-band was used with the TST-2 scheme in the simulations.

The IAE values that resulted when the depropanizer bottoms composition,  $X_B$ , was controlled using the TST-2 algorithm are compared with the corresponding results using the ST-1 algorithm in Table 4.9. The control performance of the TST-2 scheme is shown by the responses presented in Figs. 4.27 and 4.28. The TST-2 algorithm outperforms the ST-1 algorithm for these two tests. Furthermore, it should be noted that for the MD4 test the use of the ST-1 scheme resulted in unstable behavior while the TST-2 scheme controlled  $X_B$  better than the PI scheme. However, the control behavior obtained using the TST-2 algorithm was found to be inferior to the performance achieved using either the SM-1 or SM-2 scheme. The effect of truncating 7 parameters from standard ST-1 algorithm on parameter adaptation is obvious when the parameter trajectories of the TST-2 schemes displayed in Fig. 4.27 are compared with the corresponding trajectories of the ST-1 schemes (c.f. Fig. 4.10) for the MD2 test. The parameter trajectories of the TST-2 schemes are obviously "smoother" than those of the ST-1 scheme.

Table 4.9  
Comparison of Control Performance of the TST-2 and ST-1 AIC Schemes

<u>Test Code</u>	<u>IAE : TST-2 (mol fract-min)</u>	<u>Reference Figures</u>	<u>IAE : ST-1 (mol frac-min)</u>
MD2	0.381	4.27	0.626
MD4	1.155	4.28	unstable

#### 4.6 Summary

The performance of three adaptive inferential control (AIC) schemes, designated as ST-1, SM-1, and SM-2, have been applied to control the bottoms



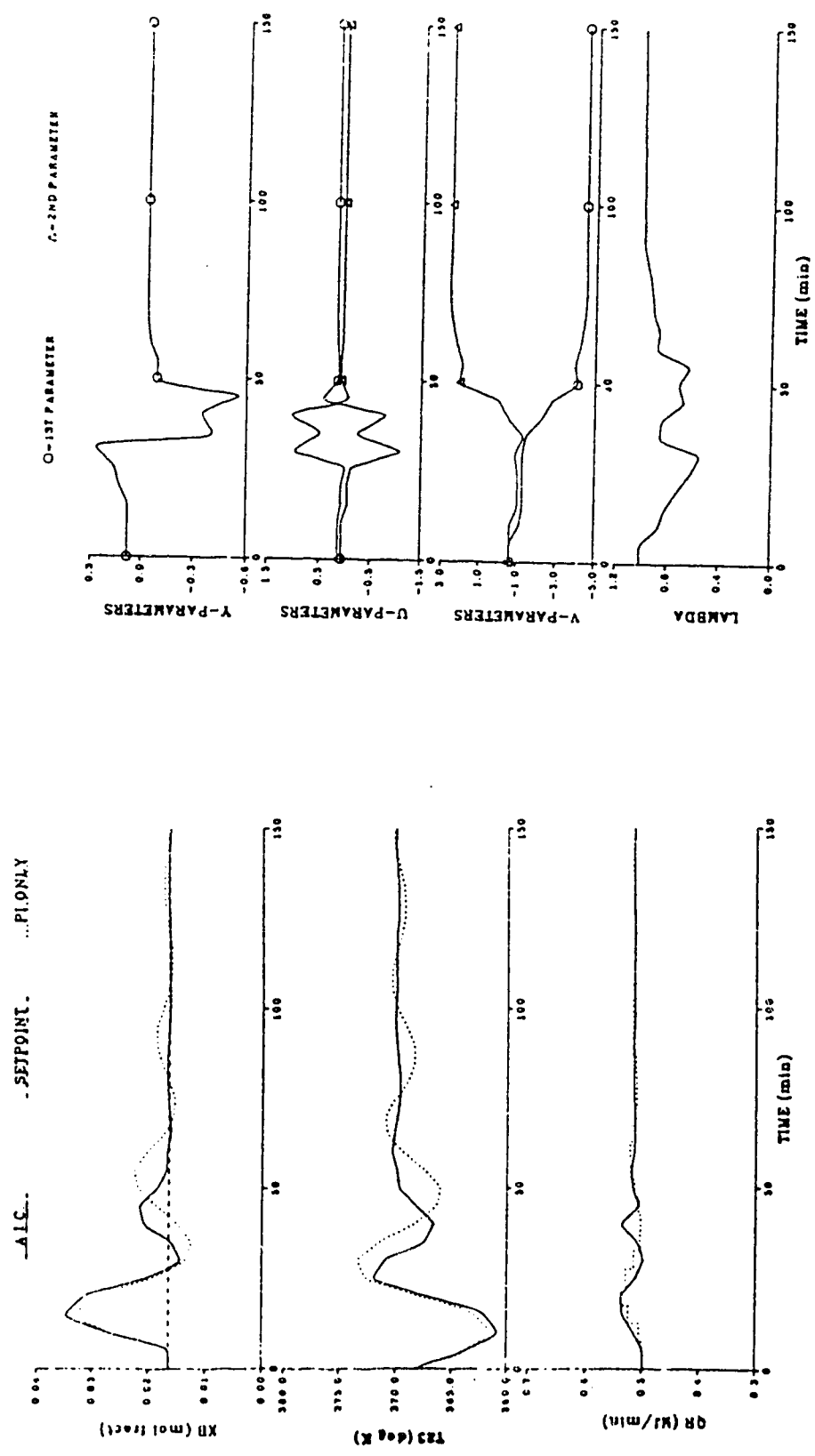


Figure 4.27 Comparison of Conventional PI and TST-2 AIC Control Performance for a +20% Step Change in Feed Rate and AIC Parameter Trajectories (15% Dead-band with AIC)

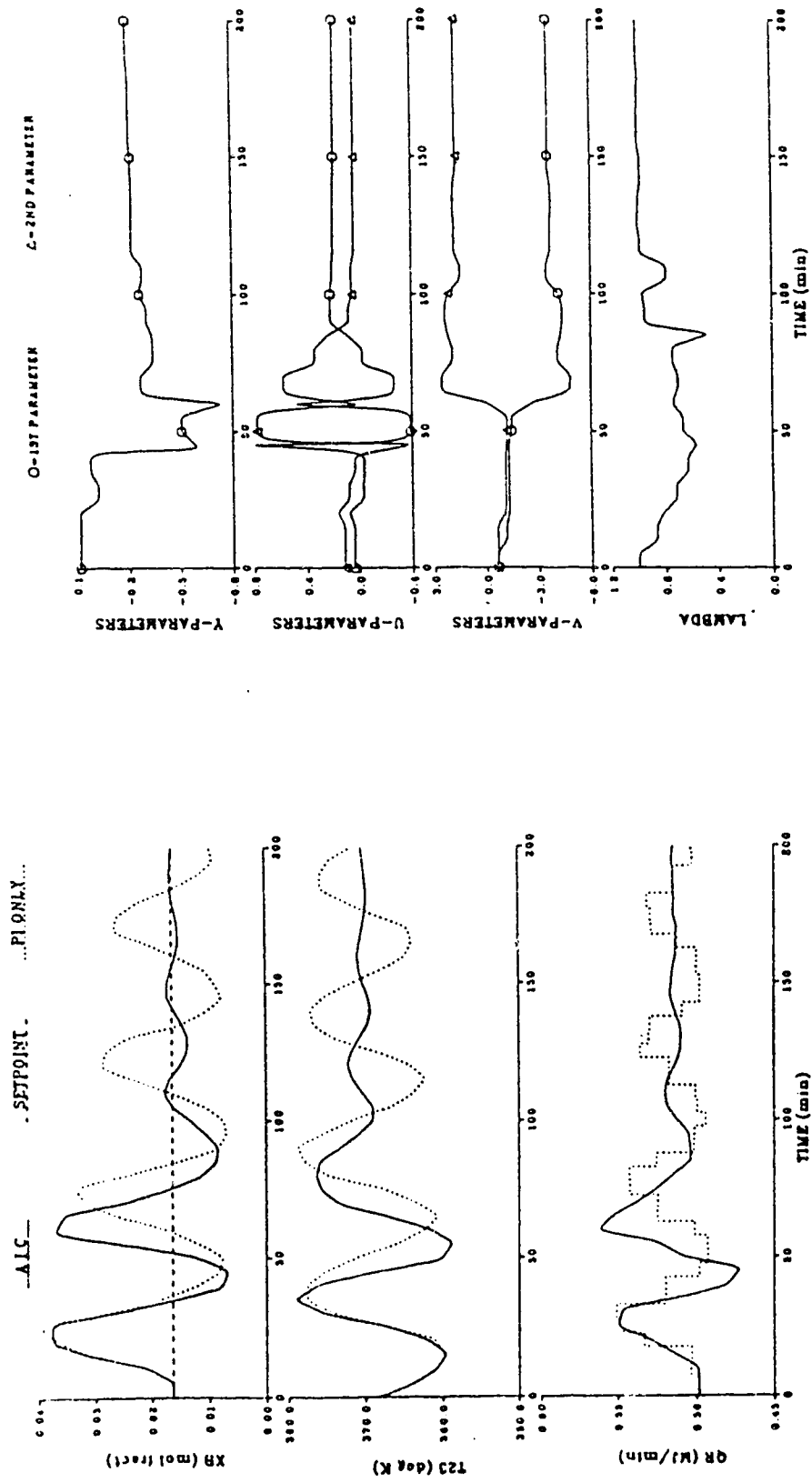


Figure 4.28 Comparison of Conventional PI and TST-2 AIC Control Performance for Simultaneous Increases in Feed Rate and Analyzer Cycle Time and AIC Parameter Trajectories (15% Dead-band with AIC)

LK composition of a depropanizer column by simulation using DYCONDIST, a nonlinear, general purpose column simulator. The simulation results indicated that the standard algorithm, ST-1, should not be used for nonlinear and/or time-varying processes because of the large number of algorithm model parameters that must be identified. The two simplified algorithms, SM-1 and SM-2, which required the identification of fewer parameters, outperformed the standard scheme, ST-1, for most of the test disturbances. However, the ST-1 scheme provided the best performance for servo control of all the algorithms evaluated because the process does not exhibit strong nonlinear behavior for a set point change. The best regulatory control performance was obtained using the SM-1 algorithm, which only involves the identification of 3 parameters. The effect of the use of a dead-band on the AIC algorithm performance was investigated. Use of a dead-band was found to stabilize the control behavior during the initial adaptation period.

When the liquid temperature of a less sensitive tray,  $T_{27}$ , was used as secondary output instead of  $T_{23}$ , control performance actually improved for tests MD2 and MD4. One possible reason is that  $T_{23}$  was too sensitive to the disturbance, causing more drifting in the  $v$ -parameters. Yet, it can be concluded from the results that using either of the stage liquid temperatures with the simplified algorithms provided superior performance compared with that achieved using either the ST-1 or the PI control scheme.

Tests of the truncated first order standard algorithm (TST-2) showed that better control performance could be achieved than was possible using the standard algorithm but SM-1 and SM-2 schemes provided superior control performance than that achieved using the TST-2 scheme. Nevertheless, when

applying AIC algorithms to the control of nonlinear processes, all three (TST-2, SM-1 and SM-2) should be evaluated to establish which algorithm will provide the most satisfactory control behavior for the disturbance(s) of interest.

## Chapter 5 : Experimental Results

### 5.1 Introduction

The objectives of the experimental phase of this study were somewhat different from those of the simulation investigation. In order to limit the time devoted to the experimental study, a detailed comparison between the control performance of the conventional PI feedback control scheme and that achieved using the AIC schemes, as performed in the simulation phase of this work, was not conducted. During the experimental studies, emphasis was directed to implement, with minimum amount of tuning, the AIC schemes for closed loop control of bottoms composition of a pilot scale binary distillation column. The performance of the AIC algorithms was examined when the process was subjected to feed disturbances or set point changes. The pilot scale distillation column used for the experimental study is described in Section 5.2. Details of the implementation of the control law for controlling the bottoms composition of the column using a microcomputer computer are presented in Section 5.3. Experimental results are discussed in Section 5.4.

### 5.2 Description of the Equipment

A schematic diagram of the pilot scale distillation column used in this work, which is located in the Department of Chemical Engineering at the University of Alberta, is shown in Fig. 5.1. The 22.5 cm diameter column contains eight trays with tray spacing of 30.5 cm. Each tray contains four bubble caps arranged in a square pattern. Feed supply enters at tray 4, with an option of supplying feed at tray 5. The column is equipped with a

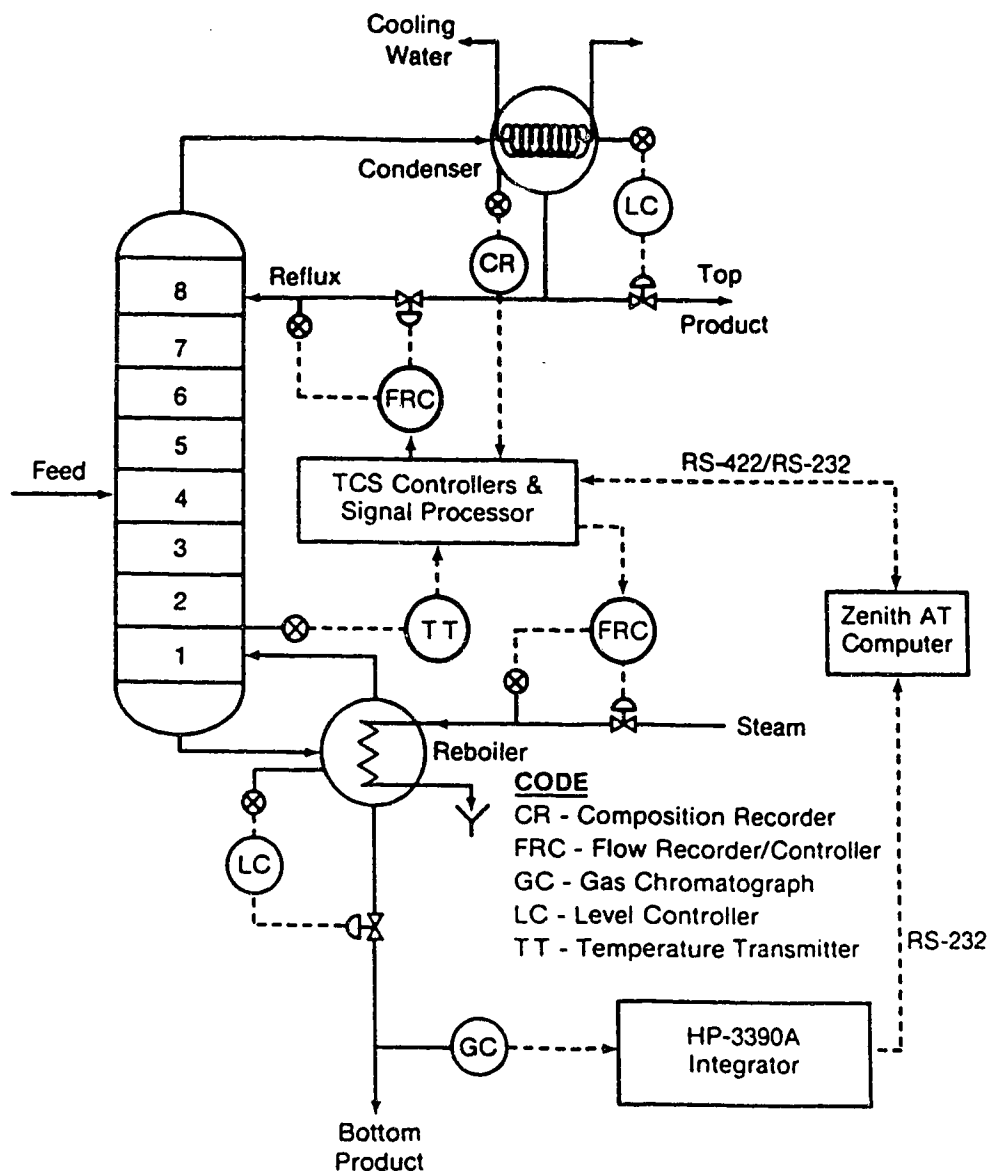


Figure 5.1 Schematic Diagram of the Binary Distillation Column

total condenser and a vertical thermosyphon reboiler with the liquid levels in the condenser and the reboiler regulated by manipulating the top and bottoms product flow rates respectively using two local analog PI controller. The column pressure is maintained at atmospheric pressure by manipulating the cooling water flow rate to the condenser. The typical operating conditions used during the experimental runs are listed in Table 5.1. The description that follows will concentrate on the changes that have been made to the equipment since the studies performed by Vagi (1988). Additional details of the column and the associated equipment are given by Svreck (1967), Lieuson (1980), Kan (1982), Langman (1987) and Vagi (1988).

Table 5.1  
Typical Steady State Operating Conditions of the  
Binary Distillation Column

Flow Rates :

Feed	17.2 g/s
Bottom Product	8.7 g/s
Top Product	8.5 g/s
Reflux	12.1 g/s
Steam	10.3 g/s

Compositions :

Feed	49.7 mass % MeOH
Top	95.0 mass % MeOH
Bottom	5.0 mass % MeOH

Several changes have been made to the associated equipment since the work of Langman (1987) and Vagi (1988). These changes were made to enable

the control of the column using three TCS (Turnbull Control Systems) 6300 series digital controllers, a TCS 6433 programmable signal processor and a Zenith PC/AT compatible computer equipped with two serial ports. The material that follows describe the communication link between the Zenith computer and the TCS controllers and signal processor to collect process measurements as well as to transmit control signals to the process. The hardware and software associated with this distillation column are documented in detail by Pacey (1973) and Shook (1989).

### 5.2.1 Software

The previous controller implementation was accomplished using a LSI 11/03 16 bit microcomputer (Langman, 1987; Vagi, 1988). Because of the limited memory available in the LSI, a Zenith PC/AT compatible computer, with 1 Mbyte of memory, has been used in the current work.

The computer is equipped with two serial ports for communications as described in the next section. Except for several low level subroutines for communicating with the serial ports written in Microsoft Macro-assembly language, all subroutines and the main control program have been written in ANSI FORTRAN 77 using Microsoft FORTRAN (version 4.1). The operating environment is Microsoft MS-DOS (version 3.3 Plus).

### 5.2.2 Communications

Two serial ports are installed in the personal computer. The integrator report is sent to serial port 2 (COM2) via the RS-232C integrator report line. The process measurements available from the three TCS controllers and the signal processor are accessed via the TCS RS-422



supervisory link. The data from the RS-422 link is converted to a RS-232 communication signal by a RS-422 to RS-232 converter. The converted RS-232 signal is then transmitted to serial port 1 (COM1) of the Zenith computer. Some FORTRAN and ASSEMBLY language subroutines resident in the computer receive the data sent to the serial ports.

### 5.2.3 Top Composition Control

The top composition is measured by an in-line capacitance cell. The capacitance and the temperature of the methanol-water solution are measured and the concentration is calculated by a microprocessor-based instrument fabricated by the Electronics Division of the Department of Technical Services (Svrcek, 1970). The instrument output voltage signal is sent to one TCS 6366 programmable controller. The stored calibration in the TCS 6366 controller is such that the range of input voltage corresponds to a composition range of 90 to 100 mass percent methanol. Top composition is controlled to a set point of 95 mass percent methanol by manipulating the reflux flow rate using this digital controller. The TCS controller output is a remote set point which is sent to a pneumatic PI controller. The pneumatic controller will then adjust the reflux valve position to give the desired reflux flow rate.

### 5.2.4 Feed Flow Control

The feed flow rate during each experimental run was set by the parameters read into the FORTRAN control program when the program was executed. The control signal was transmitted, via the RS-422/RS-232

communication link, to a TCS 6350 digital controller which sent a remote set point to a pneumatic PI flow rate controller.

#### 5.2.5 Bottoms Composition Control

The bottoms composition is measured by an HP-5722A gas chromatograph (GC). Automatic sampling of the bottoms product, for the GC, has been described in detail by Vagi (1988). An HP-3390A integrator has replaced the HP-1000 computer used previously for analyzing the signal from the GC. The ASCII composition report from the integrator is sent to a serial port of the Zenith personal computer via a RS-232C serial communication line. In the Zenith computer, there is a serial port which receives the report from the integrator. Two FORTRAN subroutines resident in the computer are used to extract the bottoms composition from the integrator report.

For this study, the overall cycle time of the GC sampling was selected to be 5 minutes, with other process measurements, such as temperatures and flow rates, being sampled at a 1 minute interval. Previous workers (Langman, 1987; Vagi, 1988) used an overall cycle time of 3 minutes but the AIC algorithms evaluated in this work are more applicable to processes with large controlled output sampling time and so a 5 minute cycle time was chosen for this work. Increasing the cycle time to 5 minutes did not affect the precision of the composition measurement. Four and a half minutes were used by the HP integrator for analysis of the chromatogram and for generation of the analysis report. Transmission of the report to the Zenith computer, via a RS-232C link, required approximately 25 seconds, followed by the sample purge. The time required for transmission of the report is quite long because the report from the HP integrator is of fixed format and the

only way to extract the composition measurement from the report is to scan the ASCII report line by line until the composition measurement is received. The sample purge was necessary to return the detector current to the base line value in preparation of the next sample. At the end of the 5 minutes, the FORTRAN control program resident in the Zenith computer initialized the sample injection. Further details of the sampling mechanism are described by Vagi (1988).

### 5.2.6 Temperature Measurements

There are a large number of iron-constantan thermocouples installed at various locations to measure liquid temperatures. Currently, four liquid temperatures can be accessed by the Zenith computer. The small voltage (mV) signals from four thermocouples, which measure the liquid temperatures at trays 1, 2 and 6 and the GC return line, are transmitted to the TCS 6432 signal processor which enables the temperature signals to be read via a RS-422 supervisory link.

### 5.3 Estimation Equations, Identification and Initialization

As mentioned in the previous section, the cycle time of the gas chromatograph was 5 minutes and the tray temperatures and flow rates were sampled at 1 minute intervals. The control objective is the regulation of the bottoms product composition,  $X_B$ , to its set point via manipulating the steam flow rate. The estimation equations for the ST-1, SM-1 and SM-2 schemes are the same as those presented in Chapter 3 (c.f. Eqs. 3.5 - 3.7). Since the liquid temperature at tray 2 is the most sensitive tray temperature to feed disturbances (c.f. Table 2.1), this temperature was

selected as the secondary output ( $v$ ) for evaluation of the AIC algorithm. A proportional plus integral controller (c.f. Eq. 3.8) was used in each AIC scheme. The control performance achieved using each AIC scheme was compared to that obtained using the conventional feedback PI controller.

The initial settings for the proportional plus integral controller, established using the process reaction curve method and the Cohen-Coon formulae (Stephanopoulos, 1984), were calculated to be  $K_p = -0.27 \frac{\text{g/s}}{\text{mass \%}}$  and  $K_I = -0.017 \frac{\text{g/s}}{\text{mass \%}-\text{min}}$ . The controller settings for the PI control scheme were tuned to obtain a minimum IAE value for a 25% step disturbance in the feed rate. The final settings were found to be  $K_p = -0.32 \frac{\text{g/s}}{\text{mass \%}}$  and  $K_I = -0.018 \frac{\text{g/s}}{\text{mass \%}-\text{min}}$ . As mentioned in Section 5.1, the AIC schemes were applied to regulate the bottoms composition with minimum amount of tuning effort. Therefore, the same final controller settings were used in the AIC schemes.

As in the simulation work presented in Chapter 4, all values used in the regressor vector are scaled deviation values (c.f. Eq. 4.1). For the experiments, the nominal values of the controlled variable ( $y$ ), manipulated variable ( $u$ ) and secondary variable ( $v$ ) were set to the corresponding initial process values. Since the deviations of  $y$ ,  $u$  and  $v$  from its nominal values were all in the order of  $10^1$ , the scaling factors used for  $y$ ,  $u$  and  $v$  were equal to 1.0. The dead-band on the AIC scheme (c.f. Eq. 2.41) used was arbitrarily chosen to be 10%.

The RLS identification algorithm employs a fixed forgetting factor,  $\lambda$ , and covariance resetting (c.f. Section 2.3.3). The value of  $\lambda$  was selected to be 0.98. The covariance matrix,  $P$ , was initialized to 100 times the identity matrix ( $I$ ).  $P$  was reset to  $\alpha^*I$  whenever the trace of  $P$  dropped

below a specified value,  $P_{\min}$ . To determine the values of  $\alpha$  and  $P_{\min}$  which would provide satisfactory results, the RLS parameter identification and the controlled output estimation for the ST-1 scheme were "turned on" during the controller settings tuning runs. The predicted values of  $X_B$  were then compared with the actual measured  $X_B$ . The values of  $\alpha$  and  $P_{\min}$  that resulted in the best prediction of  $X_B$  were used for all the experimental tests. The ST-1 scheme was chosen for tuning  $\alpha$  and  $P_{\min}$  because this scheme had the largest number of parameters and so the values of  $\alpha$  and  $P_{\min}$  selected for the ST-1 scheme would work satisfactory for the simplified algorithms. The  $\alpha$  and  $P_{\min}$  values were selected to be 2.0 and  $0.3 \cdot n$  respectively, where  $n$  is the number of parameters to be identified.

To apply any adaptive control schemes, it is important to obtain good initial parameters for the parameter vector. The initial parameters for the AIC algorithms were obtained in the following manner :

- (1)  $X_B$  was regulated to its set point using the conventional PI control scheme initially;
- (2) the regressor vector was initialized at time  $t=0$  minute;
- (3) RLS identification and adaptive inferential estimation were switch "on" at  $t=20$  minutes with  $X_B$  still controlled using the PI scheme;
- (4) at  $t=120$  minutes, the PI control scheme was switched "off" and the AIC algorithm switched "on" to control  $X_B$ ;
- (5) From observations during the controller tuning runs, after three hours of RLS identification, the predicted values of  $X_B$  generated by the ST-1 AIC algorithm were quite accurate, indicating that the parameters had converged to reliable values. Thus, for both the

feed rate disturbance and set point change tests, the change was introduced at  $t=180$  minutes.

To compare the control performance of the PI, ST-1 SM-1 and SM-2 schemes, the IAE index for each scheme was calculated for the period after the initial three hours "tune-in" period.

#### 5.4 Results

The performance of the four control schemes, PI, ST-1, SM-1 and SM-2, have been evaluated for control of the bottoms composition of the pilot scale binary distillation column when there were feed flow rate disturbances or set point changes. As will be presented in the next section, the control performance of the ST-1 scheme was very poor for a 25% step increase in feed rate. Therefore, the ST-1 scheme was not evaluated for a decrease in feed rate or changes in set point.

##### 5.4.1 Step Increase in Feed Rate of 25%

Table 5.2 provides a summary of the IAE performance values for each AIC scheme and the conventional feedback PI control scheme for a 25% step increase in feed rate. It should be noted that the IAE values in Table 5.2 were calculated from time  $t=180$  minutes, the time at which the disturbance was introduced. The closed loop responses obtained using the ST-1, SM-1 and SM-2 control strategies are compared in Figs. 5.2 to 5.4 with the controlled responses that resulted from utilizing the PI scheme. Each of these figures also shows the parameter trajectories and the trajectory of the trace of the covariance matrix. As mentioned in Chapter 3, for the sake of clarity, only 7 of the 12 parameters of the ST-1 algorithm are displayed in the parameter

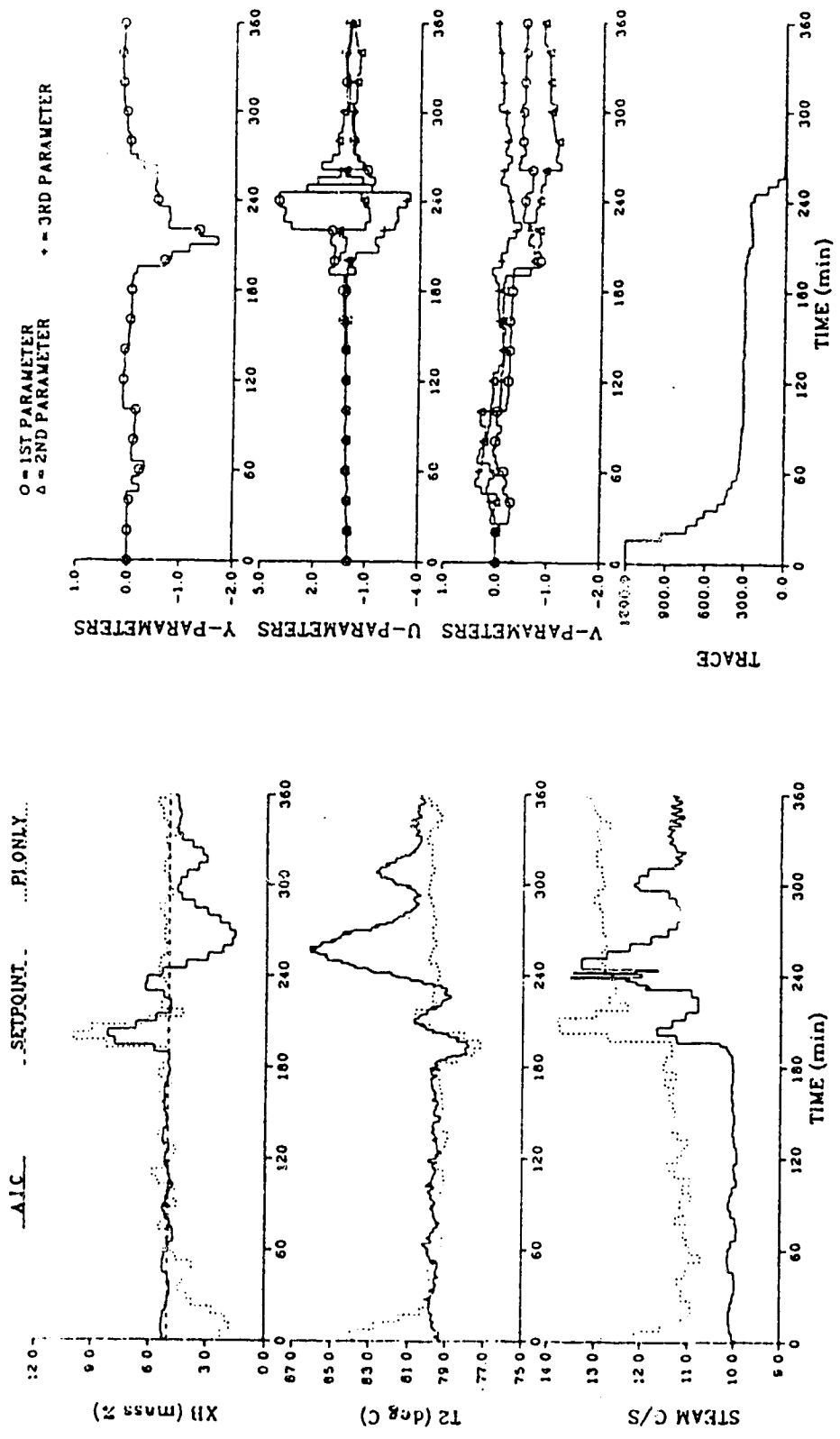


Figure 5.2 Comparison of Conventional PI and ST-1 AIC Control Performance for a +25% Step Change in Feed Rate and AIC Parameter Trajectories

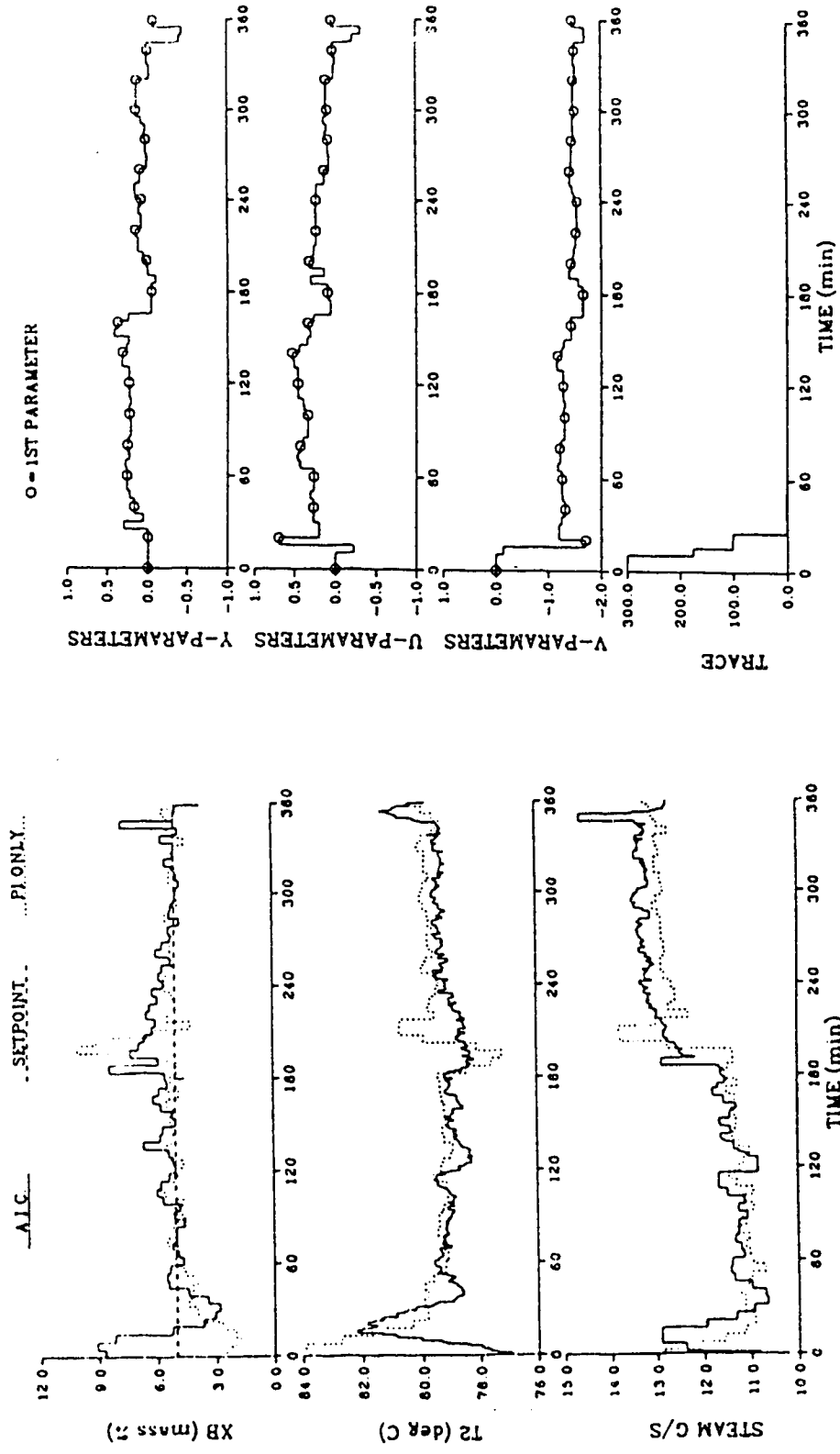


Figure 5.3 Comparison of Conventional PI and SM-1 AIC Control Performance for a +25% Step Change in Feed Rate and AIC Parameter Trajectories



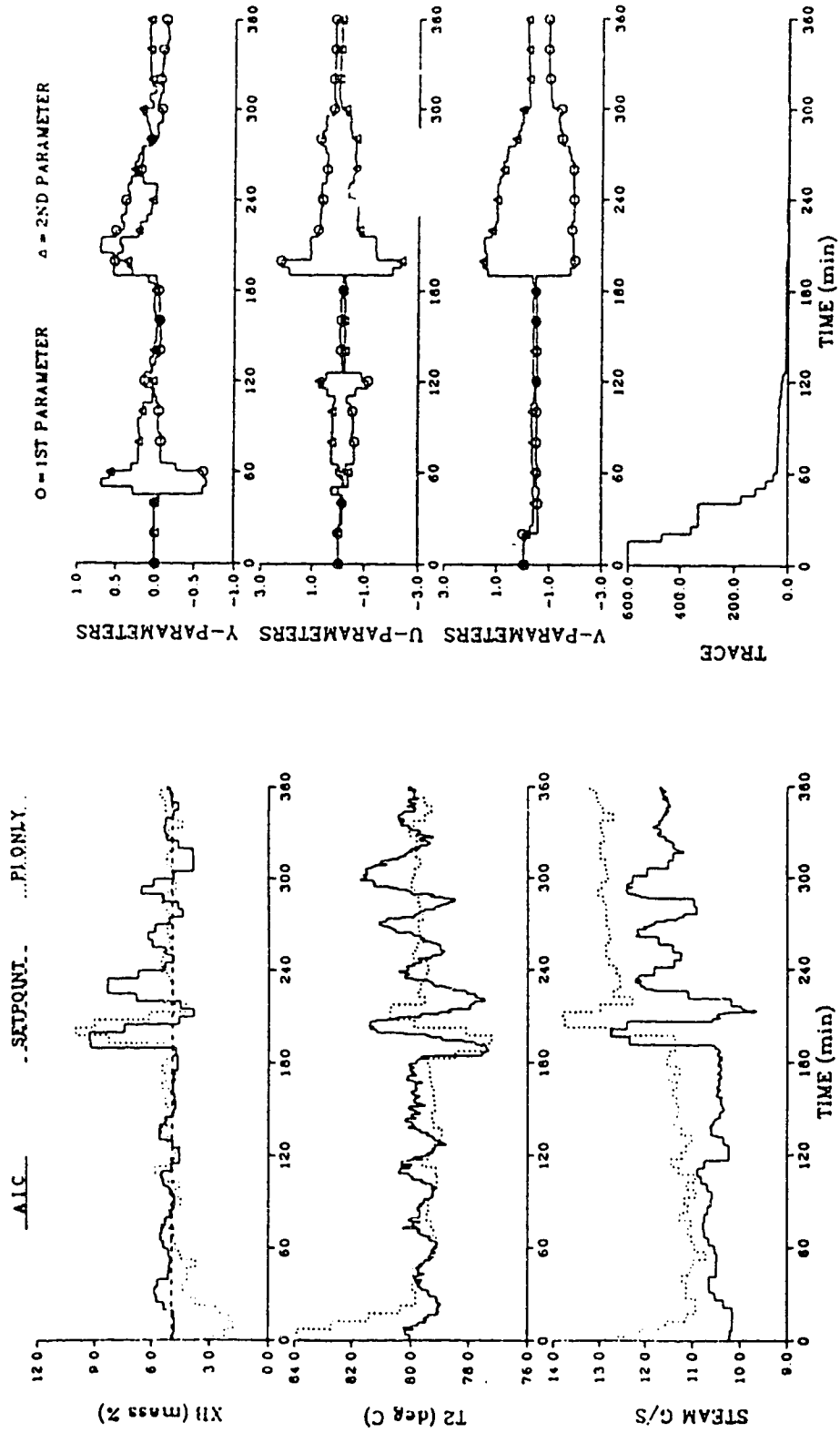


Figure 5.4 Comparison of Conventional PI and SM-2 AIC Control Performance for a +25% Step Change in Feed Rate and AIC Parameter Trajectories

trajectories. The best control performance for the feed disturbance, resulting in a minimum IAE value of 106.4, was obtained using the PI scheme. The IAE performance indices resulted from employing the SM-1 and SM-2 algorithms were found to be 32% and 72% larger than the minimum IAE value achieved using the PI scheme. The ST-1 scheme provided unacceptable control behavior, as can be seen from the  $X_B$  trajectories displayed in Figs. 5.2. The controlled responses obtained by utilizing the SM-2 algorithm were quite oscillatory. Both the PI and SM-1 schemes were able to regulate  $X_B$  to within ten percent of its set point value of five mass percent methanol only 80 minutes (i.e  $t=260$  minutes) after the disturbance was introduced while neither the ST-1 nor SM-2 scheme were able to achieve this performance until  $t=320$  minutes. It should be noted that the control performance of the SM-1 scheme was quite satisfactory considering the fact that the controller settings of the fixed PI controller in the adaptive scheme were never tuned. The SM-1 scheme should be able to provide comparable or even better control behavior than the PI scheme if its controller settings were tuned for this feed disturbance.

Table 5.2  
Summary of Control Performance for a +25%  
Step Change in Feed Rate

<u>Control Scheme</u>	<u>IAE (mass %-minute)</u>	<u>Reference Figures</u>
PI	106.4	5.2-5.4
ST-1	229.6	5.2
SM-1	140.9	5.3
SM-2	182.9	5.4

In Fig. 5.5, the predicted values of  $X_B$  are compared with the actual  $X_B$  values for each AIC scheme. As can be observed from the top plot in this figure, the predicted  $X_B$  generated by the ST-1 algorithm was quite accurate during the initial 3 hour "tune-in" period. However, after the feed disturbance was introduced, at  $t=180$  minutes, the predicted  $X_B$  was very erratic for about 100 minutes. Although a 10% dead-band on AIC was employed, the resulting control performance was still not satisfactory because of the oscillatory behavior of the prediction, leading to fluctuations in the controlled and manipulated outputs. The predicted values of  $X_B$  obtained using the SM-2 scheme were more accurate than those obtained using the ST-1 scheme but these estimated values of  $X_B$  generated by the SM-2 scheme were not accurate enough to provide good controlled responses. In contrast to this performance the predictions generated by the SM-1 algorithm, displayed in the middle plot of Fig. 5.5, are satisfactory and clearly superior to both of the ST-1 or SM-2 schemes. The predicted  $X_B$  values almost match the actual  $X_B$  values only 20 minutes after the disturbance occurred. The accurate predictions resulted in a very smooth control behavior even though the controller settings of the PI controller used with the SM-1 algorithm were the values selected for PI feedback control.

The fast convergence of the predictions generated by the SM-1 scheme to the actual controlled output can probably be attributed to the small number of parameters that needed to be identified. It can be seen from the parameter trajectories presented in Figs. 5.2 to 5.4 that the parameters of SM-1 converged to new values only 20 minutes after the disturbance was introduced while the parameters of the ST-1 and SM-2 algorithms did not

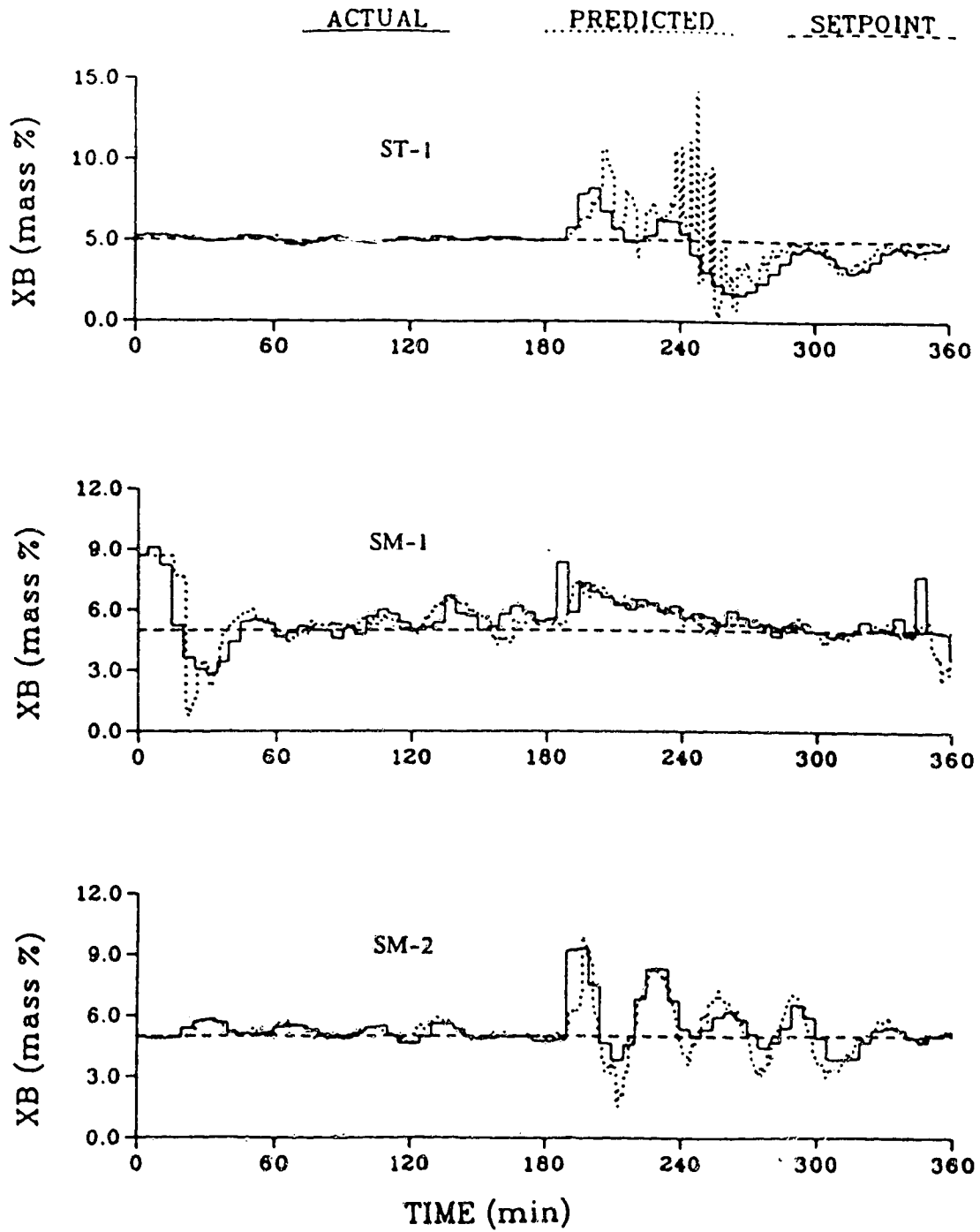


Figure 5.5 Comparison of Predicted Bottoms Composition versus Actual Bottoms Composition for a +25% Step Change in Feed Rate

converge until  $t=300$  minutes, 2 hours after the disturbance took place.

From the patterns of the trace of the covariance matrix presented in these figures, it is also obvious that the parameters of SM-1 adapted to new process characteristics much faster than was the case for either of the other two AIC schemes.

#### 5.4.2 Step Decrease in Feed Rate of 20%

The control performance of the PI, SM-1 and SM-2 schemes was also evaluated for a step decrease in feed rate. In this set of experimental runs, as described in Section 5.3, the two AIC schemes had three hours "tune-in" period. At time  $t=180$  minutes, a -20% step change in feed rate was introduced with the feed rate subsequently increased to its normal operating value at time  $t=360$  minutes and the test terminated at  $t=550$  minutes. The IAE performance indices, calculated for the period  $t=180$  to  $t=550$  minutes, are summarized in Table 5.3. The controlled responses resulted from utilizing the SM-1 and SM-2 algorithms are compared with the control behavior achieved using the PI scheme in Figs. 5.6 and 5.7, respectively. From the IAE values and the control responses presented, it is obvious that the SM-1 control scheme outperformed both the SM-2 and PI schemes for the feed rate decrease. The SM-1 algorithm was able to bring  $X_B$  slowly to its set point with some oscillations while the PI and SM-2 schemes resulted in very oscillatory  $X_B$  trajectories. The control behavior observed when SM-2 was utilized was very oscillatory, resulting in the largest IAE value for the three control schemes.

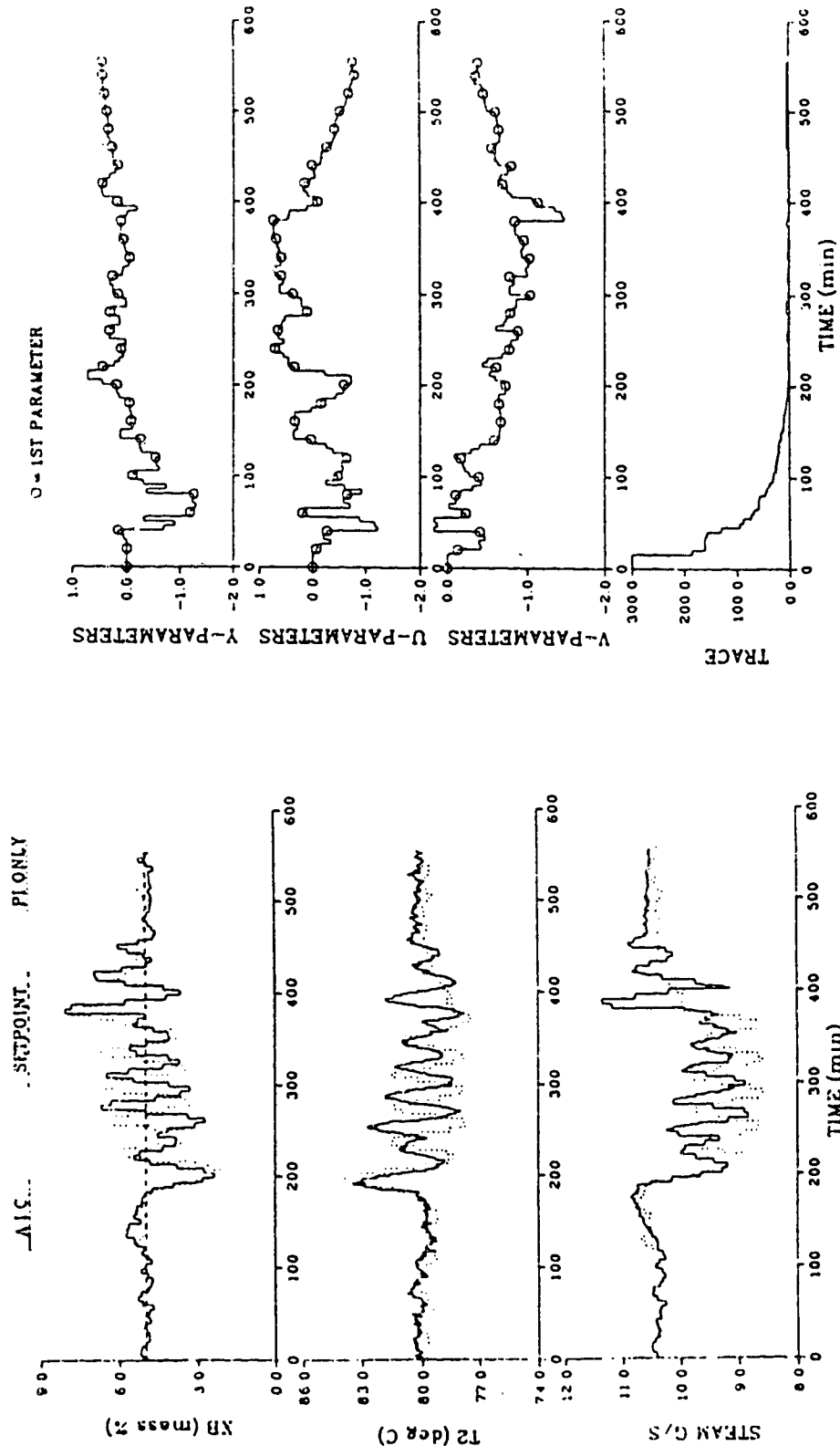


Figure 5.6 Comparison of Conventional PI and SM-1 AIC Control Performance for a -20% Step Change in Feed Rate and AIC Parameter Trajectories

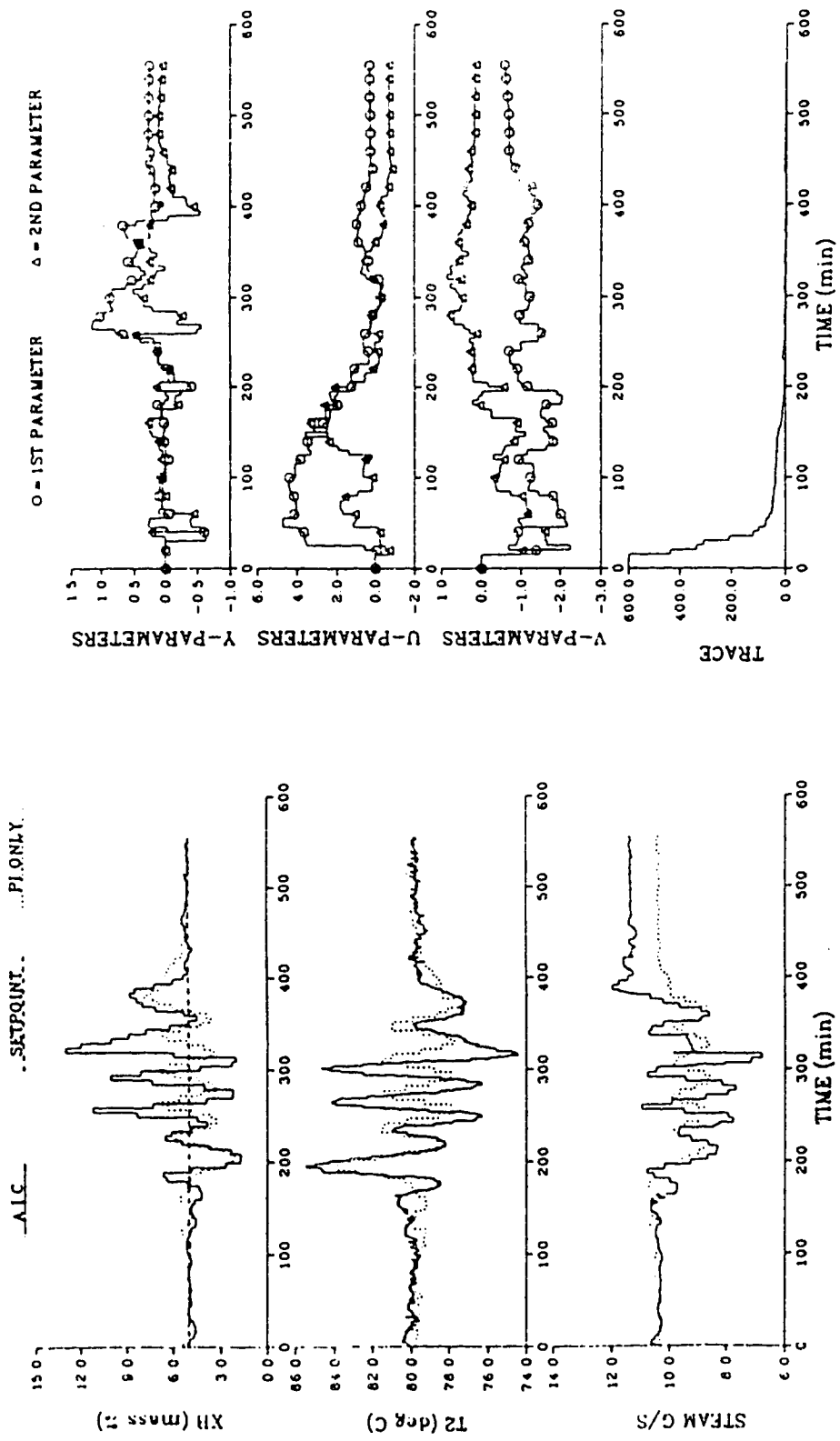


Figure 5.7 Comparison of Conventional PI and SM-2 AIC Control Performance for a -20% Step Change in Feed Rate and AIC Parameter Trajectories

Table 5.3  
Summary of Control Performance for a -20%  
Step Change in Feed Rate

Control Scheme	IAE (mass % - minute)		Reference Figures
	Decrease from Steady State	Back to Steady State	
PI	204.1	118.6	5.6-5.7
SM-1	177.1	111.2	5.6
SM-2	343.9	119.4	5.7

When the feed rate was increased to its steady state value at  $t=360$  minutes, all the three control strategies evaluated were able to regulate  $X_B$  to its set point before the end of the test period. The IAE values presented in Table 5.3 reveal that the control performance of all the three control schemes was comparable for this increase in feed rate. The minimum IAE value of 111.2, which resulted from utilizing the SM-1 scheme, is only slightly lower than the maximum IAE value which resulted when the SM-2 scheme was employed. The significant improvement in control performance when the feed rate was increased to its steady state value compared with the case when the feed rate dropped below its steady state value indicated that a decrease in feed rate is a more severe disturbance than an increase in feed rate.

The fast parameter adaptation to new process characteristics achieved using the SM-1 scheme, because of the small number of parameters involved, resulted in the superior control performance of the SM-1 scheme, as can be observed from the parameter trajectories displayed in Figs. 5.6. The adaptation patterns of the parameters of the SM-1 are "smoother" than those



of the SM-2 scheme shown in Fig. 5.7 when the feed rate was below its normal value. This explains the poor predictions generated by the SM-2 scheme compared to those of SM-1 (c.f. Fig. 5.8). When the feed rate was increased to its steady state value, since both the SM-1 and SM-2 schemes were able to adapt reasonably quick to this change to the original operating conditions, the control performance of these two AIC schemes is comparable for  $t=360$  to  $t=550$  minutes. In summary, only the SM-1 scheme can provide satisfactory control performance for this set of feed disturbances.

#### 5.4.3 Servo Control Performance

Figs. 5.9 and 5.10 display the controlled responses of the PI, SM-1 and SM-2 schemes when the process was subjected to set point changes. It should be noted that the responses for the initial three hours of "tune-in" period are not shown in these figures. The set point was changed from five mass percent methanol to six percent at time  $t=0$  minutes and it was decreased to its normal value of five mass percent methanol at  $t=180$  minutes. The IAE values obtained for this set of tests are reported in Table 5.4. The poorest performance, with a total IAE value of 98.0, resulted from employing the PI scheme. The SM-2 algorithm provided the best overall control behavior, with an minimum IAE value of 77.3, while the performance of the SM-1 scheme was comparable to that of SM-2. From the  $X_B$  responses shown in Figs 5.9 and 5.10, it can be seen that all the three control schemes evaluated were able to bring  $X_B$  to its set point within two hours for either an increase or a decrease in set point. The SM-1 scheme responded fastest to the increase in set point while the SM-2 algorithm responded fastest to the decrease in set point.

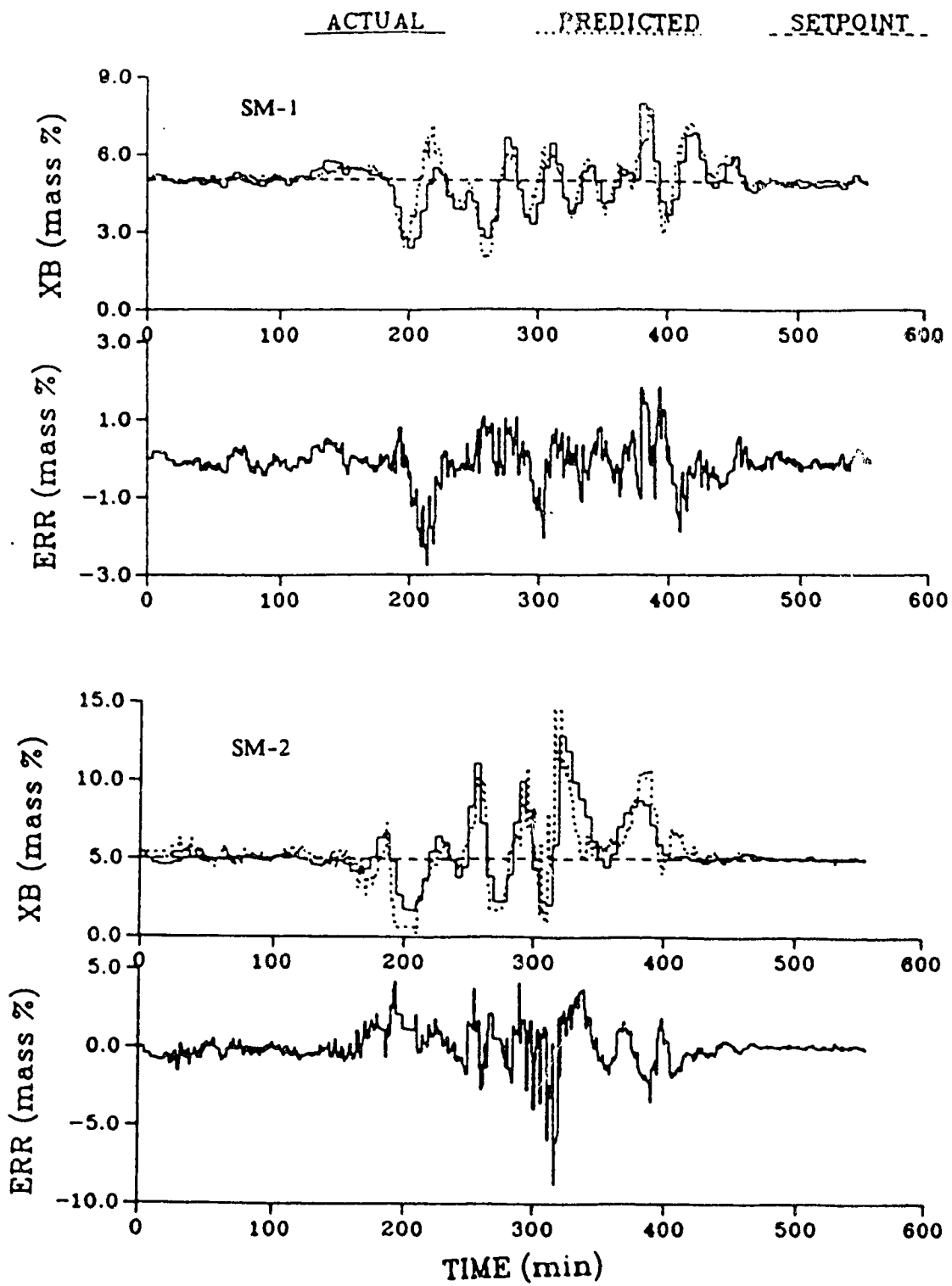


Figure 5.8 Comparison of Predicted Bottoms Composition versus Actual Bottoms Composition for -20% Step Change in Feed Rate

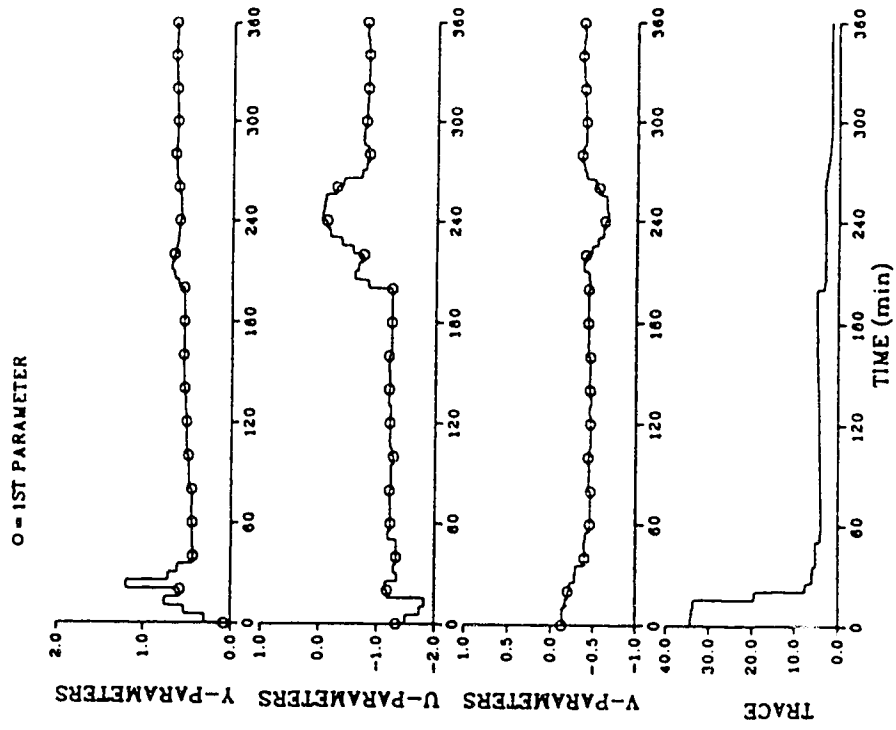
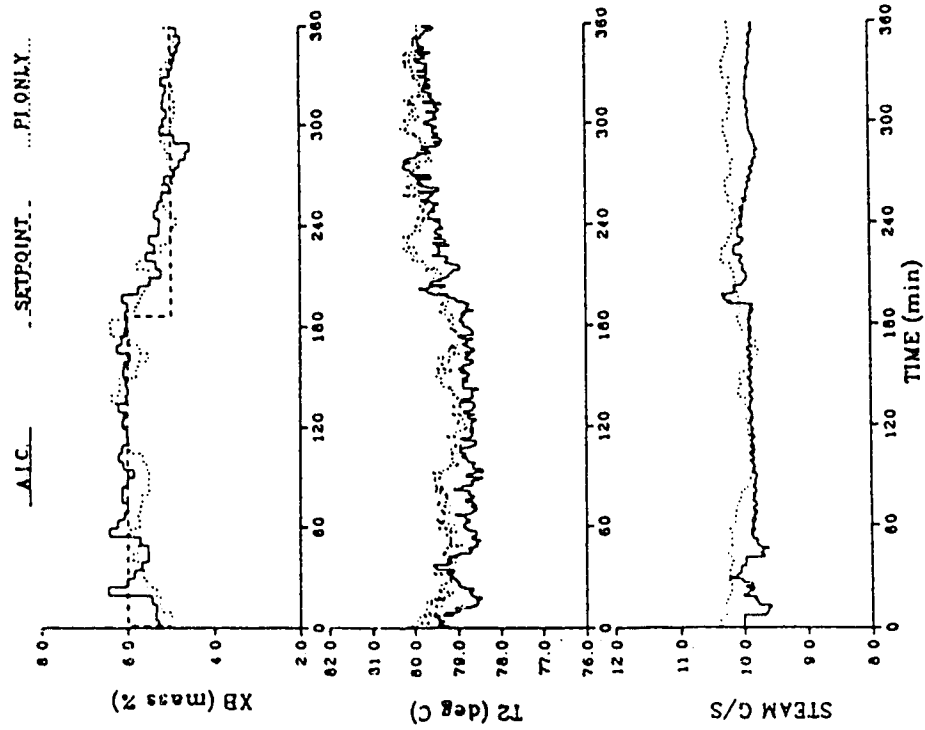


Figure 5.9 Comparison of Conventional PI and SM-1 AIC Control Performance for Step Changes of One Mass Percent Methanol Concentration in the Bottoms Composition Set Point

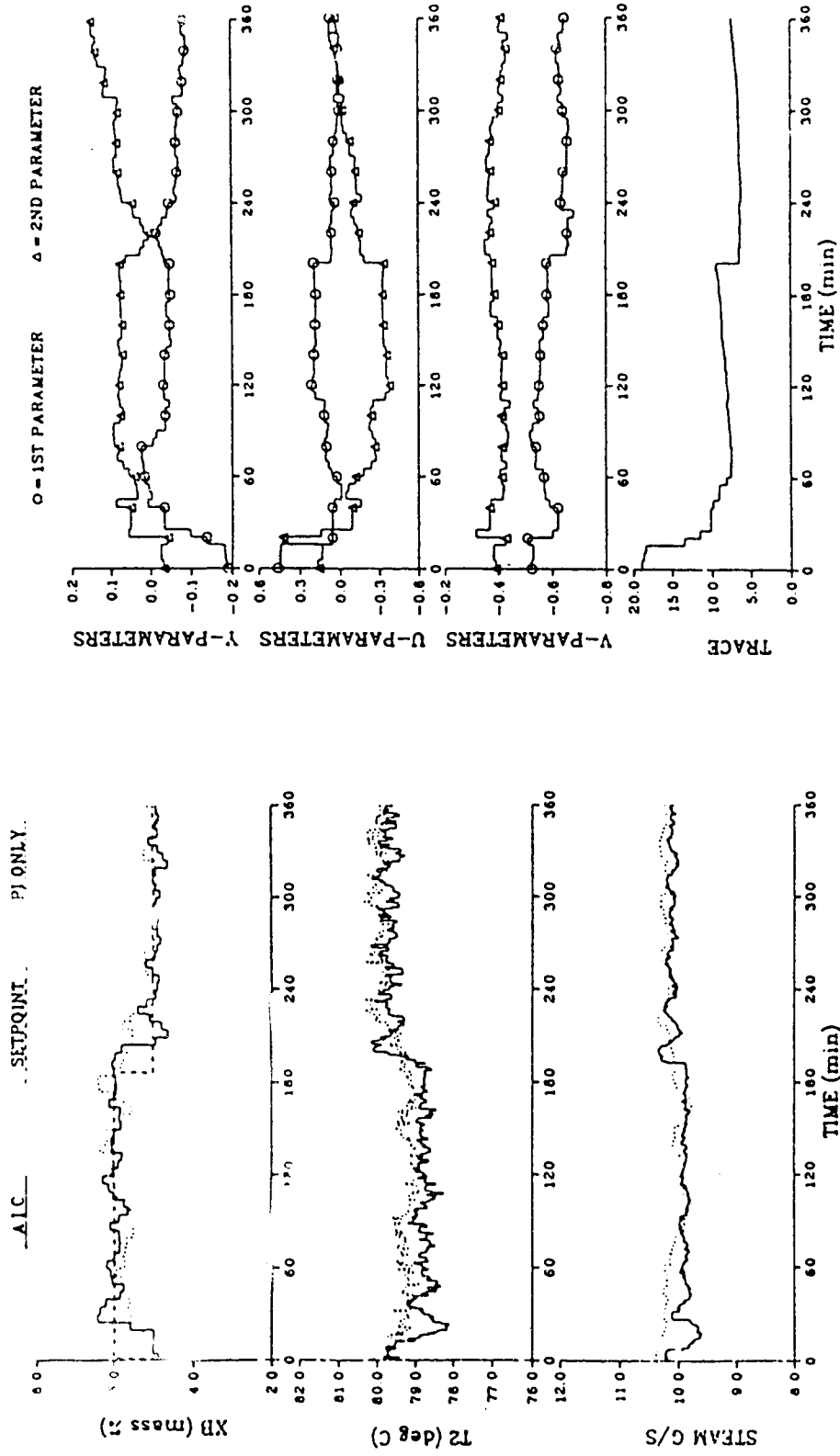


Figure 5.10 Comparison of Conventional PI and SM-2 AIC Control Performance for Step Changes of One Mass Percent Methanol Concentration in the Bottoms Composition Set Point

Table 5.4  
 Summary of Control Performance for Step Changes of One Mass Percent  
 Methanol Concentration in Bottoms Composition Set Point

<u>Control Scheme</u>	<u>Increase from Steady State</u>	<u>Back to Steady State</u>	<u>Reference Figures</u>
PI	53.0	45.0	5.9-5.10
SM-1	34.6	51.8	5.9
SM-2	40.0	37.3	5.10

It might have been expected that since the SM-2 algorithm has three more parameters to be identified than the SM-1 scheme, control performance of the SM-2 strategy would be inferior to that of SM-1 but this was not the case. A possible explanation is that unlike the column behavior for feed flow rate disturbances, the process did not exhibit very strong nonlinear behavior for changes in set point and so the SM-2 scheme was still able to quickly adapt its parameters to new values corresponding to the new set point. This resulted in accurate predictions of the controlled output, as can be seen from the prediction plots presented in Fig. 5.11. For the set point changes introduced, it can be seen that the SM-2 scheme generated more accurate predictions than SM-1 for the period  $t=180$  to  $t=360$  minutes, leading to slightly better overall control performance for SM-2. When the parameter trajectories shown in Figs. 5.9 and 5.10 are compared with the trajectories of the same algorithms for the feed disturbances (c.f. Figs 5.3, 5.4, 5.6, and 5.7), it is obvious that the parameter trajectories for the set point changes are "smoother" than those for feed disturbances, indicating that the column exhibited stronger nonlinear behavior when

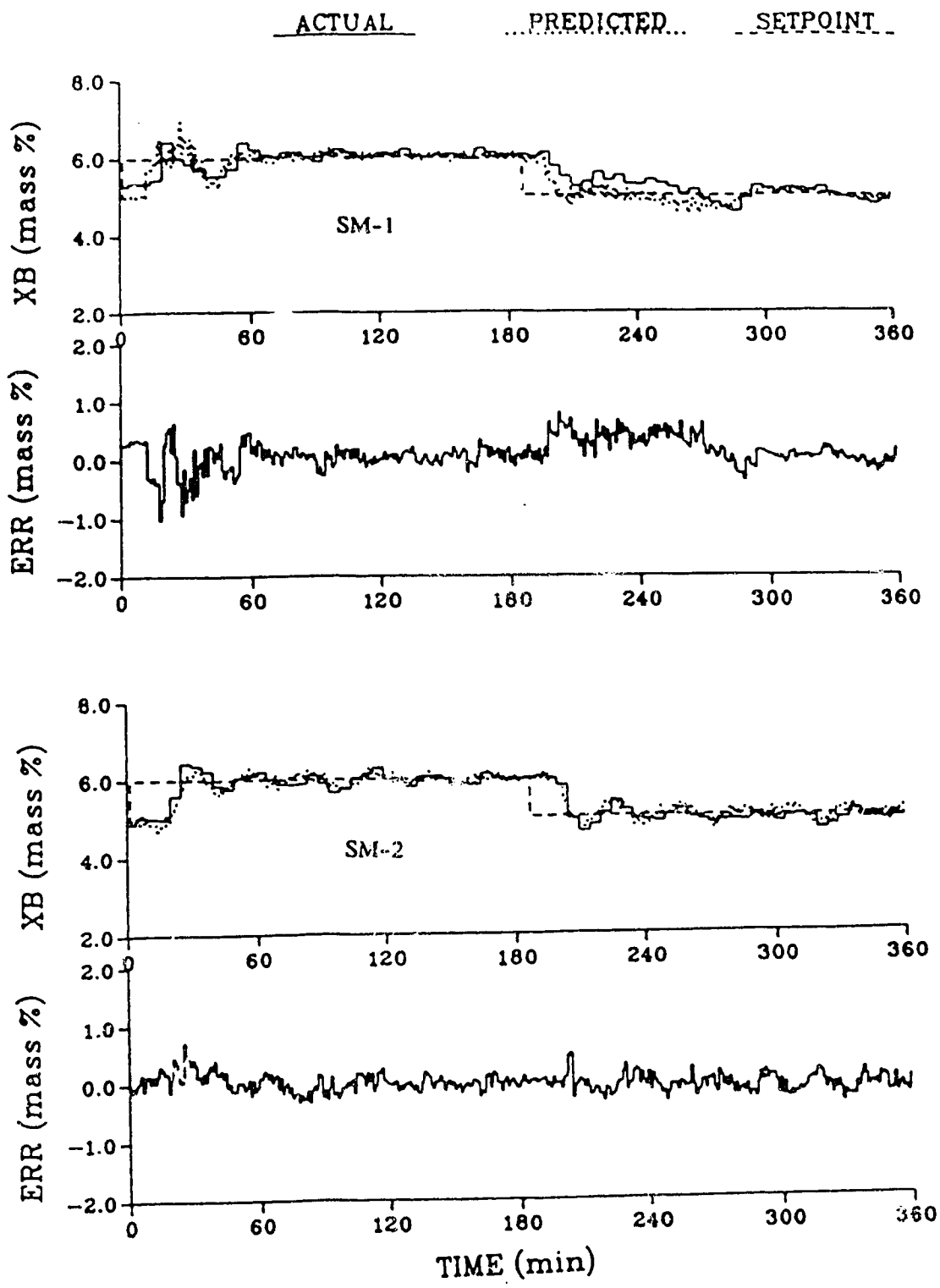


Figure 5.11 Comparison of Predicted Bottoms Composition versus Actual Bottoms Composition for Step Changes of One Mass Percent in Bottoms Composition Set Point

subjected to feed flow rate disturbances.

### 5.5 Summary

The performance of the three AIC schemes, designated as ST-1, SM-1 and SM-2, have been applied to control the bottoms product composition of a computer controlled, pilot scale binary distillation column. Experimental results showed that the standard algorithm, ST-1, could not provide satisfactory control performance for a +25% step change in feed rate because of the large number of parameters that had to be identified. Thus, use of this algorithm cannot be recommended for column control.

The simplified algorithm SM-1, which only has three parameters to be identified, is preferred over the SM-2 simplified scheme and the conventional feedback PI control scheme because SM-1 provided satisfactory control performance for both the step increase and decrease in feed rate as well as the changes in set point. The SM-2 scheme did not work satisfactorily when there were feed disturbances but it did control the bottoms composition in a satisfactory manner for the set point changes. On the basis of these results, it can be concluded that the SM-1 scheme will provide better control performance than the PI or SM-2 scheme for distillation column control.

## Chapter 6 : Conclusions and Recommendations for Future Work

### 6.1 Conclusions

This work has been concerned with the evaluation, by simulation and experimental studies, of the control performance that can be achieved using the multirate adaptive inferential estimations schemes which infer intersample values of an infrequently sampled controlled output from a more rapidly sampled secondary plant output. A first order plant model was used in the standard algorithm (ST-1 scheme) while first and second order plant models were employed with the simplified algorithm (SM-1 and SM-2 schemes respectively). Each of the three estimators obtained was combined with a fixed parameter proportional plus integral controller to form a multirate adaptive inferential control (AIC) scheme. The control performance of each AIC scheme was compared with the control behavior of a conventional PI feedback control strategy for control of bottoms compositions of distillation columns. The comparison was accomplished in three stages and the results of each stage are summarized below :

- (1) Simulation of the bottoms composition control of a binary distillation column modelled by transfer functions : The simulation results have shown that for the process model used, the standard algorithm (ST-1), though requiring the identification of 12 parameters, provided the best control performance for step changes in feed rate or set point. The performance of either of the simplified algorithms, SM-1 and SM-2, was comparable to that accomplished using the conventional PI control scheme. The



performance of all three AIC schemes was found to deteriorate when a less sensitive secondary output (tray liquid temperature at tray 6 in this case) was used instead of a sensitive secondary output (tray liquid temperature at tray 2). Because of the large number of parameters (12) that had to be identified, the effect of a poor choice of the secondary output on control performance was most profound when the standard algorithm was employed. The same phenomenon were observed for the case where the process model parameters (gains and time delays) were changed when the same step disturbance in feed rate was introduced into the process. These results have indicated that a potential problem of the speed of convergence of parameters may arise when the standard algorithm is applied to control a highly nonlinear and/or time-varying process.

- (2) Simulation of the control of the bottoms LK composition of a depropanizer column : The simulation of the control behavior of the depropanizer was performed using a nonlinear, general purpose multicomponent distillation column dynamic simulator, DYCONDIST. The simulation results showed that the standard algorithm was not suitable for control of this nonlinear process because of the large number of algorithm model parameters that must be identified. The best regulatory control performance was obtained using the SM-1 algorithm which required the identification of only 3 parameters. The SM-2 simplified scheme also outperformed either the ST-1 or PI scheme. It was shown that a different way of truncating the standard algorithm (designed as TST-2 scheme) also resulted in improved control performance over the ST-1 and the PI schemes. Use

of a dead-hand on AIC strategies was found to stabilize the control behavior during the initial adaptation period and thus its use is strongly recommended for practical applications.

- (3) Experimental evaluation of the control of the bottoms composition of a pilot scale binary distillation column : The experimental results further demonstrated the robust control performance of the SM-1 algorithm because only 3 parameters needed to be identified. The ST-1 scheme was unable to provide satisfactory control performance. Although the controller settings of the fixed PI controller used in the AIC schemes were never tuned, the SM-1 scheme was able to accomplish acceptable control behavior for a +25% step disturbance in feed rate. For the cases with -20% step disturbance in feed rate or one mass percent set point changes, the SM-1 algorithm outperformed either the SM-2 or PI scheme. The SM-2 scheme only provided good performance for servo control.

In conclusion, the simulation and experimental results show the the improvement of overall control performance using the SM-1 control algorithm. It should be noted that for adaptive control techniques to gain widespread acceptance in industry, they must be easy to implement and maintenance free. The robust control resulting from employing the SM-1 scheme in this work has indicated that this simplified algorithm has the potential to work satisfactorily in industrial processes with minimal design and tuning effort. However, the conclusions from this research are not general. Thus, when applying AIC algorithms to the control industrial processes, which are mostly nonlinear and time-varying, different simplifications of the standard algorithm should be evaluated to establish which algorithm will provide the

most satisfactory control behavior for the disturbance(s) of interest.

## 6.2 Recommendations for Future Work

The AIC algorithms studied in this thesis represent practical solutions to a problem which is commonly encountered in process control, the intermittent measurements of the primary controlled output due to the long cycle time of the measuring device. While it has been demonstrated in this work, by simulation and experimental evaluation, that the simplified (SM-1) AIC algorithm can provide improved control performance compared with the performance that can be accomplished using the conventional PI feedback control scheme for nonlinear and/or time-varying systems, a number of areas exist for future work :

- (1) The control performance of the simplified algorithms should be evaluated for systems with long sample time, such as 10 or 20 minutes, in the measured controlled output ( $y$ ), a very common situation in the chemical process industry. For a process with a long dead time, say 20 minutes, a secondary output may often be accessed at a very fast rate, say every 30 seconds, and the manipulated variable adjusted at the same rate. Thus, the maximum rate at which an estimated  $y$  can be generated is every 30 seconds. However, since the model parameters will only be updated every 20 minutes, the intersample predictions may not be accurate for satisfactory control performance. It may be preferable to perform control action every 2 or 4 minutes for robust control. The sampling rate of the secondary output which will result in good

control performance is, of course, application dependent. It will depend on the dynamics of the system. If the ratio of the dominant time constant to the sample time of the primary output is small, say 1 to 3, it may be advantageous to implement the simplified algorithm. Thus, it is worthwhile to evaluate the AIC schemes using processes with very different dynamics to investigate the sensitivity of the performance of the AIC strategy to sampling rate selection.

- (2) More experimental work is required to examine the sensitivity of AIC performance to the selection of the secondary output.
- (3) In many situations, there is more than one secondary output which can be used to infer the primary output and better control may result if more than one secondary output is used in the AIC algorithms. Work should be directed to reformulate the AIC schemes to use multiple secondary outputs and to study their performance.
- (4) An adaptive multirate estimation scheme have been proposed by Lu and Fisher (1988) to predict intersample values of the controlled output without utilizing a secondary measurement. In some situations, there may be no appropriate secondary outputs which can be used in the AIC scheme and thus the adaptive multirate estimation scheme will become useful. Detailed simulation and experimental evaluations of the adaptive multirate estimation should be done.
- (5) In order to reduce the number of tuning parameters, the RLS identification algorithms used in this work are quite simple. These algorithms may not be the "best" for practical applications.

Several RLS schemes , such as RLS with variable forgetting factor (Ydstie *et al.*, 1985) and RLS with directional forgetting factor (Rogers, 1989), have been shown to provide great potential for industrial applications. An investigation should be completed to assess various forgetting techniques in RLS identification schemes for industrial situations.

- (6) The controller used in this study is a fixed parameter proportional plus integral controller. For time-varying processes, it may be advantageous to use adaptive controllers or some long range predictive controllers. The potential exists to combine the adaptive inferential estimation scheme with other adaptive control techniques, such as self-tuning control and generalized predictive control, to obtain more powerful adaptive inferential control algorithms.
- (7) Since most difficult industrial control problems are multi-input multi-output, the formulation of the AIC schemes should be extended to handle situations where there are several infrequently sampled primary outputs and several frequently sampled secondary outputs.
- (8) For distillation column control, a feedforward strategy is often applied to improve feed disturbance rejection ability of the control scheme. It is worthwhile to incorporate feedforward control into the AIC schemes.

## References

- Åström, K.J. (1970). Introduction to Stochastic Control Theory. Academic Press, New York, New York.
- Åström, K.J. and B. Wittenmark (1984). Computer Controlled Systems. Prentice-Hall, Englewood Cliffs, New Jersey.
- Ballard, D., C. Brosilow, and C. Kahn (1978). "Dynamic Simulation of Multicomponent Distillation Columns". *Paper presented at 71st Annual AIChE Meeting*, Miami, Florida. Nov., 1978.
- Boyd, D.M. (1948a). "Fractionation Instrumentation and Control. Part I". *Petroleum Refiner*, 27, 10:115-118.
- Boyd, D.M. (1948b). "Fractionation Instrumentation and Control. Part II". *Petroleum Refiner*, 27, 11:114-117.
- Brosilow, C. and M. Tong (1978). "Inferential Control of Processes : Part II. The Structure and Dynamics of Inferential Control Systems ". *AIChE J.*, 24, 3:492-500.
- Buckley, P.S., W.L. Luyben, and J.P. Shunta (1985). Design of Distillation Column Control Systems. Instrument Society of America, Research Triangle Park, North Carolina.
- Carling, G. A. (1986). "A Multicomponent Distillation Column Simulator for Studies in Dynamics and Control". *M.Sc. Thesis*, University of Alberta.
- Carling, G.A. and R.K. Wood (1986). "The Dynamics and Control of a Depropanizer". *Proc. IFAC Symposium on Dynamics and Control of Chemical Reactors and Distillation Columns*, 167-173.

- Chanh, B.M. (1971). "Binary Distillation Column Control : Effect of Sensor Location". *M.Sc. Thesis*, University of Alberta.
- Chieh, I.-L., D.A. Mellichamp and D.E. Seborg (1983). "Adaptive Control Strategies for Distillation Columns". *Proc. 1983 ACC*, San Francisco, California. 193-199.
- Chieh, I.-L., D.E. Seborg and D.A. Mellichamp (1985). "Experimental Application of a Multivariable Self-Tuning Controller to a Multicomponent Distillation Column". *Proc. IFAC Symposium on Control of Chemical Processes*. 190-195.
- Cook, W.J. (1980). "A Modular Dynamic Simulator for Distillation Systems". *M.S. Thesis*, Case Western Reserve University.
- Deshpande, P.B. (1985). Distillation Dynamics and Control. Instrument Society of America, Research Triangle Park, North Carolina.
- Garcia, C.E. and M. Morari (1982). "Internal Model Control. 1. A Unifying Review and Some New Results". *Ind. Eng. Chem. Process Des. Dev.*, **21**, 472-484.
- Gerry, J.P., E.T. Vogel and T.F. Edgar (1983). "Adaptive Control of a Pilot Scale Distillation Column". *Proc. 1983 ACC*. San Francisco, California. 819-824.
- Goodwin, G.C. and Sin K.C. (1984). Adaptive Filtering, Prediction and Control. Prentice-Hall, Englewood Cliffs, New Jersey.
- Graupe, D. (1976). Identification of Systems. Van Nostrand and Reinhold Co., New York, New York.
- Guilandoust, M.T. and A.J. Morris (1985). "Adaptive Inferential Control of Processes with Slow Measurement Rates". *Proc. 35th Canadian Chemical Engineering Conference*, Calgary, Alberta. 213-217.

- Guilandoust, M.T., A.J. Morris and M.T. Tham (1987). "Adaptive Inferential Control". *IEE Proc.*, 134, Pt. D, 3:171-179.
- Guilandoust, M.T., A.J. Morris and M.T. Tham (1988). "An Adaptive Estimation Algorithm for Inferential Control". *Ind. Eng. Chem. Res.*, 27, 9:1658-1664.
- Henley, E.J. and J.D. Seader (1981). Equilibrium-Stage Separation Operations in Chemical Engineering. John Wiley and Sons, New York.
- Holland, C.D. (1985). "History of the Development of Distillation Computer Models". *AIChE Symposium Series*, 79, 15-38.
- Hsia, T.C. (1977). System Identification. Lexington books, D.C. Heath and Co., Toronto, Ontario.
- Joseph, B. and C. Brosilow (1978a). "Inferential Control of Processes : Part I. Steady State Analysis and Design". *AIChE J.* 24, 3:485-492.
- Joseph, B. and C. Brosilow (1978b). "Inferential Control of Processes : Part III. Construction of Optimal and Suboptimal Output Estimators". *AIChE J.*, 24, 3:500-509.
- Kailath, T. (1980). Linear Systems. Prentice-Hall, Englewood Cliffs, New Jersey.
- Kan, H.W. (1982). "Binary Distillation Column Control : Evaluation of Digital Control Algorithms". *M.Sc. Thesis*, University of Alberta.
- Langman, J.A. (1987). "Effect of Q Weighting on Self-Tuning Control of a Binary Distillation Column". *M.Sc. Thesis*, University of Alberta.
- Lieuson, H.Y. (1980). "Experimental Evaluation of Self-Tuning Control of a Binary Distillation Column". *M.Sc. Thesis*, University of Alberta.



- Ljung, L. (1987). System Identification : Theory for the User.  
Prentice-Hall, Englewood Cliffs, New Jersey.
- Ljung, L., and T. Söderström (1982). Theory and Practice of Recursive Identification. MIT Press, Cambridge, Massachusetts.
- Lu, W. (1989). "Parameter Estimation and Multirate Adaptive Control".  
*Ph.D. Thesis*, University of Alberta.
- Lu, W. and D.G. Fisher (1989). "Least Squares Output Estimation with  
Multirate Sampling". *IEEE Trans. Automat. Contr.*, 34, 6:669-672.
- Lu, W., S.L. Shah and D.G. Fisher (1989). "Multirate Constrained Adaptive  
Control". To be published in *Int. J. Control*.
- Luyben, W.L. (1969). "Feedback Control of Distillation Columns by Double  
Differential Temperature Control". *Ind. Eng. Chem. Fund.*, 8,  
4:739-744.
- Luyben, W.L. (1973). "Parallel Cascade Control". *Ind. Eng. Chem. Fund.*,  
12, 4:463-467.
- Martin-Sanchez, J.M. and S.L. Shah (1984). "Multivariable Adaptive  
Predictive Control of a Binary Distillation Column". *Automatica*, 20,  
5:607-620.
- McAvoy, T.J. and Y.H. Wang (1986). "Survey of Recent Distillation Control  
Results". *ISA Trans.*, 25, 1:5-21.
- Morari, M. (1983). "Internal Model Control - Theory and Application".  
*Preprints of 5th IFAC/IMEK Conference on Instrumentation and Automation  
in the Paper, Rubber, Plastics and Polymerization Industries*, Antwerp,  
Belgium. (Edited by A. Van Cauwenberghe).

- Morari, M and K.W. Fung (1982). "Non-linear Inferential Control". *Comput. Chem. Eng.*, 6, 4:271-281.
- Morari, M. and G. Stephanopoulos (1980a). "Optimal Selection of Secondary Measurements within the Framework of State Estimation in the Presence of Persistent Unknown Disturbances". *AIChE J.*, 26, 2:247-260.
- Morari, M. and G. Stephanopoulos (1980b). "Minimizing Unobservability in Inferential Control Schemes". *Int. J. Control*, 31, 2:367-377.
- Morris, A.J., Y. Nazer and R.K. Wood (1981). "Single and Multivariable Applications of Self-Tuning Controllers". Self-Tuning and Adaptive Control : Theory and Applications. Peter Peregrinus Ltd., Stevenage. 248-281.
- Nisenfeld, A.E. and C. Seeman (1981). Distillation Columns. Instrumentation Society of America, Research Triangle Park, North Carolina.
- Pacey, W.C. (1973). "Control of a Binary Distillation Column : An Experimental Evaluation of Feedforward and Combined Feedforward-Feedback Control Schemes". *M.Sc. Thesis*, The University of Alberta.
- Pakte, N.G., P.B. Deshpande and A.L. Chou (1982). "Evaluation of Inferential and Parallel Cascade Schemes for Distillation Control". *Ind. Eng. Chem. Proc. Des. Dev.*, 21, 266-272.
- Parrish, J.R. and C.B. Brosilow (1985). "Inferential Control Applications". *Automatica*, 21, 5:527-538.
- Parrish, J.R. and C.B. Brosilow (1988). "Nonlinear Inferential Control". *AIChE J.*, 34, 633-644.

- Prokopakis, G.J. and W.D. Seider (1981). "Adaptive Semi-Implicit Runge-Kutta Method for the Solution of Stiff Ordinary Differential Equations". *Ind. Eng. Chem. Fund.*, **20**, 3:255-266.
- Rademaker, O., J.E. Rijnsdorp and A. Maarleveld (1975). Dynamics and Control of Continuous Distillation Units. Elsevier Scientific Publishing Co., Amsterdam.
- Rogers, M.D. (1989). "Models and Methods for Recursive Identification". *M.Sc. Thesis*, The University of Alberta.
- Sastry, V.A., D.E. Seborg and R.K. Wood (1977). "Self-Tuning Regulator Applied to a Binary Distillation Column". *Automatica*, **13**, 417-424.
- Scattolini, R. (1988). "Self-Tuning Control of Systems with Infrequent and Delayed Output Sampling". *IEE Proc*, **135**, Part D, 4:213-221.
- Seborg, D.E., T.F. Edgar and S.L. Shah (1986). "Adaptive Control Strategies for Process Control : a Survey". *AIChE J.* **32**, 6:881-913.
- Shen, G.-C. (1987). *Ph.D. Thesis*, The Ohio State University, Columbus, Ohio.
- Shen, G.-C. and W.-L. Lee (1985). "Adaptive Inferential Control for Chemical Processes". *Preprints IFAC Workshop on Adaptive Control of Chemical Processes*, Frankfurt, F. R. Germany.
- Shen, G.-C. and W.-K. Lee (1988). "Adaptive Inferential Control for Chemical Processes with Perfect Measurements". *Ind. Eng. Chem. Res.*, **27**, 71-81.
- Shen, G.-C., and W.-K. Lee (1989). "Adaptive Inferential Control for Chemical Processes with Intermittent Measurements". *Ind. Eng. Chem. Res.*, **28**, 557-563.

- Shinskey, F.G. (1984). Distillation Control for Productivity and Energy Conservation, 2nd edition. McGraw-Hill , New York, New York.
- Shook, D. (1989). "Documentation of the Binary Distillation Column - Computer Instrumentation and Software". *Internal Report*, The University of Alberta.
- Söderström, T. (1980). "On Some Adaptive Controllers for Stochastic Systems with Slow Output Sampling". Methods and Applications in Adaptive Control, Springer-Verlag, New York.
- Sripada, R. and D.G. Fisher (1987). "Improved Least Squares Identification". *Int. J. Control*, 46, 1889-1913.
- Stephanopoulos, G. (1984). Chemical Process Control. Prentice-Hall , Englewood Cliffs, New Jersey.
- Svrcek, W.Y. (1967). "Dynamic Response of a Binary Distillation Column". *Ph.D. Thesis*, The University of Alberta.
- Tolliver, T.L. and L.C. McCune (1978). "Distillation Control Design Based on Steady-State Simulation". *ISA Trans.*, 17, 3:3-10.
- Tolliver, T.L. and L.C. McCune (1980). "Finding the Optimum Temperature Trays for Distillation Control". *InTech*, September, 75-80.
- Tolliver, T.L. and R.C. Waggoner (1980). "Distillation Column Control : a Review and Perspective from the CPI". *Advances in Instrumentation*, 35, 1:83-106.
- Vagi, F.J. (1988). "Experimental Evaluation of Multivariable, Multirate Self-Tuning Control of a Binary Distillation Column". *M.Sc. Thesis*, The University of Alberta.

- Vermeer, P.J. (1987). "Design and Evaluation of Practical Self-Tuning PID Controllers". *M.Sc. Thesis*, The University of Alberta.
- Vermeer, P.J., B. Roffel and P.A. Chin (1988). "Industrial Application of an Adaptive Algorithm to Overhead Composition Control". *Paper Presented at the Workshop on Adaptive Strategies for Industrial Use*. Lodge at Kananaskis, Alberta, Canada.
- Webber, W.O. (1959). "Control by Temperature Differential". *Petrol. Refiner*, **38**, 5:187-191.
- Wolovich, W.A. (1974). Linear Multivariable Systems. Springer-Verlag, New York, New York.
- Wong, T.T. (1985). "Dynamic Simulation of Multicomponent Distillation Columns". *M.Sc. Thesis*, The University of Alberta.
- Wong, T.T. and R.K. Wood (1985). "Dynamic Behaviour of a Hydrocarbon Separator". *Proc. 1985 Summer Computer Simulation Conference*. 331-336.
- Wood, C.E. (1967). "Tray Selection for Column Temperature Control". *Chem. Engr. Progress*, **64**, 1:85-88.
- Wood, R.K. and Berry, M.W. (1973). "Terminal Composition Control of a Binary Distillation Column". *Chem. Eng. Sci.*, **28**, 1707-1717.
- Ydstie, B.E., L.S. Kershebaum and R.W.H. Sargent (1985). "Theory and Application of an Extended Horizon Self-tuning Controller". *AIChE J.*, **31**, 1771-1780.
- Yiu, Y.S., G.A. Carling and R.K. Wood (1989). "Dynamics and Control of Multicomponent Distillation Columns". To be published in *Simulation*.

Yu, C.-C., and W.L. Luyben (1984). "Use of Multiple Temperatures for the Control of Multicomponent Distillation Columns ". *Ind. Eng. Chem. Proc. Des. Dev.*, 23, 3:590-597.

## Appendix A : The Concept of Observability

### A.1 The Implications of the Observability Index

Consider the plant model given by Eqs. 2.1 to 2.3, with all the noise terms being zero, i.e.

$$\underline{x}(t+1) = \begin{bmatrix} 0 & \dots & 0 & -a_1 & 0 & \dots & 0 & -\bar{a}_1 \\ & & I_{nv-1} & \vdots & \vdots & & \vdots & \vdots \\ & & & -a_{nv} & 0 & \dots & 0 & -\bar{a}_{nv} \\ 0 & \dots & 0 & -a_{nv+1} & 0 & \dots & 0 & -\bar{a}_{nv+1} \\ \vdots & & \vdots & \vdots & & & I_{ny-1} & \vdots \\ 0 & \dots & 0 & -a_n & & & & -\bar{a}_n \end{bmatrix} \underline{x}(t) + \begin{bmatrix} b_1 \\ \vdots \\ b_{nv} \\ b_{nv+1} \\ \vdots \\ b_n \end{bmatrix} u(t) \quad (\text{A.1})$$

$$v(t) = x_{nv}(t) \quad (\text{A.2})$$

$$y(t) = hx_{nv}(t) + x_n(t) \quad (\text{A.3})$$

where

$nv$  = the observability index of  $v(t)$

$n$  = the order of the process

$\underline{x}(t)$  = the state vector;  $x_{nv}$  is the  $nv$  state

$v(t)$  = secondary output

$y(t)$  = primary output

$ny = n - nv.$

$h$  = a scalar term.

Eqs. A.1 to A.3 can be rewritten into an multi-input multi-output (MIMO)

structure :

$$\begin{aligned} \underline{x}(t+1) &= \underline{A} \underline{x}(t) + \underline{B} u(t) \\ &= \begin{bmatrix} \underline{A}_{11} & \underline{A}_{12} \\ \underline{A}_{21} & \underline{A}_{22} \end{bmatrix} \underline{x}(t) + \begin{bmatrix} \underline{B}_1 \\ \underline{B}_2 \end{bmatrix} u(t) \end{aligned} \quad (\text{A.4})$$

$$\underline{Y}(t) = \begin{bmatrix} v(t) \\ y(t) \end{bmatrix} = \underline{C} \underline{x}(t) = \begin{bmatrix} \underline{C}_1 \\ \underline{C}_2 \end{bmatrix} \underline{x}(t) \quad (\text{A.5})$$

where

$$\underline{A}_{11} = \begin{bmatrix} 0 & \dots & 0 & -a_1 \\ & & \vdots & \\ & & I_{nv-1} & \\ & & & -a_{nv} \end{bmatrix} \quad (\text{A.6a})$$

$$\underline{A}_{12} = \begin{bmatrix} 0 & \dots & 0 & -\bar{a}_1 \\ \vdots & & \vdots & \\ \vdots & & \vdots & \\ 0 & \dots & 0 & -\bar{a}_{nv} \end{bmatrix} \quad (\text{A.6b})$$

$$\underline{A}_{21} = \begin{bmatrix} 0 & \dots & 0 & -a_{nv+1} \\ \vdots & & \vdots & \\ \vdots & & \vdots & \\ 0 & \dots & 0 & -a_n \end{bmatrix} \quad (\text{A.6c})$$



$$\underline{\underline{A22}} = \begin{bmatrix} 0 & \dots & 0 & -\bar{a}_{nv+1} \\ & & & \vdots \\ & I_{ny-1} & & -\bar{a}_n \end{bmatrix} \quad (\text{A.6d})$$

$$\underline{\underline{B1}} = \begin{bmatrix} b_1 & b_2 & \dots & b_{nv} \end{bmatrix}^T \quad (\text{A.7a})$$

$$\underline{\underline{B2}} = \begin{bmatrix} b_{nv+1} & b_{nv+2} & \dots & b_n \end{bmatrix}^T \quad (\text{A.7b})$$

$$\underline{\underline{C1}} = [0 \ 0 \ \dots \ 1 \ 0 \ 0 \ \dots \ 0] \quad (\text{A.8a})$$

$$\underline{\underline{C2}} = [0 \ 0 \ \dots \ 1 \ 0 \ 0 \ \dots \ h] \quad (\text{A.8b})$$

Case 1 :  $\underline{\underline{A12}}$  and  $\underline{\underline{A21}}$  are zero matrices

The observability index  $nv$ , as mentioned in Section 2.2.1, represents the number of the states that are completely observable from the secondary output. In this special case, it can be readily seen that the first  $nv$  states (i.e.  $x_1, x_2, \dots$ , and  $x_{nv}$ ) are completely observable from the secondary output  $v$  (or  $x_{nv}$ ) and the rest of the states ( $x_{nv+1}, x_{nv+2}, \dots$ , and  $x_n$ ) are completely observable from the primary output,  $y$ . However, a "better" choice of secondary output does not mean that the value of  $nv$  is larger. Similarly, a large value of  $nv$  does not imply that the secondary output selected is a good choice. The reason is that  $nv$  only represents the number (*quantity*) of different states or "dynamic modes" that can be observed from the secondary output, not the *quality* of the observation. The quality of the observation is measured by the condition number of the

observability matrix (see Section A.2).

Case 2 :  $\underline{A}_{12}$  and  $\underline{A}_{21}$  are not zero matrices

The system represented by Eqs. A.4 and A.5 can be decomposed into two sub-systems as follow

$$\begin{aligned} & [x_1(t+1) \ x_2(t+1) \ x_3(t+1) \ \dots \ x_{nv}(t+1)]^T \\ & = \underline{A}_{nv \times n} \underline{x}(t) + \underline{B}_{nv \times 1} u(t) \\ & = \begin{bmatrix} \underline{A}_{11} & \underline{A}_{12} \end{bmatrix} \underline{x}(t) + \underline{B}_1 u(t) \end{aligned} \tag{A.9a}$$

$$v(t) = \underline{C}_1 \underline{x}(t) \tag{A.9b}$$

$$\begin{aligned} & [x_{nv+1}(t+1) \ x_{nv+2}(t+1) \ x_{nv+3}(t+1) \ \dots \ x_n(t+1)]^T \\ & = \underline{A}_{ny \times n} \underline{x}(t) + \underline{B}_{ny \times 1} u(t) \\ & = \begin{bmatrix} \underline{A}_{21} & \underline{A}_{22} \end{bmatrix} \underline{x}(t) + \underline{B}_2 u(t) \end{aligned} \tag{A.10a}$$

$$y(t) = \underline{C}_2 \underline{x}(t) \tag{A.10b}$$

It can be easily shown that the rank of the observability matrix for the first sub-system (Eq. A.9) is  $nv$  and the rank of the observability matrix of the second sub-system (Eq. A.10) is  $ny$  ( $ny = n-nv$ ). In other words, from the secondary output  $v(t)$ ,  $nv$  different "states" or "dynamic modes" of the system can be observed. Correspondingly,  $ny$  different "dynamic modes" can be observed from the primary output  $y(t)$ . It should be noted that using the term "dynamic modes" instead of "states" is less ambiguous since the "dynamic modes" observed are different from the states (defined in Eqs. A.9 and A.10) because  $\underline{A}_{12}$  and  $\underline{A}_{21}$  are not zero matrices. The "dynamic modes"

observed in this case are "similar" to the states defined in Eqs. A.9 and A.10.

*NOTE* : From the theory of linear systems (Kailath, 1980), it is known that there can be many ways to express the state space model of a linear system. Two realizations of the same linear system are similar to each other if there exists a nonsingular matrix  $\Omega$  such that

$$\underline{\bar{A}} = \Omega^{-1} \underline{A} \Omega, \quad \underline{\bar{B}} = \Omega^{-1} \underline{B}, \quad \underline{\bar{C}} = \underline{C} \Omega \quad (\text{A.11})$$

The states of the two realizations can be related as

$$\underline{x}(t) = \Omega \underline{\bar{x}}(t) \quad (\text{A.12})$$

## A.2 The Effect of the Choice of the Secondary Output on Observability

If there are two secondary outputs,  $v'(t)$  and  $v''(t)$ , available, one can obtain two different but "similar" state space models of the same linear system

**Model 1** : For  $v'(t)$  as the secondary output, then

$$\underline{x}'(t+1) = \underline{A}' \underline{x}'(t) + \underline{B}' u(t) \quad (\text{A.13a})$$

$$\underline{Y}'(t) = \begin{bmatrix} v'(t) \\ y(t) \end{bmatrix} = \underline{C}' \underline{x}'(t) \quad (\text{A.13b})$$

**Model 2** : For  $v''(t)$  as the secondary output, then

$$\underline{x}''(t+1) = \underline{A}'' \underline{x}''(t) + \underline{B}'' u(t) \quad (\text{A.14a})$$

$$\underline{Y}''(t) = \begin{bmatrix} v''(t) \\ y(t) \end{bmatrix} = \underline{\underline{C}}'' \underline{x}''(t) \quad (\text{A.14b})$$

The observability matrix,  $\Psi$ , of each model is given by :

$$\text{Model 1 : } \Psi' = \left[ \underline{\underline{C}}' \quad \underline{\underline{C}}' \underline{\underline{A}}' \quad \underline{\underline{C}}' (\underline{\underline{A}}')^2 \quad \dots \quad \underline{\underline{C}}' (\underline{\underline{A}}')^{n-1} \right]^T \quad (\text{A.15})$$

$$\text{Model 2 : } \Psi'' = \left[ \underline{\underline{C}}'' \quad \underline{\underline{C}}'' \underline{\underline{A}}'' \quad \underline{\underline{C}}'' (\underline{\underline{A}}'')^2 \quad \dots \quad \underline{\underline{C}}'' (\underline{\underline{A}}'')^{n-1} \right]^T \quad (\text{A.16})$$

If  $v'(t)$  is a better choice of secondary output than  $v''(t)$ , this implies that the matrix  $\Psi'$  is "better conditioned" than  $\Psi''$  (i.e. the condition number of  $\Psi'$  is closer to 1 than the condition number of  $\Psi''$ ).

Intuitively, a secondary output,  $v'(t)$ , which is more sensitive to disturbances than  $v''(t)$ , should result in a "better conditioned" observability matrix than  $v''(t)$ . This argument will probably hold for systems that have high signal to noise ratio. For nonlinear systems, the analysis presented is not applicable and the choice of the secondary output should rely on the *a priori* knowledge of the system.

**Appendix B : Tray Liquid Holdup Data and Thermodynamic Parameters  
for Depropanizer Column**

**B.1 Tray Liquid Holdup Data**

The tray liquid holdup data used in the control simulation of the depropanizer column model are listed in this section. These data are the same as those used by Carling (1986). Stages are numbered from top to bottom, with stage 1 being the condenser and stage 31 being the reboiler.

Table B.1  
Tray Liquid Holdup Profile

<u>Stage Number</u>	<u>Holdup (kmol)</u>
2	22.0
3	21.8
4	21.5
5	21.1
6	20.5
7	19.8
8	19.0
9	17.9
10	16.8
11	15.8
12	14.8
13	16.0
14	15.9
15	15.7
16	15.5
17	15.2
18	14.9
19	14.6
20	14.2
21	13.8
22	13.4
23	13.0
24	12.8
25	12.5
26	12.3
27	12.2
28	12.1
29	12.0
30	11.9

## B.2 Thermodynamic Parameters

The thermodynamic parameters used for the five component depropanizer column simulated in Chapter 5 are listed in the following tables. All data are obtained from Wong (1985).

Table B.2  
Equilibrium Data

$$K_i = \exp\left(a_{1i} + \frac{a_{2i}}{T} + \frac{a_{3i}}{T^2}\right) \quad (T \text{ in K})$$

<u>Component</u>	<u>a<sub>1i</sub></u>	<u>a<sub>2i</sub></u>	<u>a<sub>3i</sub></u>
Ethane	0.649086E+00	0.421544E+04	-0.882222E+06
Propylene	0.391245E+01	0.186111E+04	-0.533920E+06
Propane	0.384851E+01	0.192822E+04	-0.560525E+06
Iso-butane	0.684489E+01	-0.167722E+03	-0.252485E+06
Cis-butene-2	0.658149E+01	0.174340E+02	-0.317562E+06

Table B.3  
Liquid Enthalpy Data

$$h_i = c_{1i} + c_{2i}T \quad (T \text{ in K, } h_i \text{ in kJ/kmol})$$

<u>Component</u>	<u>c<sub>1i</sub></u>	<u>c<sub>2i</sub></u>
Ethane	-3.050700	0.040113
Propylene	-3.507600	0.045986
Propane	-5.480700	0.053833
Iso-butane	-7.743300	0.038080
Cis-butene-2	-3.899100	0.059589

Table B.4  
Vapor Enthalpy Data

$$H_i = e_{1i} + e_{2i}T + e_{3i}T^2 \quad (T \text{ in K, } H_i \text{ in kJ/kmol})$$

<u>Component</u>	<u>e<sub>1i</sub></u>	<u>e<sub>2i</sub></u>	<u>e<sub>3i</sub></u>
Ethane	0.684620E+01	0.199386E-01	-0.422788E-05
Propylene	0.966230E+01	0.185670E-01	0.626584E-05
Propane	0.105420E+02	0.138070E-01	0.206430E-04
Iso-butane	0.134260E+02	0.947720E-02	0.436136E-04
Cis-butene-2	0.173470E+02	0.226330E-02	0.448513E-04